Signatures of Quantum Gravity

Aditya Varna Iyer
Oriel College
University of Oxford

A thesis submitted for the degree of

Doctor of Philosophy

Trinity 2022

Acknowledgements

This thesis is a culmination of several interesting discussions with my collaborators and fellow academics. I will forever be indebted to my supervisor, Vlatko Vedral, for starting me off on a journey of intellectual curiosity and for providing me the luxury to engage in independent thought. Vlatko reminded me to stay true to the unitary path even as I encountered several non-linear phenomena while navigating my intellectual quagmire. My heartfelt gratitude extends to my undergraduate supervisor, Wang Yi, who was instrumental in shaping my mindset as a researcher and exposed me to the field of cosmology. I also thank my collaborators, Eduardo Dias, Alexander Yosifov, Richard Howl and Gowtham Amirthya for numerous conversations, academic or otherwise and for always providing a refreshing perspective on several ideas that we shared. I was also very fortunate to have interacted with Chiara Marletto, whose contagious energy and passion for physics kept me engrossed in the big questions and encouraged me to pursue bolder fundamental ideas.

It was a privilege to be part of the Quantum Frontiers Group at Oxford which quickly developed into a place of refuge where I was privy to many fervent discussions ranging from the nature of existence to economic ideologies. My peers (the original three) Samuel Kuypers, David Felce and Jinzhao Sun stuck with me through the highs and lows of ideation and I will always cherish the wonderful time we had at Singapore. I thank Christian Schilling, Benjamin Yadin, Felix Tennie and Tristan Farrow for their mentorship. As our group grew, so did the diversity of thought which led to my continued education and exploration. For this, I thank Nicetu, Simone, Lodovico, Amy, Maria and Lucia for making the group the cohesive unit that it is today. I also thank my friends for being a constant presence in my life and for sparing their precious time to engage with my research.

This acknowledgement would barely qualify as complete without going back to the very beginning. I thank my parents Balu and Suganthy, for bringing me into this universe and for providing me with every opportunity, through personal sacrifice, converging to this undertaking of answering some of the deepest questions about the universe. To them, I dedicate this thesis. I also thank my partner Arsène for her patience, love and encouragement throughout this roller coaster journey.

Abstract

This thesis discusses the hurdles that are frequently encountered in attempts to quantize gravity or rather, while gravitizing quantum mechanics. Among the issues we consider here are the lack of observable signatures of the quantum nature of gravity despite the considerable amount of effort directed towards theoretical approaches such as string theory and loop quantum gravity, to name a few. Here, we examine observable consequences of quantum gravity through superpositions of primordial massive particles and quantum witnesses in table top experiments involving Bose Einstein Condensates. We compute the decoherence timescales of a primordial superposition and outline its effects in the form of an interference pattern, characteristic absorption spectra or entanglement effects. While it is difficult to conceive of a way to control measurements that occur in the early universe, such as the measurement of curvature perturbations during inflation, we have a significant degree of control over quantum systems in the laboratory such as Bose Einstein Condensates for which we propose a non-Gaussianity based witness of the quantum nature of gravity. Non-Gaussianities are also discussed in the context of cosmological observations where it becomes important to distinguish primoridal non-Gaussianities from secondary effects. While observing any of these signatures can give credence to the requirement that gravity should be quantum, insight can also be drawn between conflicts that exist between general relativity and quantum mechanics. One such anomaly we discuss is the cosmic censorship conjecture and its reconciliation with quantum information theory. In particular by employing the complexity-volume conjecture from the AdS/CFT correspondence, we show that for Kerr black holes, spacetime must continue across the Cauchy Horizon where solutions to the Einstein field equations break down. Finally, we introduce a formalism that attempts to bridge the gap between quantum theory and relativity by putting spacelike and timelike events on the same footing. The notion of an event, redefined as a correspondence between a system and an apparatus, gives rise to interesting predictive phenomena and allows us to apply the tools of quantum information theory in their characterisation.

Contents

List of Abbreviations

QM . . . . . . Quantum Mechanics

GR . . . . General Relativity

QI . . . . Quantum Information

QG . . . . Quantum Gravity

CG . . . . Classical Gravity

QFT . . . . . . Quantum Field Theory

CVQI . . . . . Continuous Variable Quantum Information

BMV . . . . . Bose Marletto Vedral (experiment)

CMB . . . . . Cosmic Microwave Background

SLE/TLE . . . Spacelike/Timelike Events

BEC . . . . . . Bose Einstein Condensate

PBH . . . . . . Primordial Black Hole

SCC . . . . . . Strong Cosmic Censorship

Publications Represented

Ch. 1 . . . . . Quantum signatures of gravity from superpositions of primordial massive particles, Gowtham Amirthya Neppoleon, Aditya Iyer, Vlatko Vedral, and Yi Wang, Phys. Rev. D 105, 043505 – Published 3 February 2022.

Ch. 2 . . . . . Non-Gaussianity as a Signature of a Quantum Theory of Gravity, Richard Howl, Vlatko Vedral, Devang Naik, Marios Christodoulou, Carlo Rovelli, and Aditya Iyer, PRX Quantum 2, 010325 – Published 17 February 2021.

Ch. 3 . . . . . A new look at the C0-formulation of the strong cosmic censorship conjecture, Aditya Iyer, Alexander Y Yosifov, and Vlatko Vedral, New Journal of Physics, Volume 24 - Published 25 May 2022

Ch. 4 . . . . . Signatures of causality and determinism in a quantum theory of events, Aditya Iyer, Eduardo O. Dias, and Vlatko Vedral, Phys. Rev. A 105, L010202 – Published 14 January 2022.

The feature of quantum gravity that challenges its very right to be considered as a genuine branch of theoretical physics is the singular absence of any observed property of the world that can be identified unequivocally as the result of some interplay between general relativity and quantum theory.

— Chris J. Isham, *Structural Issues in Quantum Gravity*

1 Introduction

Contents

1.1 Motivation

A longstanding endeavour since the advent of General Relativity (GR) is the unification of gravity and quantum mechanics (QM) [1–4], which is expected to resolve pathologies such as singularities in the big bang or in black holes. Notable attempts towards a quantum theory of gravity include: String Theory [5] and Loop Quantum Gravity [6]. However, observable consequences that are uniquely attributable to these theories to test their validity, remain elusive. In addition, among the limited signatures predicted, none can be verified with currently available technology and resources. While strides have been made through model specific proposals based on these theories, the differences may not be readily observable at low energy scales.

The common view is that there is no hope of experimental evidence since we need to probe GR near a very small length scale, the Planck length, where QM effects of spacetime become relevant. Such observations through collider physics would require us to build an astronomical scale particle accelerator to probe these high energy scales.

In this thesis, we will consider classes of observations at a cosmological, Ch.2 and table-top experimental level, Ch.3 to shed insights on the quantum nature of gravity. Some of these signatures are model dependent while others are model independent. In particular, we investigate cosmological events that naturally occur close to the Planck energy scale and table-top experiments on quantum systems at the Planck mass scale. We will also study conflicts that arise during unification attempts of quantum theory and gravity from a holographic perspective, Ch.4. Furthermore, we will investigate a theoretical formalism of events that resolves the asymmetry between spacelike and timelike events, offering a window into the requirements and properties of quantum theory of gravity, Ch.5.

1.2 Superpositions

A central tenet of QM is that quantum degrees of freedom can be superposed. A straightforward extension of this principle to massive particles opens up several issues that are at the heart of the conflict between GR and QM. Preserving the unitarity and linearity of quantum mechanics, we expect a massive superposition to manifest as entanglement with the metric itself which if observed would be a tell-tale sign of quantum gravitational (QG) effects.

Recent works on table-top experiments have emphasised an important scale in addition to the Planck length scale – the Planck mass, where gravitational effects of massive quantum systems become relevant, allowing us to distinguish quantum gravitational effects from classical gravity. In contrast to the Planck length $\sim 1.6 \times 10^{-35}$ m which requires extraordinarily high energy scales to probe, the Planck mass $\sim 2.2 \times 10^{-8}$ kg corresponds to laboratory scales. Due to the continuing rapid developments in quantum technology driven by quantum information theory (QI), this mass scale is hoped to be within experimental reach soon.

Proposals have been developed by Bose et.al. [7] and Vedral et.al. [8], for an experiment to detect evidence of QG using techniques of QI and quantum technology. The Bose-Marletto-Vedral (BMV) proposal considers a witness of the creation of entanglement between two masses that were initially superposed at two locations to be a tell tale sign of the quantum nature of the gravitational field mediating their interaction. Exciting advances in creating massive superpositions, e.g. [9], indicate that the BMV experiment could be performed in the near future. Other proposals of a similar nature describing tests of QG motivated by QI insights include [10–13]. A comprehensive review of the advances in experimental and theoretical work on quantum experiments that will be able to probe relativistic effects of gravity on quantum properties can be found in [14].

The BMV proposal demonstrates the utility of QI concepts in developing novel and promising tests of QG. The extension of this analysis to continuous variable QI (CVQI) to develop a new witness that is motivated by the different ways in which matter must interact in a QG or CG theory, is a topic of discussion in this thesis. This new witness is the production or change of non-Gaussianity in the quantum state of matter. It is complementary to an entanglement witness of QG since it is applicable to types of tests of QG that are inaccessible to an entanglement witness, and vice-versa. A particular example we consider is witnessing non-Gaussianity in systems consisting of gravitationally interacting identical bosons in the same state and masses whose wavefunctions overlap. This opens new systems to tests of QG using a promising QI approach. An advantage of this protocol is that it requires a single quantum system as opposed to two in the BMV prescription. This work adds to the body of existing literature on gravitational witnesses in condensates, notably those considered in [15] on phononic excitations in a BEC where they satisfy the Klein–Gordon equation on a curved background metric. It is shown that changes in the spacetime metric through a non-uniform acceleration of the BEC cavity trap produces phononic excitations that can be detected. The effect of an oscillating gravitational field on BEC phonon modes has been considered in [16] that could serve as a possible experimental realization of [15].

Another domain where superpositions are considered is in the context of the early universe. While common laboratory systems are susceptible to decoherence, cosmology may provide exotic objects that are robust against decoherence. In particular, the dominant contribution to the mass of the universe comes from dark matter which does not interact with the standard model sector and can only be witnessed through its gravitational interactions. This allows for the possibility of Schrodinger-cat-like states of dark matter in the absence of appreciable interactions. In this thesis, we study the decoherence of a primordial massive superposition to shed some insight on the relevant mass scales that would allow for a quantum superposition from the early universe to survive until present times.

1.3 Early Universe Cosmology

The early universe is often seen as a test bed for quantum effects where primordial processes such as inflation are assumed to be driven by quantum fields. Inflation [17–19] is the leading paradigm of the early Universe that was formulated as a solution to the "big bang puzzles" of standard cosmology, namely the horizon problem and the flatness problem. As a bonus inflation also proved to be a consistent theory of structure formation in the Universe, explaining the anisotropies in the primordial cosmic microwave background (CMB) and the large scale structure of galaxies through quantum fluctuations in the scalar field driving inflation, dubbed the inflaton.

One of the most promising places to look for evidence of quantum gravity is through cosmological observations. In particular, it is hoped that such evidence could be found in the cosmic microwave background (CMB). If gravity is indeed quantum mechanical, the fluctuations of the inflaton should lead to the creation of real gravitational fluctuations from the vacuum. Such fluctuations will modify the trajectory of photons from last scattering, which (in addition to other effects) modifies the red-shifting process and leads to temperature fluctuations in the sky. However, if gravity is always a classical process, then there will be no creation of gravitational fluctuations from the vacuum and thus no quantum contribution to the temperature fluctuations due to the inflationary process.

Inflation will only amplify scalar and tensor (spin-2) field quantum fluctuations in 3+1 dimensions. The inflaton itself (if it is indeed a scalar field) should then have its quantum fluctuations magnified. These will enter the scalar power spectrum of the CMB. For the gravitational fluctuations, there are both scalar (essentially the Newtonian potential) and tensor (gravitons) fluctuations. The gravitons will enter the tensor power spectrum of the CMB. It is thought that, for consistency of the theory, the gravitational scalar fluctuations must enter the scalar power spectrum with the inflaton (in fact these should really be considered as inseparable as these are related through the perturbed Einstein equations).

The dynamics of the inflaton, provides the negative pressure needed for the exponential expansion of the Universe. The action governing the simplest models of inflation is as follows,

$$S = \int d^4x\sqrt{-g}\left[\frac{M_{pl}^2}{2}\mathcal{R} - \frac{1}{2}g^{\mu\nu}\partial_\mu\phi\partial_\nu\phi - V(\phi)\right] \tag{1.1}$$

In linear cosmological perturbation theory, the metric tensor and the inflaton are expanded around a background such that, $g^{\mu\nu} = \gamma^{\mu\nu} + h^{\mu\nu}$ and $\phi = \bar{\phi} + \delta\phi$ where $\gamma^{\mu\nu}$ and $\bar{\phi}$ are the background metric and scalar field respectively. The metric perturbations, $h^{\mu\nu}$ can be resolved into scalar, vector and tensor components as follows,

$$h_{\mu\nu} = a^2(\eta)\begin{pmatrix} 2\Phi & -B_{|i} \\ -B_{|i} & 2(\psi_{ij} - E_{|ij}) \end{pmatrix} \tag{1.2}$$

The scalar part of the metric perturbation (Φ) combines with the inflaton perturbations resulting in a gauge-invariant scalar perturbation $\delta\zeta$ that can be treated conveniently,

$$\delta\zeta = a\left(\delta\phi + \bar{\phi}'(B - E') + z\Psi\right) \tag{1.3}$$

where Ψ is the gauge-invariant Bardeen variable that is identical to the Newtonian potential Φ for a particular gauge choice. We have deliberately chosen Φ to represent the Newtonian potential and ϕ to represent the inflaton as these sectors evolve together under the inflationary action.

The action for the perturbations then reduces to that of a parametric harmonic oscillator.

$$S_{pert} = \frac{1}{2}\int d^4x \left[\delta\zeta'^2 - c_s^2(\delta\zeta_{,i})^2 + \frac{z''}{z}\delta\zeta^2\right] \tag{1.4}$$

It has been shown in [20] that at the end of inflation each Fourier mode is evolved from the vacuum state $\otimes_k |0_k, 0{-}k\rangle$ into a two-mode squeezed state $|\psi_{sq}\rangle$ which belongs to the wider class of quantum states called Gaussian states,

$$|\psi_{sq}\rangle = \bigotimes_k \frac{1}{\cosh r_k}\sum_{n=0}^{\infty} e^{-2in\varphi_k}\tanh^n r_k \, |n_k, n_{-k}\rangle \tag{1.5}$$

Where $|n_k\rangle$ is a number state of mode k with occupation number n and r_k, φ_k are the squeezing parameter and angle respectively. Through this treatment, it is apparent that quantum field theory (QFT) in curved space time preserves the Gaussianity of states and non interacting theories do not generate non-Gaussianity. A more detailed commentary on this generic property of semiclassical gravity is provided in Appendix A. Also note that one can obtain a direct relation between the slow roll parameters and the degree of entanglement as shown through the computation of the Von Neumann entropy and its relation to the scale factor in [21]. Further, in [22] the entanglement between the modes of a fermionic field in the FRW universe was studied and found to be lower than the bosonic case. This suggests that the nature of the quantum field plays an important role in determining response of entanglement to the dynamics of the expanding universe.

An interesting question to ask at this point would be: if we could perform a Bell inequality violating experiment in cosmology as the state is highly entangled. This would confirm that the inflationary fluctuations are of quantum origin and not simply stochastic in nature. However upon further consideration we note that a key missing ingredient for Bell violation in cosmology is the lack of non-commuting observables. While the dominant contribution to the CMB temperature fluctuations stems from the curvature modes $\zeta(x)$, its conjugate momentum, $\Pi(x)$ is suppressed over many e-folds during inflation.

A simple setup would start with two scalar fields ϕ and σ to serve as the system and the appartus whose joint Hilbert space would be, $\mathcal{F} = \mathcal{F}_\phi \otimes \mathcal{F}_\sigma$, where

$\mathcal{F}_\phi$ and $\mathcal{F}_\sigma$ are the Fock spaces of ϕ and σ. Observables are regarded to be operators on $\mathcal{F}_\phi$ and $\mathcal{F}_\sigma$. In this case, for a quantum state $|\psi\rangle \in \mathcal{F}$ the expectation value of an observable $\mathcal{O}$ is,

$$\langle\psi|\mathcal{O}|\psi\rangle = \mathbf{Tr}_\phi[\mathcal{O}\rho_\phi]\,, \tag{1.6}$$

where

$$\rho_\phi \equiv \mathbf{Tr}_\sigma|\psi\rangle\langle\psi|\,, \tag{1.7}$$

is the reduced density matrix, and $\mathbf{Tr}_\phi$ and $\mathbf{Tr}_\sigma$ are the trace operations in $\mathcal{F}_\phi$ and $\mathcal{F}_\sigma$, respectively. In general, the reduced density matrix ρ_ϕ represents a mixed state due to quantum entanglement between $\mathcal{F}_\phi$ and $\mathcal{F}_\sigma$ unless the quantum state of the total system is a direct product of a state in $\mathcal{F}_\phi$ and a state in $\mathcal{F}_\sigma$.

The key, seemingly insurmountable hurdle is that, unlike table-top experiments where we have free reign to manipulate quantum systems, there exists only one universe which has already chosen a measurement basis. Strides have been made in [23] to develop baroque models of the early universe involving multiple fields to replicate a system-apparatus interaction and treating different patches of the universe as independent runs of an experiment on identically prepared initial states. These models do accommodate a possibility for Bell inequality violation, however introducing non minimal assumptions such as additional fields, interacting in a contrived manner makes distinguishing observable effects a phenomenological problem. This motivates us to consider the possibility of witnessing quantum effects due to relics left behind by primordial processes like inflation in Ch.2 and non-Gaussianity as a quantum witness in Ch.3.

As a side remark, the field of relativistic quantum information has seen several developments pertaining to the entanglement of the vacuum state of a free field [24–26]. It is worth stressing at this point that notions of entanglement are underpinned by the choice of the tensor-product decomposition of the joint Hilbert space of the whole system. In Minkowski space we could consider decomposing a free scalar field into plane wave modes or employ a Rindler wedge type decomposition. In these cases the vacuum state can be expressed as,

$$|0\rangle = \bigotimes_k |0\rangle_k \tag{1.8}$$

which is a product state of the Fourier modes denoted by k, or the two mode squeezed state similar to (1.3) in the Rindler wedge decomposition which is bipartite entangled. For example the Unruh effect [27] is related to the entanglement structure obtained by decomposing spacetime into two regions, $R_1 : x < 0$ and $R_2 : x > 0$. The violation of Bell's inequalities has also been discussed in this context in [24].

While projective measurements work well operationally in non-relativistic quantum mechanics and are routinely used in the construction of Bell's inequalities, in quantum field theory, projective measurements are not compatible with relativistic causality. In fact, local projectors of finite rank do not exist in QFT [28, 29]. Furthemore, localized ideal measurements such as infinite rank projectors considered in [28] also suffer from faster-than-light signalling as considered in a work by Sorkin [30]. Other measurement schemes involve coupling with particle detectors which are localized non-relativistic quantum systems to quantum fields, including the Unruh-DeWitt model [31]. These models are used in the characterisation of entanglement harvesting from the vacuum state [32]. While point like detector models are compatible with relativistic causality, some divergences emerge due to their singular nature. To remedy this issue smeared detectors [33, 34] have been considered that maintain causality within the bounds of the smearing length scale. These results, together with the fact that detector models can realistically represent the way fields are measured experimentally [35], make this option especially appealing for modelling measurements in QFT. Finite-size detectors with a position-dependent coupling strength were studied in [36] that naturally couple to peaked frequency distributions of Rindler, Minkowski and Unruh modes. Such models are suitable to analyze entanglement harvesting in noninertial frames. Some open questions remain regarding the mechanism of going from a field state and a detector that are originally decoupled and uncorrelated to a experimental measurement. We will not be considering projective measurements on fields or particle detector based measurements in this thesis. The ardent reader is encouraged to refer to the collection of papers in [37] for an excellent background on the issues discussed above, and in general the field of relativistic quantum information.

1.4 AdS CFT

Among recent theoretical frameworks developed for a quantum theory of gravity is the Anti-de Sitter/Conformal Field Theory correspondence (AdS/CFT) [38]. This correspondence relates quantum gravity in d dimensions to non-gravitational QFTs in $d-1$ dimensions. The QFTs considered are conformally symmetric, hence UV complete. The states defined in these CFTs like any other quantum state possess quantum correlations that are well understood from a quantum information theoretic perspective. These dual states on the CFT side correspond to a spacetime geometry and gravitating systems on the AdS side. Their dynamics are governed by the Einstein field equations.

Recall, that in condensed matter systems while studying collective phenomena, new weakly coupled degrees of freedom emerge dynamically in the study of strongly coupled systems. These emergent excitations, are in turn described by their own fields which is akin to the holographic duality [39]. The interesting twist in the bulk-boundary correspondence for spacetime, however, is that these emergent fields live in a space with one extra dimension with the dual theory being a theory of gravity. It seems natural that the first hints of a gauge/gravity duality were seen in string theory where branes contain a gauge theory living in their world volume. However, the study of the correspondence has been extended to include very different domains, ranging from the analysis of the strong coupling dynamics of QCD and electroweak to applications in condensed matter physics such as holographic superconductors. For instance the strong-coupling QCD analysis of ultrarelativistic processes like heavy ion collisions [40, 41] is impossible with the present state of the QCD theory while some insights can be derived from an AdS/CFT based analysis. In the following we present a digression to review the AdS/CFT correspondence, the more familiar reader may skip this section.

1.4.1 Review

The Bekenstein-Hawking formula for black hole entropy, S_{BH} is given as,

$$S_{BH} = \frac{1}{4G} A_H \tag{1.9}$$

where G is the gravitational constant and A_H is the area of the event horizon. In standard QFT, entropy is an extensive quantity and scales with the volume of a spatial region i.e. for a spatial region of $d-1$ dimensions (R_{d-1}), $S_{QFT} \propto \mathrm{Vol}(R_{d-1})$. It is here that we see the first hints of a holographic description, as entropy is no longer an extensive quantity, in a system with gravitational degrees of freedom.

If one were to treat an R_{d-1} QFT on a lattice with $d-1$ spatial dimensions and spatial extent R, with spacing ϵ to serve as a UV cutoff, the total number of associated degrees of freedom, N_γ^{QFT} of the QFT, with γ degrees of freedom per lattice scales as,

$$N_\gamma^{QFT} = \left(\frac{R}{\epsilon}\right)^{d-1} \gamma \tag{1.10}$$

γ which is also referred to as the central charge characterizes CFTs. For instance $SU(N)$ gauge CFTs have $\gamma \sim N^2$.

The holographic principle states that given a closed surface in spacetime enclosing a quantum gravitational system, all information contained in the interior of the surface can be holographically projected onto the surface. Furthemore, the gravitational theory governing the bulk physics can be described by a gauge field theory on the boundary surface. This taken together with the Bekenstein-Hawking formula suggests that the number of degrees of freedom contained in a certain region equals the maximum entropy where A_H can be reinterpreted as the area of the region at boundary of AdS in d spatial dimensions.

Comparing (1.10) and (1.9), given that $A_H = \left(\frac{RL}{\epsilon}\right)^{d-1}$ we have,

$$\gamma = \frac{1}{4}\left(\frac{L}{l_p}\right)^{d-1} \tag{1.11}$$

A classical gravity dual to the CFT exists in the limit of large γ which is precisely why AdS/CFT is formulated in the context of large N for $SU(N)$ gauge theories.

A theory is regarded to be classical when the coefficient multiplying its action is large. In this case the path integral is dominated by a saddle point. The action of a gravitational theory in the AdS_d spacetime of radius L, contains a factor L^{d-1}/G. As the Planck length $l_p \propto G^{d+2}$, we conclude that the classical gravity theory is reliable if, $\gamma \gg 1$ which happens when the AdS radius is large in Planck units. Thus, a QFT has a classical gravity dual when γ is large, or equivalently if there is a large number of degrees of freedom per unit volume or a large number of species (which corresponds to large N for $SU(N)$ gauge theories).

The prototypical example of the correspondence was studied in the context of N coincident D3 branes in String theory. More precisely, type IIB string theory in $AdS_5 \times S^5$ is dual to 4 dimensional $\mathcal{N} = 4$ supersymmetric Yang Mills gauge theory (SYM) with gauge group SU(N) and coupling constant g_{SYM} which is a conformal field theory. This duality holds for all values of N and coupling constants, however it is commonly studied in the limit of large N and finite but small string coupling constant where, the gravity side reduces to classical type IIB supergravity which can lending itself to a perturbative analysis but the gauge theory (SYM) becomes strongly coupled and can not treated perturbatively. This is why AdS/ CFT offers a powerful window into the study of strongly coupled field theories. There is a one–to–one correspondence between the symmetries, scales, degrees of freedom and dynamics of the two theories for which we refer the astute reader to [42] as it is beyond the scope of this thesis.

Since at its heart, AdS/CFT is a correspondence between weakly/strongly coupled theories, we will conclude our digression with a simple illustration of the black hole entropy correspondence on both sides of the theory.

The entropy density, s, of an AdS_d black hole with Hawking temperature T, can be computed from the Bekenstein-Hawking relation and is found to be,

$$s = \frac{A_H}{4G_d} = \frac{1}{4G_d}\left(\frac{4\pi}{d-1}\right)^{d-2} L^{d-2}\, T^{d-2} \tag{1.12}$$

This in terms of the QFT central charge γ can be expressed as,

$$s = \left(\frac{4\pi}{d-1}\right)^{d-2} \gamma\, T^{d-2} \tag{1.13}$$

In the case of $\mathcal{N} = 4$ SYM, we take $d = 5$ and $\gamma = N^2/2\pi$ and the entropy density is given as,

$$s_{black\,hole} = \frac{\pi^2}{2} N^2 T^3 \tag{1.14}$$

From the expression of the entropy density in (1.14) we can obtain the value of the pressure related to the entropy by $s = \frac{\partial p}{\partial T}$,

$$p = \frac{\pi^2}{8} N^2 T^4 \tag{1.15}$$

Hence from the first law of thermodynamics, $\mathcal{E} = -p + Ts$, where the energy density $\mathcal{E}$ is,

$$\mathcal{E} = \frac{3\pi^2}{8} N^2 T^4 \tag{1.16}$$

Having obtained the values of s, p and $\mathcal{E}$ in the strong coupling limit, let us consider a gas of non-interacting massless relativistic bosons and fermions which corresponds to the weak coupling limit. The partition function in the canonical ensemble for bosons and fermions respectively is,

$$\frac{\log Z_b}{V_3} = \frac{\pi^2}{90} T^3 \tag{1.17}$$

and,

$$\frac{\log Z_f}{V_3} = \frac{7\pi^2}{720} T^3 \tag{1.18}$$

The entropy density is therefore,

$$s = \frac{\partial}{\partial T}\left[T \frac{\log Z}{V_3}\right] = 4 \frac{\log Z}{V_3} \tag{1.19}$$

It follows that,

$$s_b = \frac{2\pi^2}{45} T^3 \tag{1.20}$$

$$s_f = \frac{7\pi^2}{180} T^3 \tag{1.21}$$

In $\mathcal{N} = 4$ SYM there are 2 gauge bosons and 6 scalar fields which brings the total boson number to $8N^2$ while the number of fermions corresponding to 4 Weyl Spinors is $8N^2$ as well due to the supersymmetric nature of the theory.

Therefore, the total entropy density s_{gas} of $\mathcal{N} = 4$ SYM when the coupling constant is zero is,

$$s_{gas} = 8N^2 \left[\frac{2\pi^2}{45} + \frac{7\pi^2}{180}\right] T^3 = \frac{2\pi^2}{3} N^2 T^3 \tag{1.22}$$

We immediately observe that the entropy for the ideal gas is related to the black hole entropy as follows,

$$s_{black\,hole} = \frac{3}{4} s_{gas} \tag{1.23}$$

A similar analysis calculation can be made for p and $\mathcal{E}$ which demonstrates that the AdS/CFT correspondence predicts that the values of s, p and ϵ at infinite coupling differ from their values at zero coupling by a multiplicative factor 3/4. These reductions of the entropy, pressure and energy density as the coupling is increased are in very good agreement with the results obtained in lattice simulations for different gauge theories [43].

While AdS/CFT consists of many conjectures [42] that are yet to be experimentally verified, they offer a window into the properties of candidate quantum gravity theories. CFTs themselves are better understood and are routinely discussed in condensed matter physics. Observables on both sides of the theory are translated by a dictionary mapping. For instance, the spin 2 generator of translational symmetry is mapped to the metric tensor, CFT scalars to scalar fields gravitating in the bulk with a correspondence between their respective correlation functions [42]. The simplest example is that of a thermal state on the CFT side which is mapped to a black hole in AdS where the thermal entropy of the CFT state corresponds to the Bekenstein entropy of the black hole.

A natural line of inquiry follows from attempting to relate the interior of black holes to their CFT state. In particular, it is well known that in the interior of an eternal black hole space and time invert roles. Subsequently, just as the way time flows forward in the exterior of a black hole its interior region must continue growing. More precisely, by this growth of the interior, we mean that the length of a spacelike curve at a fixed interior radius grows towards the singularity. Proponents of AdS/CFT including Susskind have advocated that the growth of the interior region (a gauge invariant observable) must be captured by a corresponding CFT quantity, which eventually was found to be best represented by the quantum state complexity [44–46]. Interestingly, the complexity continues to grow even after the black hole has reached thermal equilibrium.

In Ch.4, we will consider a particular application of the complexity theory of gates in the context the AdS/CFT correspondence to provide new insights on GR effects in rotating black holes. In particular it is interesting to see how insights from quantum theory can change our viewpoint on the pathologies that emerge in GR such as singularities in rotating black holes and the related cosmic censorship conjecture [47].

1.5 Events

At an experiential level, time is one of the most intuitive physical concepts. However, its precise characterisation is still a very much an open problem in the foundations of physics, in particular in quantum theory [48–52]. Relativity introduces the notion of events as coordinates in spacetime where every observer has their own clock. The transformations between different observers and reference frames also transforms clock time itself, which suggests that time behaves dynamically. However, in quantum mechanics, time is an independent parameter with respect to which the Schrodinger evolution of quantum systems takes place.

In the description of multi-systems, the quantum state of each subsystem lives in a separate Hilbert space (e.g. $\rho_i \in \mathcal{H}_i$) and the full state description, ρ is achieved through a tensor product such that $\rho \in \mathcal{H} = \bigotimes_i \mathcal{H}_i$. The tensor product indicates that these systems can be treated separately while the joint state description also exists and is well defined at each instant of time. An equivalent notion does not generalize to state descriptions over an extended period of time due to the lack of a tensor product space. In fact one would expect such notions to generalise over a spatio-temporal tensor product.

To resolve this conflict, in Ch.5, we extend the classical concept of an event to the quantum domain by defining an event as a transfer of information between physical systems. This allows us to describe spacelike and timelike (causally connected) events on an equal footing by utilizing detectors coupled to timers that store information about a given system and the moment of measurement.

This approach has some semblances to the Page Wootters picture [53], where time emerges from a stationary universe. Here we recover the Schrodinger equation for a system, from the correlation between that system $\mathcal{S}$ and the rest of the universe $\mathcal{R}$ [54]. In this case, the environment serves as the system's clock and since the clock does not interact with the system, $\mathcal{S}$ evolves with respect to a variable β that labels the eigenvalues of a suitable clock observable. This motivates us to develop a formalism of events that incorporates measurement records. In fact the distinguishable states of the record are responsible for the emergence of time.

By tracing out the system and focusing on the detectors' and timers' states, events are represented by a tensor product structure. Furthermore, including a time register gives rise to a temporal superposition analogous to the familiar spatial superposition in quantum mechanics. We verify that the presence of coherence can ensure a causal connection between events. We also propose a causal correlation function involving the detection times to characterize the type of events. Our formalism allows us to extend quantum information concepts to spacelike and timelike events. For instance, similar to measurements on spatially entangled systems, we observe that in the limit of "instantaneous" measurements, a deterministic relationship emerges between causally connected events; i.e. observing the state of one of the systems (in our case, knowing a previous event), enables us to learn precisely the state of the other system (we delineate a later event).

1.6 Way Forward

The issues discussed in the previous sections must not be treated in isolation. Several approaches to quantum gravity rely heavily on novel theoretical insights alone. Approaches to quantum gravity must bridge the gap between theory and observation to make falsifiable predictions and to guarantee consistency with all observed phenomena. Experimental proposals at the frontiers of quantum information theory and gravity aim to do precisely this Ch.2, 3. A complementary mode of investigation is to examine the conflicts between classical GR and QM in greater detail to gain insight into the ways conventional pathologies can be resolved Ch.4. Finally, establishing generic notions such as that of an event, can be readily carried forward to any theoretical framework of quantum gravity Ch.5.

So, the good news is that all seems fine with quantum gravity in the standard Heisenberg field theoretic approach. We can use the lowest order to experimentally confirm that gravity must be quantum ... The bad news might be that we may never be able to test most of them. Unless, of course, some observations from the early universe, or extreme astronomical objects like black holes and neutron stars come to rescue.

— Vlatko Vedral *Are There Any Real Problems With Quantum Gravity?*

2

Signatures from Superpositions of Primordial Massive Particles

Contents

This chapter is based on a paper written in collaboration with Gowtham Neppoleon, Yi Wang and Vlatko Vedral. The author of this thesis computed the decoherence time of a primordial massive superposition and investigated the observational implications.

2.1 Introduction

A first step in the search of quantum effects in the early universe is to investigate the relics left behind by primordial processes i.e., primordial massive particles. Examples of primordial massive particles include dark matter candidates that may be created in the reheating era, or primordial black holes (PBHs) that are sourced by primordial fluctuations that re-enter the horizon. In the radiation dominated era of the universe these primordial particles interact with the photon background leading to decoherence in their positional degree of freedom. This leads to the interesting question of whether such primordial particles can persist in a superposition up to current times and their associated quantum signatures. In ordinary macroscopic systems often seen in the laboratory, interactions with the surrounding environment, such as interactions with matter or spurious electromagnetic effects lead to decoherence. The environmental degrees of freedom effectively perform a measurement on the sub system of interest. The large number of degrees of freedom of the environments accelerates the process of decoherence often occurring on timescales less than seconds. In this chapter we will compute the decoherence timescale associated with a superposed state of a primordial massive particle and the range of masses for which the superposition persists to present time.

Recent literature has investigated the gravitational decoherence of light dark-matter for well-chosen initial states, through the study of scattering processes with the environment, both in a Newtonian [55] and general relativistic context [56, 57]. While Ref. [56] has considered decoherence by a single scattering particle in terms of the decay of the system's off-diagonal density matrix elements, with a special focus of light dark matter with coherent oscillations, we consider heavy dark matter and decoherence due to a thermal environment of particles interacting with the system through gravity. This analysis is performed for an arbitrary initial state of the system. Furthermore, we investigate the implications of a coherent massive superposition for the quantum nature of gravity. In particular, we outline observational consequences relating to interference patterns produced by such superpositions, quantum gravitational bound states, and entanglement witnesses.

2.2 Coherence of the Superposition

Primordial massive particles are sourced as early as during reheating and propagate to the radiation and matter dominated universe up to present times. In the following, we will consider decoherence due to photons as a representative example of the interactions that persist during the early universe. The massive particle is modeled by a scalar field χ which interacts with the photon bath, described by the Lagrangian,

$$\mathcal{L} = \frac{1}{2}\partial_\mu \chi^\dagger(\mathbf{x}) \cdot \partial^\mu \chi(\mathbf{x}) - \frac{1}{2}M^2\chi^2 + \frac{1}{4}F^{\mu\nu}(\mathbf{x})F_{\mu\nu}(\mathbf{x}) - V, \tag{2.1}$$

where M is the mass of the massive particle and $F_{\mu\nu}$ is the electromagnetic stress energy tensor. Note that we have employed natural units, $\hbar = c = G = 1$. In these units, the gravitational potential of interaction, V between these fields is,

$$V = \int \mathrm{d}^3\mathbf{x}\ \mathrm{d}^3\mathbf{x}'\frac{M}{|\mathbf{x} - \mathbf{x}'|}\chi^\dagger(\mathbf{x})\chi(\mathbf{x})\,\varrho(\mathbf{x}'). \tag{2.2}$$

Here, $\varrho(\mathbf{x})$ is the photon energy density at $\mathbf{x}$ which is defined in terms of the energy of single photon, $\epsilon_\mathbf{k} = k$ as,

$$\varrho(\mathbf{x}) = \int \mathrm{d}^3\mathbf{k}\ \mathrm{e}^{\mathrm{i}\,\mathbf{k}\cdot\mathbf{x}}\,\epsilon_\mathbf{k}\, b^\dagger_\mathbf{k} b_\mathbf{k}. \tag{2.3}$$

In Eq.(2.2) we have employed the Newtonian approximation as opposed to a weak field GR approach. However, the difference due to this is expected to be an order 1 deviation from our result for the decoherence time scales which we calculate here. As we are interested in an order of magnitude comparison of this time to the age of the universe as a preliminary illustration, the Newtonian approximation would suffice. Secondly, while decoherence has been studied extensively in QED, mostly in the context of quantum optics, these studies focus either on the absorption and emission of photons in a cavity, or interactions with vacuum fluctuations, as opposed to their gravitational effect on a scalar particle.

The decoherence of the state of the massive particle is studied in Appendix B in terms of the decay of $\mathrm{tr}\,\rho^2$ where ρ is its reduced density matrix. For brevity, we begin by considering the Fourier transformed interaction Hamiltonian,

$$H_{\mathrm{int}} = \int \mathrm{d}^3\mathbf{p}\ \mathrm{d}^3\mathbf{k}\ \nu(\mathbf{k})\,\epsilon_\mathbf{k}\, a^\dagger_\mathbf{p} a_{\mathbf{p}+\mathbf{k}}\, b^\dagger_\mathbf{k} b_\mathbf{k}, \tag{2.4}$$

where $\nu(k) = M/\pi k^2$ is the Fourier transform of gravitational potential $\phi(\mathbf{x}) = M/|\mathbf{x}|$, derived as follows,

$$\begin{aligned}\nu(\mathbf{k}) &= \frac{1}{2\pi}\int \mathrm{d}^3\mathbf{x}\ \mathrm{e}^{-\,\mathrm{i}\,\mathbf{k}\cdot\mathbf{x}}\,\phi(\mathbf{x})\\ &= \frac{M}{2\pi}\int_0^\infty \mathrm{d}x\ x\,\frac{\sin kx}{kx}.\end{aligned} \tag{2.5}$$

We see that this integral is oscillatory and thus does not converge. Hence, we modify the potential to include a Yukawa term $\mathrm{e}^{-\lambda x}$ for $\lambda > 0$ and set it to 0 after integration. That is,

$$\phi(\mathbf{x}) = \frac{M}{x}\,\mathrm{e}^{-\lambda x}. \tag{2.6}$$

Then,

$$\begin{aligned} \nu(\mathbf{k}) &= \frac{M}{2\pi}\int_0^\infty \mathrm{d}x\; x \int_{-1}^{1} \mathrm{d}t\; \mathrm{e}^{-\,\mathrm{i}\,kxt-\lambda x} \\ &= \frac{M}{\pi}\,\frac{1}{k^2+\lambda^2} \overset{\lambda\to 0}{=} \frac{M}{\pi k^2}, \end{aligned} \tag{2.7}$$

A resemblance can immediately been seen to scattering processes in Eq.(2.4). Let ρ_T be the density matrix of the system and environment combined, and $\rho_\mathcal{E}$ be the reduced density matrix of the environment. The unitary evolution of ρ_T under H_{int} interaction is given by, $\rho_T(t) = \exp\left(-\,\mathrm{i}\,Ht\right)\rho_T(0)\,\exp\left(\mathrm{i}\,Ht\right)$. Since we are interested in the description of the primordial particle (in terms of its reduced density matrix ρ), we trace out the photon environment and obtain the well-known Lindblad form for the master equation [58],

$$\begin{aligned} \frac{\mathrm{d}\rho}{\mathrm{d}t}\,\Delta t = \mathrm{i}[\mathrm{tr}_\mathcal{E}(U_1\rho_\mathcal{E}) - \mathrm{tr}_\mathcal{E}(B\rho_\mathcal{E}),\rho]+ \\ \mathrm{tr}_\mathcal{E}\left(U_1\rho_T U_1 - \frac{1}{2}U_1^2\rho_T - \frac{1}{2}\rho_T U_1^2\right), \end{aligned} \tag{2.8}$$

where $U_1 = -\int_{-\infty}^{\infty}\mathrm{d}t\,H_{\text{int}}(t)$ is the time evolution operator, and B is some Hermitian operator which drops out in the one particle sector. Here, Δt is the timescale over which we study the evolution of ρ. This timescale is small compared to the evolution of the system but large compared to the evolution of the environment. The right hand side of this equation is also proportional to Δt, details of which can be found in Ref. [58].

We now represent the density matrix as the function $\rho(\mathbf{k},\mathbf{k}') := \langle\mathbf{k}|\rho|\mathbf{k}'\rangle$, and compute the rate of change of $\mathrm{tr}\,\rho^2$ as an indicator of the purity of the state. We obtain,

$$\frac{\mathrm{d}(\mathrm{tr}\,\rho^2)}{\mathrm{d}t} = -\frac{1}{\pi}\int \mathrm{d}^3\mathbf{q}\;|\nu(q)|^2\,\epsilon_\mathbf{q}^2\,n_\mathbf{q}(n_\mathbf{q}+1)\,\Lambda(q), \tag{2.9}$$

where $\Lambda(q)$ is defined by,

$$\Lambda(q) := \mathrm{tr}\,\rho^2 - \mathrm{Re}\int \mathrm{d}^3\mathbf{k}\ \mathrm{d}^3\mathbf{s}\,\rho(\mathbf{k},\mathbf{s})\rho(\mathbf{s}-q\,\hat{z},\mathbf{k}-q\,\hat{z}). \tag{2.10}$$

Having shown that $\Lambda(q) \in [0, \mathrm{tr}\,\rho^2]$, we obtain,

$$\frac{\mathrm{d}(\mathrm{tr}\,\rho^2)}{\mathrm{d}t} = -\Gamma\,\mathrm{tr}\,\rho^2, \tag{2.11}$$

where the decay rate $\Gamma \in [0, \Gamma_0]$, with,

$$\Gamma_0 = \frac{4M^2}{\pi^2}\int_0^\infty \frac{\mathrm{d}q}{q^2}\epsilon_{\mathbf{q}}^2 n_{\mathbf{q}}(n_{\mathbf{q}}+1). \tag{2.12}$$

Further details of this calculation can be found in Appendix B. Setting $\epsilon_{\mathbf{q}} = q$, and $n_{\mathbf{q}}$ to be the number density corresponding to the Planck distribution, the integral can be explicitly evaluated to yield,

$$\Gamma_0 = \left[\left(\frac{16}{15\pi^2} - \frac{96\zeta(5)}{\pi^6}\right)\frac{1}{\beta^5} + \frac{8\zeta(3)}{\pi^4}\frac{1}{\beta^3}\right]M^2. \tag{2.13}$$

where $\zeta(x)$ is the Riemann zeta function. Thus, we have derived an upper bound on the rate of decoherence of the massive particle due to the photons that scales as the squared mass. Note that our approach of using $\mathrm{tr}\,\rho^2$ to quantify purity is basis-independent, although we have used the momentum basis to perform intermediate calculations for simplicity.

We neglect the decoherence due to baryonic matter in our estimate. While, the source of gravitational decoherence comes from both the background density of matter and radiation, we argue that radiation is the main source of decoherence. This is trivial in the radiation dominated era. In the matter dominated era, the matter has already formed localised distributions such as stars and galaxies. While the gravitational field due to these large structures could potentially become strong, it is homogeneous in the small spatial region around the particle. This homogeneous gravitational field is equivalent to acceleration by the equivalence principle and does not contribute to any significant decoherence.

That being said, the result in Eq.(2.12) is also generally applicable to decoherence caused by the baryonic matter with $\epsilon_{\mathbf{q}} = m^2$ and $n_{\mathbf{q}}$ taken to be the Fermi-Dirac distribution $(1+\exp\beta q^2/2m)^{-1}$ in the non-relativistic limit. However, in this case

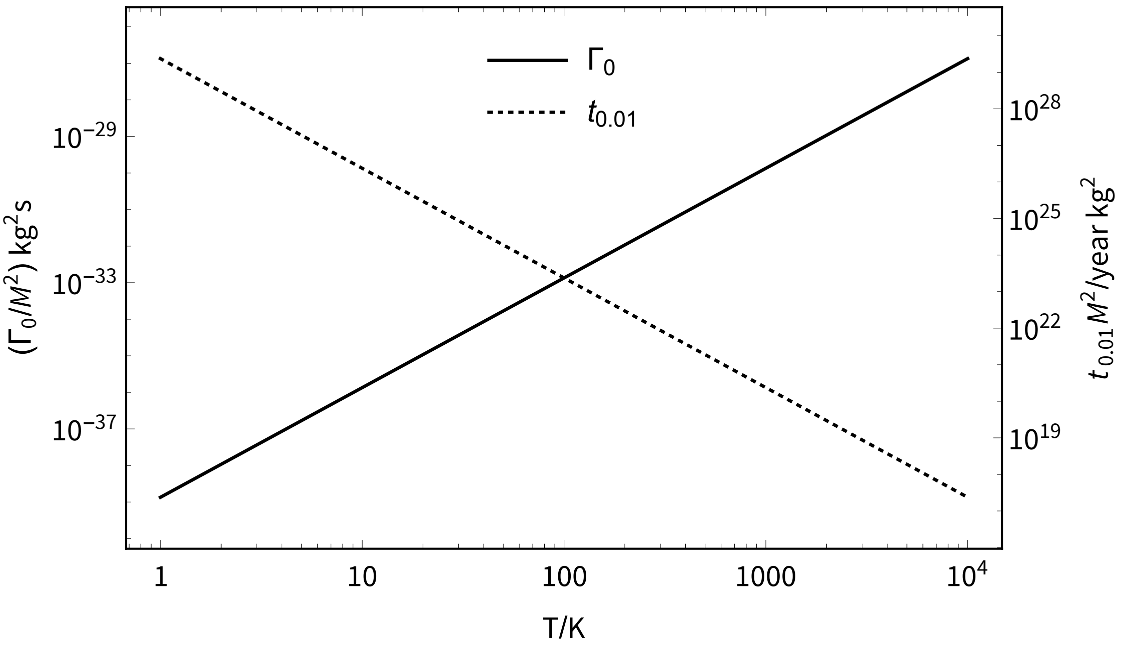

Figure 2.1: Plots of the maximum decoherence rate Γ_0 and time taken for 1% decoherence due to background photons $t_{0.01}$ of a 1 kg primordial particle as a function of the temperature of the universe. Note that Γ_0 scales as M^2 while $t_{0.01}$ scales as M^{-2}.

the integrand in Eq.(2.12) is $\propto q^{-2}$ in the IR limit, and hence the integral diverges. We resolve this issue by using a better upper bound than $\operatorname{tr}\rho^2$ in the derivation of Eq.(2.12). We show in Appendix B that indeed in the IR limit, this introduces a factor $\propto q^2$ that alleviates the divergence. It must be noted that this argument also holds for photons and will yield a better bound Γ_0 in place of Eq.(2.13).

We observe in Figure 2.1 that for a range of temperatures spanning the current temperature (2.7 K) of the universe to that at the time of recombination (3000 K) the decoherence rate is mild enough such that even a single percentage drop in purity (the corresponding time taken is $t_{0.01} = -\ln(0.99)/\Gamma_0$) occurs at timescales several orders greater than the age of the universe for $M = 1$kg. Considering the M^{-2} dependence of this time, we can safely neglect decoherence for particles at a mass scale of order 10^7 kg or lower. While we can extend our discussion to more massive candidates of dark matter, such as Massive Compact Halo Objects (MACHOs) [59–61], they decohere rather quickly as calculated above. However, it is still possible to observe effects of quantum spread as their localization in position can only be of order of the wavelength of the CMB photons.

Similarly, we also compute the minimum spread associated with a primordial particle in the time when decoherence is negligible. For demonstration, we consider an initial Gaussian state of the primordial particle with initial spread s_0. After time t the spread of the wavefunction is,

$$s(t) = \sqrt{\frac{s_0^4 + (\hbar t/m)^2}{s_0^2}}. \tag{2.14}$$

This can be minimized in s_0 to give the minimum value of $s(t)$ to be,

$$s_{\min}(t) = \sqrt{\frac{2\hbar t}{m}}. \tag{2.15}$$

For instance, for a primordial particle of mass 10^{11} GeV formed during early universe, $t \approx 14$ billion years and we get the minimum spread today as $s_{\min} \approx 0.72\,\mathrm{m}$. Note that this is only the minimal wave function spread considering the uncertainty principle. The initial condition of the particle may allow more dramatic spread of the wave function, depending on the production mechanism of the primordial particle.

2.3 Observable Consequences

Having shown that a class of massive particles do not decohere significantly since their formation, through the interaction with photons in the radiation dominated universe, we will discuss how a superposition of massive particles and its QG effects can be observed. We will consider three classes of observations — (i) Experiments that distinguish between classical spreads and quantum superpositions of the stress energy tensor, (ii) stationary states and transitions, and (iii) signatures of entanglement.

The quantum nature of gravity, unlike standard field theory, comprises two distinct aspects — whether the metric can exist in a superposition, and whether there is a quantized force carrier for gravity – the graviton. Of the three proposed signatures, the first allows us to probe the quantum nature of the metric. The second signature explores the existence of atom-like bound states for superpositions with a discrete absorption spectrum hinting at the existence of gravitons. Finally, detecting entanglement between the components of the bipartite system interacting gravitationally demonstrates that the gravitational field mediating the interaction is quantum.

2.3.1 Superposition Effects

One of the key questions we wish to answer about the nature of quantum gravity is, how superpositions of matter affect the construction of the stress-energy tensor and in turn affect the associated gravitational field. In a semi-classical treatment of QFT in curved space time, one might consider a background value of the stress energy tensor which is in actuality an expectation value over possible quantum states of the universe, effectively treating the stress energy tensor classically. Alternatively, in a fully quantum approach [62], one may consider a many-worlds scenario – one for each distribution of matter and all of them superposed linearly.

As an illustration consider the following – It is well known that massive objects distort the path of passing light around them giving rise to gravitational lensing. We investigate how this phenomenon will occur with a massive object (such as primordial black hole (PBH) or a heavy particle) with a spread in wave function. Consider a detector on Earth that measures the angular intensity $I(\theta, \phi)$ of radiation coming from different azimuths θ and declinations ϕ. Let $T_{\mu\nu}$ be the stress energy tensor associated with the superposed massive object with its center described by a wavefunction $\psi(\mathbf{x})$, and let $\alpha(\theta, \phi, T_{\mu\nu})$ be the corresponding angular amplitude of radiation from a distant source, lensed by $T_{\mu\nu}$ and observed on Earth in that direction. Then, we may compute a semi-classical average $T_{\mu\nu}$ defined by,

$$\langle T_{\mu\nu}(\mathbf{x})\rangle = \int \mathrm{d}^3\mathbf{x}'|\psi(\mathbf{x}')|^2\tau_{\mu\nu}(\mathbf{x}-\mathbf{x}'), \tag{2.16}$$

where $\tau_{\mu\nu}(\mathbf{x})$ is the the energy momentum tensor at $\mathbf{x}$ of the massive object centered at the origin. In the semi-classical picture, we will expect to observe a lensing pattern due to this expectation value, $\langle T_{\mu\nu}\rangle$ whose intensity I_{cl} is given by,

$$I_{\mathrm{cl}}(\theta, \phi) = \left|\alpha\Big(\theta, \phi, \langle T_{\mu\nu}\rangle\Big)\right|^2. \tag{2.17}$$

However, we can alternatively consider a coherent sum over the amplitudes given by,

$$I_{\mathrm{qg}}(\theta, \phi) = \left|\int \mathrm{d}^3\mathbf{x}'\psi(\mathbf{x}')\alpha(\theta, \phi, S_{\mathbf{x}'}\tau_{\mu\nu})\right|^2, \tag{2.18}$$

where $S_{\mathbf{x}'}\tau_{\mu\nu}$ is the shifted energy momentum tensor, $S_{\mathbf{x}'}\tau_{\mu\nu}(\mathbf{x}) = \tau_{\mu\nu}(\mathbf{x}+\mathbf{x}')$. We will expect these intensities I_{cl} and I_{qg} to be qualitatively different which would in turn be an observable signature. $I_{\rm cl}$ would be equivalent to the lensing pattern produced by an extended object, while $I_{\rm qg}$ would show the emergence of a diffraction pattern corresponding to the interference of Einstein rings generated by each individual branch of the PBH superposition.

This effect resembles Feynman's thought experiment [63] to witness the quantum effects of gravitational field through a double slit experiment with single particles in presence of gravitational field. It has been argued that this does not prove the existence of non-commuting complementary observables of the gravitational field [11] and thus does not prove that the gravitational field is quantum in the quantum information theoretic sense. However, in this work, we have demonstrated that a cosmological massive particle can persist in a superposition. Thus, in the case of a coherent sum over amplitudes in Eq.(2.18), we are adding geodesics corresponding to different stress energy tensors, rather than only considering the effect of gravitational field on the phase. While, this is still not conclusive evidence of quantum nature in the quantum information theoretic sense, we expect the interference pattern to be more exotic than a simple double slit pattern that could be reasonably produced by an alternative classical mechanism. A more rigorous signature of the quantum nature of the gravitational field could be constructed by considering the role of entanglement, as discussed subsequently under entanglement effects.

2.3.2 Stationary States and Transitions

A quantum system of heavy massive particles, possibly belonging to the dark matter sector can now exist in a quantum bound state [64, 65]. As an illustration, consider a pair of such particles of mass M bound by mutual gravitation. We expect that this system would not emit gravitational waves as long as it is in a stationary quantum state. However, similar to atoms, this system would absorb and emit gravitational waves during transitions.

First, we compute the spectrum of energies by quantizing the total angular momentum similar to the Bohr atom. The total energy of a state with principal quantum number n is,

$$E_n = -\frac{G^2M^5}{4\hbar^2 n^2} = -1.84 \times 10^{-32} \left(\frac{Mc^2}{10^{11}\,\mathrm{GeV}}\right)^5 \frac{1}{n^2}\ \mathrm{J}. \tag{2.19}$$

The corresponding orbit radius from the common center of mass is,

$$r_n = \frac{\hbar^2 n^2}{GM^3} = 29.1 \left(\frac{10^{11}\,\mathrm{GeV}}{Mc^2}\right)^3 n^2\ \mathrm{pm}. \tag{2.20}$$

Note that the radius of this orbit is much smaller than the minimal uncertainty in position of a 10^{11} GeV mass, calculated using Eq.(2.15). Similarly, the velocity of the particle in orbit is given by,

$$v_n = \frac{Gm^2}{2n\hbar} = 10.1 \left(\frac{Mc^2}{10^{11}\,\mathrm{GeV}}\right)^2 \frac{1}{n}\ (\mathrm{nm/s}). \tag{2.21}$$

Note that this approximation is only valid when $v_n \ll c$, or correspondingly $M \ll 10^{19}\,\mathrm{GeV/c^2}$, which is expected generally of dark matter particles. Imagine the scenario when a gravitational wave passes through a cloud of these bound states. As the spectrum of energies is discrete, we would expect to see absorption lines similar to the Hydrogen atom spectrum. The frequencies of such lines can be expressed in terms of the principal quantum numbers of initial and final states n and m as,

$$\begin{aligned}\nu_{nm} &= \frac{E_0}{\hbar}\left(\frac{1}{m^2} - \frac{1}{n^2}\right) \\ &= 174 \left(\frac{Mc^2}{10^{11}\,\mathrm{GeV}}\right)^5 \left(\frac{1}{m^2} - \frac{1}{n^2}\right) \mathrm{Hz}.\end{aligned} \tag{2.22}$$

The gravitational cross section for absorption has been calculated to be of the order l_p^2 [64]. Although this is very small, we can consider the augmenting effect of dark matter prevalent over astronomical distances. While we may not observe very dark lines like the EM atoms, we could expect dips in the GW spectrum. Furthermore, this effect will depend on whether we can get a small enough line width, corresponding to a large intensity drop at specific frequencies. Despite the significant observational challenge this poses, it is worthwhile to investigate this possibility thoroughly as it is among the few known direct indicators of the graviton.

2.3.3 Entanglement Effects

Having shown that a primordial massive particle can exist in a coherent quantum state, it is natural to expect the emergence of entanglement in superpositions of composite systems. For instance, similar to the entanglement between the proton and electron of the hydrogen atom, constituent primordial particles of binary systems will also be entangled.

The entangled pair would undergo interference which is markedly different from the unentangled case [11, 66]. However, it remains a challenge to identify the complementary observables [67–69] that need to be measured on the subsystems to construct an entanglement witness. We also remark that the transfer of entanglement effects between the primordial entangled pair and other interacting species that scatter off the pair or interact gravitationally with it could be witnessed through the correlation functions of the scattered particles. We emphasize the importance of this effect as the creation of entanglement between particles whose interaction is mediated solely by gravity is a direct witness of the quantum nature of the gravitational field [11, 66].

Generalizing the above arguments to many body systems, one could consider a massive condensate of primordial particles, similar to axion stars. A class of witnesses predicated on the non-Gaussianity [70] of the state can be used as a probe of the quantum nature of the self-gravitational effects.

Furthermore, we can consider a stationary state of two particles as discussed earlier. We may assume that the total state of the two-particle system is pure, which is reasonable given that there is limited decoherence from the environment. As an entanglement witness, we may measure the $\operatorname{tr}\rho_1^2$, where ρ_1 is the reduced density matrix of one of the particles (labelled as 1). We can then conclude that the particles are entangled if the value of $\operatorname{tr}\rho_1^2$ deviates significantly from unity.

2.4 Discussion

The early universe forms a natural test bed for QG phenomena. A promising place to look for signatures is in primordial massive particles that include relics generated from the inflationary universe during reheating and persist onto the radiation and matter dominated eras. Since primordial particles occur at various mass scales we have chosen the representative example of 10^7 kg whose decoherence timescale scales as M^2. This further yields an upper bound of on the mass of primordial particles that we expect to survive in a coherent state till present time upon interacting with the various constituents of the universe across its evolutionary history. This is significant from the standpoint of quantum gravity where massive superpositions are expected to get entangled to the gravitational field probing its quantum nature. We remark here that while gravitationally induced state reduction can occur due to a conflict between the superposition principle of QM and equivalence principle of GR, the timescales involved are much larger than the decoherence timescales we consider here for the range of masses discussed.

Our work provides a natural foray into the foundations of quantum gravity and helps ascertain the necessary postulates expected in candidate theories of quantum gravity. There are a host of issues that deserve further consideration. In particular the difference between semiclassical and quantum gravity can be explored through the discrepancy between the interference patterns I_{cl} and I_{qg} introduced in Eq.(2.17) and Eq.(2.18) which warrant a more involved calculation. We have discussed the possibility of absorption lines due to gravitationally bound states which deserve further investigation. For instance, a more realistic resonant absorption model can be setup for the absorption lines and the detailed signatures that ensue can be explored. If the constituent particles have mass of order 10^{11} GeV, the dark lines will lie in the observable frequency range of the LIGO. While the gravitational cross-section for the absorption of radiation is small (estimated to be of the order l_p^2 [71]), the observability would depend on proximity and concentration of dark matter clouds. If observed, this effect could constitute a direct evidence of the graviton. In our future work, we aim for a complete treatment of this problem involving, assessing the spatial distribution of dark matter, the line widths of the transitions and the location of the source of gravitational waves. In addition, we would also consider bound systems consisting of more than two particles. Overall, these studies will provide an estimate of the sensitivities required for various detection methods employed to observe this effect.

But aside from that possibility [that quantum mechanics fails], if you believe in quantum mechanics up to any level then you have to believe in gravitational quantization in order to describe this experiment.

— Richard Feynman, *Chapel Hill Conference*

3

Non-Gaussianity as a Signature of Quantum Gravity

Contents

This chapter is based on a paper written in collaboration with Richard Howl, Vlatko Vedral, Devang Naik, Marios Christodoulou and Carlo Rovelli. The author of this thesis worked on the theoretical characterisation of Non-Gaussianity as a witness of the quantum effects of gravitational self interaction, both in condensates and potentially the early universe.

3.1 Introduction

As early as the Chapel hill conference of 1957, Feynman proposed a thought experiment to witness the quantum nature of gravity. This involved the interference of a massive object that was prepared in a superposition of two different positions and interacting with the background gravitational field. However, it is well known now, that the phase differences required to witness interference effects can be induced by an entirely classical gravitational field as well such as the familiar gravitational redshift effect. In order to demonstrate the quantum nature of gravity it is necessary to show that the gravitational field itself can exist in a superposition. This principle of requiring two non-commuting observables motivated several entanglement based tests of QG including the BMV experiment.

An assumption frequently used in entanglement based witnesses is that classical gravity (CG) acts as a local operations and communication channel (LOCC) [68]. It follows then, that as a local classical-information mediator [11, 66], CG can never create entanglement. However, it is in theory possible that CG could cause two spatially separated quantum matter systems to directly couple with one another, invalidating the LOCC and classical-information mediator arguments and leading to entanglement generation in experiments. For instance, such direct CG interactions could be due to non-local effects associated with CG, or even quasi-local CG effects, such as tunnelling between two quantum matter systems.

An illustrative example was discussed in the previous chapters where, modes of a quantum field such as the inflaton could become entangled even in a classically expanding universe [72–74]. This motivates us to consider other approaches besides entanglement as a witness of QG [75, 76]. One such witness that we will develop further here is the creation of non-Gaussianity in the quantum field of matter, when we promote classical gravitational degrees of freedom to quantum operators.

Quantum information is encoded in discrete variables, such as qubits, or continuous variables, like the eigenstates of a harmonic oscillator. The continuous variable equivalent of encoding quantum information (CVQI), is generically applicable to quantum field theory where fields can be considered as collections of harmonic oscillators, thereby allowing us to analyse their information theoretic properties (such as entropy). Here we apply CVQI to QG, and show that a true signature of QG would be the creation of non-Gaussianity, a continuous-variable resource that is necessary for universal quantum computation [77]. Non-Gaussianity is

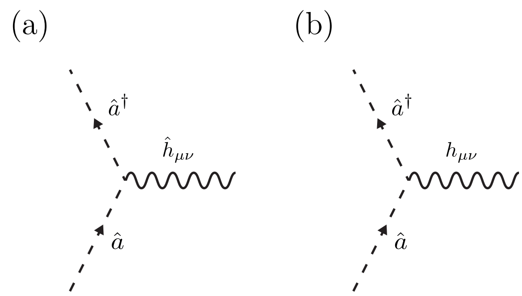

Figure 3.1: (a) Basic Feynman diagram for matter interacting with QG where matter emits a graviton, which is associated with $\hat{h}_{\mu\nu}$. For simplicity, we represent matter by a real scalar field such that $\hat{a}^\dagger$ and $\hat{a}$ are the creation and annihilation operators of matter. The interaction is then associated with three quantum operators and, therefore, can induce non-Gaussianity. (b) We can illustrate the analogous interaction between matter and classical gravity with a similar diagram except that now the gravitational leg represents a classical gravitational wave $h_{\mu\nu}$ rather than a graviton. Since this CG interaction is associated with just two quantum operators $\hat{a}^\dagger$ and $\hat{a}$, it cannot, in contrast to the QG interaction, induce non-Gaussianity. Note that, although these diagrams represent weak-field, perturbative gravitational interactions, the fact that CG cannot create non-Gaussianity also applies to the strong-field, non-perturbative regime of gravity, as shown in Section 3.2.

generated through non-quadratic quantum operators in the interaction Hamiltonian of quantum systems [78, 79] which in the context of gravity implies that only QG, compared to CG, can generate it (provided the usual suspects of quantum interactions such as electromagnetic effects are suppressed).

The simplest illustration of this effect is to consider the gravitational interaction between matter to be mediated by gravitons. While we do not delve into the properties of the graviton itself, it is representative of a perturbative weak field theory. As illustrated in Figure 3.1, the corresponding Feynman diagram contains three quantum operators and, therefore, induces non-Gaussianity. On the other hand, in CG, we consider an expectation value of the gravitational interaction that leaves a quadratic Hamiltonian, which preserves Gaussianity [80].

Yet another advantage of using non-Gaussianity as indicator is that unlike entanglement based witnesses that are reliant on LOCC or classical-information mediator arguments, it is not reliant on the non-existence of direct CG interactions. Therefore, as long as we are working in an experimental situation where non-gravitational quantum interactions can be neglected (just as in tests based on entanglement [11, 66, 68]), non-Gaussianity can be used as a signature of QG in experimental tests without the need for the additional assumption of there being no direct CG interactions [11, 66, 68]. A further advantage of a non-Gaussianity signature is that a single system can be non-Gaussian, allowing for tests of QG that are based on just a single rather than multi-partite system. We illustrate this with a table-top test of QG that uses a single Bose-Einstein condensate (BEC) in a single location.

In addition to being just a single quantum system without any spatial superposition, our experimental proposal also uses a type of quantum technology (BECs) for which certain massive quantum states have already been created [81, 82]. This is in contrast to proposals based on opto-mechanical setups where massive non-classical states have yet to be generated. BECs also offer a contrasting method to distinguish the QG signal from electromagnetic noise. As with previous table-top proposals, it is vital that we can attribute the searched for QG effect from the analogous effect that is generated through electromagnetic interactions. For the BMV this effect is entanglement, which electromagnetic as well as gravitational interactions will naturally generate, whereas, in the test proposed here this is non-Gaussianity, which electromagnetic interactions would also naturally generate since they are fundamentally quantum interactions. However, electromagnetic interactions (unlike gravity which couples to everything) can be screened out by exploiting Feshbach resonances that generically occur in BECs. Optical and magnetic Feshbach resonances can be used in BEC experiments to control the strength of the electromagnetic interactions between the atoms by the application of an external magnetic or optical field [83].

By completely suppressing the electromagnetic interactions without affecting the strength of the gravitational interactions, a non-Gaussian signal can be attributed to only to gravity. This method contrasts with that used in opto-mechanical proposals where the distance between micro-objects is increased to a level where gravitational interactions are greater than the electromagnetic van der Waals interactions. In that case, both the electromagnetic and gravitational interactions are suppressed by increasing the distance, whereas applying an external magnetic or optical field to a BEC only affects the former.

3.2 Non-Gaussianity as a Signature of Quantum Gravity

The Wigner function [84] is an equivalent representation of a quantum system like the density operator $\hat{\rho}$. The Wigner function can be regarded as a quasi-probability distribution over phase space, much in the same way probability distributions are used in classical statistical mechanics (canonical ensembles etc...). A key difference, however lies in the fact that the Wigner function can take on negative values which is an indicator that a system is quantum mechanical without an equivalent classical description.

An explicit example of the Wigner function construction can be seen in the following. For a free scalar field, the Hamiltonian can be written as a collection of quantum simple harmonic oscillators: $\hat{H} = \sum_k \hbar\omega_k[\hat{a}_k^\dagger \hat{a}_k + 1/2]$, where $\hat{a}_k^\dagger$ and $\hat{a}_k$ are creation and annihilation operators of mode k; ω_k is the angular frequency; and we have assumed a discrete mode spectrum for simplicity [85]. Furthermore, the standard quadrature operators that are position and momentum-like operators can be defined as follows, $\hat{x}_k := \hat{a}_k + \hat{a}_k^\dagger$ and $\hat{p}_k := i(\hat{a}_k^\dagger - \hat{a})$. These observables posess a continuous eigenspectra: $\hat{x}_k|x\rangle_k = x_k|x\rangle_k$ and $\hat{p}_k|p\rangle_k = p_k|p\rangle_k$. The eigenvalues, x_k and p_k, in turn span a continuous phase space which we encodes quantum information [80]. Configurations in the this phase space describe the entire quantum system. A similar approach can be extended to general bosonic and fermionic quantum fields [86]. For a field with one degree of freedom (single mode), the Wigner function is given by the following transformation,

$$W_{\hat{\rho}}(x,p) = \frac{1}{2\pi}\int dy\, e^{-iyp}\langle x+y|\hat{\rho}|x-y\rangle. \tag{3.1}$$

The only states that have negative Wigner functions are non-Gaussian states, such as Fock states or Schrodinger cat states. Gaussian states, on the other hand, such as coherent states, squeezed states and thermal states, have only positive Wigner functions. Here a Gaussian state of a quantum field is defined as one for which its Wigner function is a Gaussian distribution [80]. Such a state is fully characterized by the first and second moments of the quadrature operators, or, equivalently, by the one and two-point correlation functions of the quantum field [78–80].

The distinction between Gaussian and non-Gaussian states can also be seen in the form of the Hamiltonian that they evolve under. Hamiltonians where the highest order of the interaction terms is quadratic in the quadrature operators (position, momentum etc...), or equivalently in annihilation and creation operators, in the second quantized picture, preserve the Gaussian nature of states. That is, the Hamiltonian must be of the form,

$$\hat{H} = \sum_k \boldsymbol{\lambda}_k(t)\hat{\boldsymbol{x}}_k + \sum_{k,l} \hat{\boldsymbol{x}}_k^T \boldsymbol{\mu}_{kl}(t)\hat{\boldsymbol{x}}_l, \tag{3.2}$$

where $\hat{\boldsymbol{x}}_k^T := (\hat{x}_k, \hat{p}_k)$, and $\boldsymbol{\lambda}_k(t)$ and $\boldsymbol{\mu}_{kl}(t)$ are 2×1 and 2×2 real-valued matrices of arbitrary functions of time. Although we have assumed a discrete, finite mode spectrum here for simplicity, the extension to infinite and continuous modes is straightforward [78, 79].

The Hamiltonian Eq.(3.2) preserves Gaussianity since it is associated with a general Bogoliubov transformation, which is a linear transformation of the quadratures (and, therefore, phase space) that preserves their commutation relations [80]. Any other Hamiltonian, i.e. one that is not linear or quadratic in quantum operators, will in general create non-Gaussianity [77, 80].

Note that a free quantum field has a Hamiltonian that is of the form Eq.(3.2) since it only contains the kinetic and mass terms, and so is necessarily quadratic in the field. For example, the free Hamiltonian for a real scalar quantum field $\hat{\phi}$ is [85],

$$\hat{H} = \frac{1}{2}\int d^3\boldsymbol{r}\left[(\partial_t\hat{\phi})^2 + (\nabla\hat{\phi})^2 + m^2\hat{\phi}^2\right] \tag{3.3}$$

where m is the mass of the field. Expanding the field in annihilation and creation operators $\hat{\phi} = \sum_k [u_k(t)\hat{a}_k + v(t)\hat{a}_k^\dagger]$, results in a Hamiltonian of the form Eq.(3.2) [85].

Now consider interacting this quantum field with a classical entity $\mathcal{G}$, which could depend on space and time. Taking the classical interaction to not induce quantum self-interactions of $\hat{\phi}$, then $\mathcal{G}$ and $\hat{\phi}$ can only interact through Hamiltonian terms that are linear or quadratic in $\hat{\phi}$. For example, the classical interaction could occur through a Hamiltonian term such as $(\nabla\hat{\phi})^2 f[\mathcal{G}]$, where f is a real functional of $\mathcal{G}$. Then, expanding $\hat{\phi}$ in annihilation and creation operators, we would still find a Hamiltonian that is of the form Eq.(3.2), with $\mathcal{G}$ just absorbed into the time-dependent coupling constants. That is, the Hamiltonian of the classical interaction preserves Gaussianity, and this would apply to a classical interaction with any type of quantum field, not just a real scalar field $\hat{\phi}$.

In contrast, if we quantize $\mathcal{G}$, such that we interact $\hat{\phi}$ (or any other type of quantum field) with a quantum entity, then it is possible for the resulting Hamiltonian to be higher order than quadratic in quantum operators, and thus induce non-Gaussianity. Therefore, any sign of the creation of non-Gaussianity in the state of a quantum field would be evidence of a quantum interaction.

Due to the universal coupling of gravity, we can apply this argument to determine whether gravity obeys a quantum or classical theory. In this case, if we are working in a situation where all other quantum interactions can be neglected, the matter Hamiltonian contains only the kinetic and mass terms of the matter quantum field, to which gravity couples. If there were terms that were neither linear nor quadratic in the quantum matter field, and which thus induce quantum self-interactions of matter, then these would have to be associated with a non-gravitational force since these terms must also be present in flat space. Therefore, as we are assuming a situation where all interactions other than gravity can be ignored, these terms are not present.

For example, if, for simplicity, we used a real scalar field $\hat{\phi}$ to describe matter and ignored a possible quadratic Ricci scalar coupling term then the Hamiltonian of CG would be Eq.(3.3) but with $\sqrt{\mathfrak{g}}$ multiplying each term, where $\mathfrak{g}$ is the determinant of the spatial metric [87]. This Hamiltonian would preserve Gaussianity. In contrast, in QG there must be an operator associated with the gravitational field, which would result in Gaussianity no longer being preserved. For instance, in loop QG, $\mathfrak{g}$ would be quantized in this example [87], and in linearized QG, we would perturb the gravitational metric around a classical spacetime background metric and quantize only the perturbation [88]. Similarly, in the non-relativistic Newtonian limit, only the temporal component of the perturbed metric would be used, which is quantized and associated with the Newtonian gravitational potential Φ.

In summary, creation of non-Gaussianity would provide evidence for a quantum theory of gravity. In fact, since all known fundamental interactions with matter, such as electromagnetism, have interaction Hamiltonians with terms that are quadratic in matter fields. [85], non-Gaussianity could also be used to evidence that these are indeed quantum interactions.

3.3 Testing Quantum Gravity with a Single Quantum System

Like in the previous chapter, we will now consider the observable signatures of quantum gravity. We turn to the application of a Wigner Negativity witness in a table-top test of QG (Figure 3.2) involving a BEC prepared at a single location. It is worth emphasising that the experiment considered is not amenable to an entanglement based witness of QG.

3.3.1 Signatures in a Bose-Einstein condensate

Bose Einstein Condensation is a quintessentially quantum phenomenon where, for low enough temperatures, the ground state of a quantum system is macroscopically occupied. For simplicity, we describe our condensate with a non-relativistic scalar quantum field $\hat{\Psi}(\boldsymbol{r})$, which creates an atom at position $\boldsymbol{r}$. Here, $\hat{\Psi}(\boldsymbol{r}) \approx \psi(\boldsymbol{r})\hat{a}$, where $\psi(\boldsymbol{r})$ is the wave-function of a condensed atom, and $\hat{a}$ is the annihilation operator for the condensate [83].

On account of the system being composed of massive atoms we expect them to interact gravitationally with each other. In the following, we will employ the non-relativistic (Newtonian) approximation of gravity. The fully classical interaction Hamiltonian for Newtonian gravity is,

$$H_{int} = \frac{1}{2}\int d^3\boldsymbol{r}\rho(\boldsymbol{r})\Phi(\boldsymbol{r}), \tag{3.4}$$

where $\Phi(\boldsymbol{r})$ is the classical Newtonian potential and $\rho(\boldsymbol{r})$ is the classical mass density.

If gravity is indeed quantum, it is necessary to quantize both the matter source $\rho(\boldsymbol{r})$ and the potential $\Phi(\boldsymbol{r})$. However in CG, one quantizes only the source $\rho(\boldsymbol{r})$. This difference gives rise to the following respective QG and CG interaction Hamiltonians,

$$\hat{H}_{QG} = \frac{1}{2}m \int d^3\boldsymbol{r} : \hat{\Psi}^\dagger(\boldsymbol{r})\hat{\Psi}(\boldsymbol{r})\hat{\Phi}(\boldsymbol{r}) : \tag{3.5}$$

$$\hat{H}_{CG} = m \int d^3\boldsymbol{r}\hat{\Psi}^\dagger(\boldsymbol{r})\hat{\Psi}(\boldsymbol{r})\Phi[\varPsi](t, \boldsymbol{r}), \tag{3.6}$$

Here we have taken $\hat{\rho}(\boldsymbol{r}) = m\hat{\Psi}^\dagger(\boldsymbol{r})\hat{\Psi}^\dagger(\boldsymbol{r})$ and :: refers to normal ordering, m is the mass of the atoms, and we have made explicit that the classical potential Φ can be a functional of the quantum state $\varPsi$ of the BEC, for which we have dropped a factor of 1/2. Solving the quantized version of Poisson's equation, we have,

$$\hat{\Phi}(\boldsymbol{r}) = -Gm \int d^3\boldsymbol{r'} \, \frac{\hat{\Psi}^\dagger(\boldsymbol{r'})\hat{\Psi}(\boldsymbol{r'})}{|\boldsymbol{r} - \boldsymbol{r'}|}, \tag{3.7}$$

where G is the gravitational constant. In contrast, depending on the chosen CG theory, Φ is a certain quantum average of this expression (for example, in the CG Schrodinger-Newton theory, which is the Newtonian limit of the semi-classical CG theory, $\Phi = \langle\hat{\Phi}\rangle$.

Using $\hat{\Psi}(\boldsymbol{r}) = \psi(\boldsymbol{r})\hat{a}$, the above interaction Hamiltonians for the BEC reduce to,

$$\hat{H}_{QG} = \frac{1}{2}\lambda_{QG}\hat{a}^\dagger\hat{a}^\dagger\hat{a}\hat{a}, \tag{3.8}$$

$$\hat{H}_{CG} = \lambda_{CG}[\varPsi]\hat{a}^\dagger\hat{a}, \tag{3.9}$$

where,

$$\lambda_{QG} := -Gm^2 \int d^3\boldsymbol{r}\, d^3\boldsymbol{r'} \frac{|\psi(\boldsymbol{r'})|^2|\psi(\boldsymbol{r})|^2}{|\boldsymbol{r} - \boldsymbol{r'}|}, \tag{3.10}$$

$$\lambda_{CG}[\varPsi](t) := Gm \int d^3\boldsymbol{r}|\psi(\boldsymbol{r})|^2\Phi[\varPsi](t, \boldsymbol{r}). \tag{3.11}$$

The QG interaction Hamiltonian Eq.(3.8) can also be derived as the non-relativistic limit of linearized QG where we consider the four-point Feynman diagram with a single virtual graviton propagator, and then effectively integrate out gravitational degrees of freedom [89–91]. All QG theories must limit to the above quantum version of Newtonian gravity and so Eq.(3.8) is the Hamiltonian for general QG self-interactions of a BEC. Likewise, all CG theories must limit to Eq.(3.9) for CG self-interactions of a BEC in the Newtonian limit, such that Eq.(3.8) – Eq.(3.9) are not dependent on a specific model of CG or QG. Similar Hamiltonians have been derived using cold atoms in a double-well potential [92].

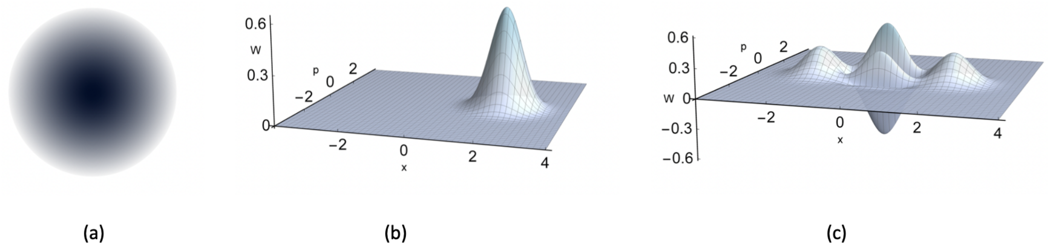

Figure 3.2: Illustration of the proposal outlined in Section 3.3 for a table-top test of QG. (a) A single spherical BEC of 10^9 atoms and radius $R = 200\,\mu$m is left to self-interact gravitationally for around $t = 2\,$s. If QG acts, non-Gaussianity is induced in its quantum state, whereas, if CG acts, Gaussianity is preserved. Each atom is equally delocalized across the extent of the BEC but, since the BEC is in a spherical harmonic trap, the density of the BEC is greatest at its centre and drops off to zero asymptomatically, as illustrated. The BEC is initially in a Gaussian state, and (b) displays its Wigner function W. Here, for simplicity, a coherent state $|\alpha\rangle$ is assumed, but this can also be squeezed to improve the signal-to-noise ratio, as discussed in Section 3.3. If QG acts, and the interaction time were long enough, then gravity could even force the coherent state to a Yurke-Stoler cat state $(|\alpha\rangle + i|-\alpha\rangle)/\sqrt{2}$. The Wigner function for such a non-Gaussian state is illustrated in (c). If, however, CG acts, then the state will remain Gaussian. In the non-relativistic CG limit, the state will in fact remain a coherent state, whereas, relativistic CG effects would, in principle, squeeze the state but keep it Gaussian. In practice, the interaction time would not be long enough for such a dramatic effect as a coherent state changing to a Yurke-Stoler state, and instead smaller deviations from a Gaussian distribution are looked for (see Section 3.3). Note that $\alpha = 2$ is used in the plots, whereas, in practice, the BEC will have an amplitude of around $|\alpha| = 10^{4.5}$, the square-root of the number of atoms.

From the Hamiltonians Eq.(3.8) – Eq.(3.9), we can see that, as long as all other quantum interactions can be neglected, only the QG Hamiltonian Eq.(3.8) can induce non-Gaussianity in the quantum state of the BEC field, with the CG Hamiltonian Eq.(3.9) preserving Gaussianity since it is quadratic in quantum operators. Therefore, any sign of non-Gaussianity being created in the BEC would be evidence of QG. Note that entanglement cannot be used as a witness here since this is just a single-mode system. In fact, the QG Hamiltonian is analogous to the Kerr interaction, which induces non-Gaussianity in quantum optics.

3.3.2 Measurement Scheme

As shown above, measuring creation of non-Gaussianity in the BEC would provide evidence of QG. In order to detect non-Gaussianity, we consider measurements of high-order cumulants [93]. For a Gaussian distribution, all cumulants higher than second order vanish and, therefore, a non-zero value of such cumulants is a signature of non-Gaussianity. Here we concentrate on the fourth-order cumulant κ_4, since κ_3 is also zero for a symmetric non-Gaussian distribution. Defining a generalized quadrature as $\hat{q}(\varphi) = \hat{a}e^{-i\varphi} + \hat{a}^\dagger e^{i\varphi}$, we have,

$$\kappa_4 := \langle \hat{q}^4 \rangle - 4\langle \hat{q} \rangle \langle \hat{q}^3 \rangle - 3\langle \hat{q}^2 \rangle^2 + 12\langle \hat{q}^2 \rangle \langle \hat{q} \rangle^2 - 6\langle \hat{q} \rangle^4. \tag{3.12}$$

In an experiment, only a finite sample can be used to estimate κ_4 and we desire unbiased estimators, which are the k statistics: $\langle k_n \rangle = \kappa_n$. The noise in the estimation of κ_4 is then the standard deviation of k_4, such that the signal-to-noise ratio (SNR) for the measurement is,

$$\mathrm{SNR} = |\kappa_4| / \sqrt{\mathrm{Var}(k_4)}, \tag{3.13}$$

where, for a large number of independent measurements $\mathcal{M}$, $\mathrm{Var}(k_4) \propto 1/\mathcal{M}$.

In order to make the SNR as large as possible, we use quantum metrology, where highly quantum states can improve the estimation of parameters that are not associated with observables. This is also effectively used in the BMV proposal where the initial quantum states are N00N-like states [94]. However, rather than using a N00N state, here we consider a squeezed state, which is a Gaussian state that often provides similar performance in quantum metrology to N00N states but which is usually far less demanding to create. Assuming that QG acts, i.e. that the gravitational interaction has the Hamiltonian of QG Eq.(3.8), and taking the limit that $\chi := |\lambda_{QG}|/\hbar$ is small and that the number of atoms N of the BEC is large, the SNR can be of order $\chi t N^2 \sqrt{\mathcal{M}}$, where t is the interaction time. Assuming a weakly interacting BEC of mass M in a spherical harmonic trap with frequency ω_0, the BEC wavefunction is [83],

$$\psi(\boldsymbol{r}) = \frac{1}{\pi^{3/4} R^{3/2}} e^{-r^2/(2R^2)}, \tag{3.14}$$

where $R := \sqrt{\hbar/(m\omega_0)}$ is the effective radius of the spherical BEC and $r := |\boldsymbol{r}|$. Using Eq.(3.10), this results in [94]:

$$\chi t N^2 \equiv \sqrt{\frac{2}{\pi}} \frac{G M^2 t}{\hbar R}, \tag{3.15}$$

which is $t/\hbar$ times the gravitational self-energy of the BEC. Note that, with the replacement of R with d, and neglecting the numerical factor, this expression is the same as the relative phase generated in the BMV proposal between the two microspheres that are separated by the smallest possible distance d that, when ignoring all other distances, leads to an entangled state [11, 66, 68]. It is demonstrated in the BMV proposal that a value of order one for this phase is achieved when $d = 200\,\mu$m, $t \approx 2\,$s and $M = 10^{-14}\,$kg [68, 69]. However, since the SNR here scales with $\sqrt{\mathcal{M}}$, we can lower the total mass required by increasing the number of measurements. For example, to achieve an SNR of 5 for a ^{133}Cs BEC, we could use $R = 200\,\mu$m, $t = 2\,$s and $M = 10^{-15}\,$kg with around 40,000 measurements. Such a mass corresponds to around 4×10^9 atoms, which is only a little larger than what has been achieved so far: in 1998 a ^{1}H BEC was created with over 10^9 atoms [95], and in 2006 a ^{23}Na BEC had over 10^8 atoms [96]. However, the number of atoms required can be reduced by further increasing $\mathcal{M}$.

It is worth noting the relation of the quantities computed to the Planck mass. Using Eq.(3.15), we can write the SNR for one measurement in this case as [97],

$$\frac{M}{M_P}\frac{\delta\tau}{t_P}, \tag{3.16}$$

where M_P is the Planck mass, t_P is the Planck time, and $\delta\tau := \sqrt{2/\pi}GMt/(Rc^2)$. This expression can also be derived by dividing the BEC into two halves, considering the gravitational interaction of one with the other and the time dilation $\delta\tau$ induced in GR in the centre of each half. If we fix the SNR of one measurement, then Eq.(3.16) illustrates that as M gets closer to M_P, it seems that we can probe more minute gravitational field intensities and thus further access its possible quantum properties.

An experimental implementation of this scheme would be to use a spin-1 BEC where the $m_F = \pm 1$ states are prepared in large coherent states and then a magnetic field is used to drive spin-mixing collisions to generate a quadrature squeezed state in the $m_F = 0$ condensate. In a spin-1 BEC, the interaction Hamiltonian is [98],

$$\begin{aligned}\hat{H} = \hbar\kappa &\left[\hat{a}_0^2\hat{a}_+^\dagger\hat{a}_-^\dagger + \left(\hat{a}_0^\dagger\right)^2\hat{a}_+\hat{a}_-\right]\\ &+ \hbar\kappa\left(\hat{a}_0^\dagger\hat{a}_0 - \frac{1}{2}\right)\left(\hat{a}_+^\dagger\hat{a}_+ + \hat{a}_-^\dagger\hat{a}_-\right)\\ &+ \hbar q\left(\hat{a}_+^\dagger\hat{a}_+ + \hat{a}_-^\dagger\hat{a}_-\right),\end{aligned} \tag{3.17}$$

where $\hat{a}_0$ is the annihilation operator of the $m_F = 0$ mode and $\hat{a}_\pm$ are the annihilation operators of the $m_F = \pm 1$ modes. By dynamically tuning q with a magnetic field, the quadratic Zeeman shift (third term) cancels collisional shifts due to s-wave scattering of the three modes (second term) [99]. Taking the $m_F = \pm 1$ modes to be in large coherent states ($N_\pm \gg 1$) so that $\hat{a}_\pm \approx \sqrt{N_\pm}$, Eq.(3.17) then acts as effectively,

$$\hat{H} = \hbar N \kappa \left[\hat{a}_0^2 + \left(\hat{a}_0^\dagger \right)^2 \right], \tag{3.18}$$

where $N := \sqrt{N_+ N_-}$, which results in a single-mode quadrature squeezed state for the $m_F = 0$ mode. Spin-squeezing experiments have already been performed in cold atoms and BECs [100], where normally it is the $m_F = 0$ mode that is taken to be the large coherent mode and then a two-mode squeezed state is created for the $m_F = \pm 1$ modes.

After the system has evolved for a time t, the non-Gaussianity of the BEC field would then be measured. To achieve this, a homodyne or heterodyne scheme could be used [101, 102], where moments up to fourth order are looked for in the intensity difference, providing a direct map for obtaining κ_4. Observing a non-zero value for κ_3, which only requires the third-order moment in homodyne detection, would be sufficient for detecting non-Gaussianity, and the third-order correlation function of atoms due to electromagnetic self-interactions has already been measured in experiments [103]. However, κ_3 is predicted to be zero if the initial state of the BEC is a squeezed vacuum state, in which case κ_4 needs to be analysed. For κ_4, the techniques used in [103] could be extended to measure the fourth-order correlations to obtain κ_4 through homodyne detection. This would require single-atom counting in a quantum gas with high efficiency on small length scales, and recent advances have opened up very promising approaches to single-atom counting. Rather than performing a homodyne or heterodyne measurement, another option would be to determine the Wigner function of the BEC, either using full state tomography with projective measurements (see e.g. [104] for such measurements on cold atoms and BECs), or through 'direct' measurement with weak measurements of the position quadrature and projective measurements of the momentum quadrature (this has so far been achieved with photons [105, 106], but could be extended to atoms [105]).

3.3.3 Characterizing other interactions

In the following we will discuss the various sources of noise that may affect the non-Gaussian signal and possible ways to distinguish them. An advantage to considering a non-Gaussian signal is that we can immediately neglect all processes generating Gaussian noise since these will not affect the non-Gaussian measurement. The largest contributing non-Gaussian noise would be expected to come from the electromagnetic interactions between the atoms of the BEC. A BEC is very dilute and the atoms are neutral overall, but there are still, in general, weak electromagnetic interactions between the atoms due to van der Waals and magnetic dipole dipole interactions (MDDIs). At the low temperatures at which BECs operate, the Hamiltonian for a BEC with electromagnetic interactions is [107, 108],

$$\begin{aligned}\hat{H} = \int d^3\boldsymbol{r}\bigg[&-\frac{\hbar^2}{2m}\hat{\Psi}^\dagger(\boldsymbol{r})\nabla^2\hat{\Psi}(\boldsymbol{r}) + V_T(\boldsymbol{r})\hat{\Psi}^\dagger(\boldsymbol{r})\hat{\Psi}(\boldsymbol{r}) \\ &+\frac{1}{2}\int d^3\boldsymbol{r'}\Big[\hat{\Psi}^\dagger(\boldsymbol{r})\hat{\Psi}^\dagger(\boldsymbol{r'})\hat{\Psi}(\boldsymbol{r})\hat{\Psi}(\boldsymbol{r'})\Big(g_s\delta^{(3)}(\boldsymbol{r}-\boldsymbol{r'}) \\ &+ g_d\frac{1-3\cos^2\vartheta}{|\boldsymbol{r}-\boldsymbol{r'}|^3}\Big)\Big]\bigg], \end{aligned} \tag{3.19}$$

where the first term is the kinetic part, $V_T(\boldsymbol{r}) = m\omega_0^2 r^2/2$ is the spherical trapping potential, $g_s := 4\pi\hbar^2 a_s/m$ is the s-wave scattering coupling constant, $g_d := \mu_0\mu^2/(4\pi)$ parametrizes the strength of the MDDIs, and ϑ is the polar angle of $\boldsymbol{r}-\boldsymbol{r'}$, with a_s the s-wave scattering length, μ the magnetic moment of the atom and μ_0 the permeability of free space. Using $\hat{\Psi}(\boldsymbol{r}) = \psi(\boldsymbol{r})\hat{a}$ and Eq.(3.14), the above Hamiltonian reduces to:

$$\hat{H} = \hbar\omega\hat{a}^\dagger\hat{a} + \frac{1}{2}\lambda_s\hat{a}^\dagger\hat{a}^\dagger\hat{a}\hat{a}, \tag{3.20}$$

where,

$$\hbar\omega := \hbar\omega_0 + \frac{3}{4}m\omega_0^2 R^2, \tag{3.21}$$

$$\lambda_s := \frac{g}{2\sqrt{2}\pi^{3/2}R^3} \equiv \sqrt{\frac{2}{\pi}}\frac{a_s\hbar^2}{mR^3}. \tag{3.22}$$

Note that the MDDIs have cancelled out due to the spherical symmetry of the BEC, leaving behind only the s-wave interactions. This interaction term has the same form as the quantum gravitational interaction Eq.(3.8), and so we need to be able to distinguish between the electromagnetic and gravitational interactions in order to attribute non-Gaussianity to only gravitational interactions. One way to achieve this is to use magnetic or optical Feshbach resonances, which are extraordinary processes particular to cold atom and BEC experiments. Here an external magnetic or optical field is used to resonantly couple a molecular bound state to a colliding atom pair, enabling the strength of the electromagnetic interactions to be controlled [83].

Usually Feshbach resonances are used to increase the electromagnetic interaction strength between atoms in BECs. However, they also allow for the electromagnetic interaction to be in principle switched off, i.e. $\lambda_s = 0$, without affecting the strength of the gravitational interaction. This is achieved by applying a magnetic field of strength B to the BEC, which results in the s-wave scattering length becoming a function of B [83],

$$a_s(B) = a_s^{bg}\left[1 - \frac{\Delta}{B - B_0}\right], \tag{3.23}$$

where a_s^{bg} is the background scattering length, B_0 denotes the resonance position and Δ is the resonance width. The s-wave interactions can then be minimized by setting $B \to B_0 + \Delta$. The experimental goal is to attribute non-Gaussianity largely to QG interactions in the BEC. However, in reality the applied magnetic field is $B = B_0 + \Delta + \delta B$ where δB is the error in setting its value which we shall equate to the resolution limit. It is up to this limit in tuning B that we can distinguish gravitational non-Gaussianity from the electromagnetic. In this case the error, δa_s in a_s is given by,

$$\delta a_s = a_s^{bg}\left[\frac{\delta B}{\Delta}\right] \tag{3.24}$$

This in turn affects the value of the coupling constant λ_s given in Eq.(3.22). SQUID sensors [109] and atomic magnetometers [110] can achieve femtotesla scale magnetic field resolutions. For ^{133}Cs, the ideal scenario where $a_s = 0$ is when $B = 17\,\mathrm{G}$ [111], leaving behind only the QG interactions which are unaffected by the applied magnetic field. However, considering the resolution limit and Eq.(3.24), we note that for λ_{QG} to be comparable to λ_s, $\delta B \sim 10^{-14}\,\mathrm{G}$ which is 3 orders of magnitude below the current state of the art [112]. While ^{133}Cs has $a_s^{bg} = 1720\,\mathrm{a}_0$ (where a_0 is the Bohr radius), one can consider condensates of ^{39}K with $a_s^{bg} = -29\,\mathrm{a}_0$ [113] or ^{88}Sr with $a_s^{bg} < 13\,\mathrm{a}_0$ [114]. In this case it follows from Eq.(3.24) that $\delta B \sim 10^{-12}\,\mathrm{G}$, which looks to be within technological reach. We can further reduce this value by considering larger condensates with $R > 200\,\mu$m. The small s-wave scattering length of ^{88}Sr is also controllable through an optical Feshbach resonance [115].

Rather than working with a spherical BEC where MDDIs cancel, we could alternatively use a harmonic trap to create a quasi-1D or quasi-2D geometry (extreme pro-late or oblate spheroidal geometries) [83]. In this case, instead of tuning the s-wave scattering length to zero, we can tune it to cancel the MDDIs such that we again have small electromagnetic interactions. We could also use pure 2D or 1D Bose gases where the trapping geometry has one or two dimensions with characteristic size much smaller than both two- and three-body length scales [83], leading to a drastic reduction in collisional electromagnetic effects [83], but not gravitational effects. In this case, there may be no phase transition to a BEC but there can still be macroscopic occupation of the ground state.

Furthemore, instead of eliminating the noise from the electromagnetic interactions, we could use distinguishing features between the electromagnetic and gravitational interactions, such as how their strengths vary with the trapping potential and the magnitude of an applied magnetic field. For example, for a spherical trap, the effective strength of the electromagnetic interaction scales as $1/R^3$, whereas gravity scales as $1/R$ - see Eq.(3.22) and Eq.(3.15). The different scaling is due to the fact that the electromagnetic interactions are already partially screened due to the atoms having overall neutral charge, whereas the coupling of gravity is universal and so cannot be screened. With an applied magnetic field, it is even possible to change the s-wave interactions from being repulsive to attractive and vice-a-verse, which is clearly impossible to achieve with gravity

We also note other effects such as three-body elastic collisions, that often limit the size and lifetime of condensates. These are usually neglected in comparison to two-body elastic collisions, which need to be accounted for while computing the SNR. Three-body recombination occurs when three atoms in the condensate collide to form a molecule (diatomic bound state) and a single atom, both of which can escape the trap due to their large kinetic energy. The corresponding interaction Hamiltonian can be written as,

$$\hat{H}_3 = \int d^3\boldsymbol{r} \left[\hat{\Psi}^3(\boldsymbol{r})\hat{\Psi}^\dagger_F(\boldsymbol{r})\hat{\Phi}^{\dagger\,3}_F(\boldsymbol{r}) + h.c.\right] \tag{3.25}$$

where Ψ_F and Φ_F are the annihalation operators for the free atom and the free molecule respectively.

3.4 Classical Interaction Effects

A classical interaction can create entanglement if this involves the respective quantum systems directly interacting with each other. For example, consider two BECs that are in the two spatial arms of a double-well potential. In the two-mode approximation, we can write the full quantum field of the atoms as $\hat{\Psi}(\boldsymbol{r}) = \psi_L(\boldsymbol{r})\hat{a}_L + \psi_R(\boldsymbol{r})\hat{a}_R$ where $\hat{a}_L$ and $\hat{a}_R$ respectively destroy an atom in the left and right well, and ψ_L and ψ_R are the corresponding mode wavefunctions [83]. In the case of CG, and taking the Newtonian approximation for simplicity, there will, in principle, be terms of the form $\lambda_{LR}\hat{a}^\dagger_L\hat{a}_R + h.c.$, in the Hamiltonian, where $\lambda_{LR} := m\int d^3\boldsymbol{r}\psi^*_L(\boldsymbol{r})\psi_R(\boldsymbol{r})\Phi[\Psi](\boldsymbol{r}, t)$. These are beam-splitting terms such that, if λ_{LR} is non-zero due to, for example, the mode wavefunctions overlapping, and either BEC is in a non-classical state, then the terms will induce entanglement between the BECs. There is an electromagnetic analogue of this effect where a double-well trapping potential, which is approximated to be classical, causes or contributes to entanglement between the two wells. This entangling process is often referred to as "quantum tunnelling" in cold atom experiments [83]. However, since the entangling-inducing terms are quadratic, they will not induce non-Gaussianity, illustrating that, although a direct classical interaction with matter can create entanglement, it cannot create non-Gaussianity in the quantum field of matter.

Note that here we are working with "mode" entanglement, i.e. entanglement between modes of a quantum field. If instead we attempted to use a first-quantization picture and describe the full system using a many-body wave-function, then it is possible to argue that the initial state of the full system is already entangled and that Newtonian CG is not creating entanglement in this picture [81, 82]. This is because there is so-called "particle" entanglement before and after the effective CG beam splitter. For example, the initial state could be $|\alpha\rangle_L|\xi\rangle_R$, with $|\alpha\rangle$ a coherent state and $|\xi\rangle$ a squeezed state, which, in a quasi first-quantization picture, is particle entangled but not mode entangled. This occurs because, in the first quantization picture, a beam splitter does not couple the left and right wells. However, in the relativistic CG limit we would also have, in principle, two-mode squeezing operations such as $\hat{a}_L\hat{a}_R + \hat{a}_L^\dagger\hat{a}_R^\dagger$, that can result in a two-mode squeezed state, which is particle entangled. Therefore, in full generality and in either picture, CG can, in principle, create entanglement. In contrast, in the first-quantization picture, it is possible for Newtonian CG to create non-Gaussian "particle" Wigner functions. For example, the many-body wavefunction of our single-well BEC experiment could start off Gaussian but become non-Gaussian under CG. However, in the more fundamental second quantization picture, the state of matter i.e., the state of the quantum field of matter, always remains Gaussian under CG.

3.5 Alternative Theories of Gravity

Einstein's GR can be formulated as an action theory with the action principle being used to derive the field equations. The action S of GR can be decomposed into the Einstein-Hilbert action S_{EH}, that only contains gravitational degrees of freedom, and the matter action S_M, which tells us how matter and gravity interact,

$$S = S_{EH} + S_M, \tag{3.26}$$

where:

$$S_{EH} = \frac{c^4}{16\pi G}\int d^4x\sqrt{g}R, \tag{3.27}$$

with R the Ricci scalar; and for a real scalar matter field ϕ,

$$S_M = \frac{1}{2}\int \sqrt{g}\Big[g^{\mu\nu}\partial_\mu\phi\partial_\nu\phi - (m^2 + \varepsilon R)\phi^2\Big], \tag{3.28}$$

with ε a numerical factor. The matter actions for spin-1/2 and spin-1 fields are provided in Appendix A.

The argument that we have presented for non-Gaussianity being an indicator of QG only uses the matter action S_M and says nothing of the purely gravitational action S_{EH}. It relies on the fact that S_M must be, in the absence of all non-gravitational quantum interactions, quadratic in the matter fields such that a classical theory of gravity will preserve Gaussianity. If S_M had terms that coupled gravitational degrees of freedom with non-linear or non-quadratic functions of the matter fields then, in flat spacetime, such terms would still exist and this would result in a new non-gravitational interaction, which we have excluded.

Many theories of gravity have been suggested as alternatives to Einstein's GR [116]. These tend to consider alternative forms for the gravitational action S_{EH}. For example, in $f(R)$ theories of gravity, the R in S_{EH} is replaced with some function of the Ricci scalar $f(R)$. Using the argument above, as long as we can exclude all other relevant quantum interactions, non-Gaussianity can still be used as evidence of a quantum rather than classical version of these alternative theories of gravity.

3.6 Non-Gaussianity in Cosmology

Cosmological correlation functions are extrapolated through satellite probes of the CMB such as the Planck experiment. Among the various signals studied in the early universe, it is expected that temperature fluctuations of the cosmic microwave background (CMB) could follow a non-Gaussian distribution. Precision studies of the power spectrum have indicated that the temperature fluctuations in the CMB are consistent with a Gaussian distribution. However with better technology and increasing resolution, it is possible that non-Gaussianity could be detected in the near future, providing important insights into structure formation in our Universe.

The inflationary perturbations laid down the seeds of the temperature fluctuations expressed in the CMB at the surface of last scattering. While tracking the quantum origin of these perturbations it is imperative to keep track of quantum mechanical effects that occur at or before horizon exit, and classical non-linear/ decohering effects after horizon exit.

The simplest models of inflation are ruled out by current observations of the CMB, necessitating the investigation of multiple fields driving the inflationary process and the phenomenology associated with different inflationary potentials. The Hamiltonians for these models are similar to those which are used to illustrate that non-Gaussianity in the quantum state of matter can be used as evidence of QG (Eq.(A.5)). An important difference, however, is that realistic models of inflation incorporate a non-quadratic potential $V(\hat{\phi})$ due to self-interactions of the inflaton.

Cosmological non-Gaussian signatures may occur as the scalar sector of the metric couples with the inflaton which in turn evolves with the inflationary potential. It is in principle possible for purely classical gravitational effects to enhance non-Gaussianity inflation if the scalar sector coupling to the inflaton is chosen to be classical. Unlike our experimental proposal we have no control over this phenomenon where it is impossible to screen out other interactions besides gravity. Even if future probes of the CMB discover non-Gaussian signatures, a proper measure of non-Gaussianity such as the SNR considered in Eq.(3.13) needs to be applied to the CMB statistics, where each patch of the sky is treated as an independent measurement.

Yet another issue we have no control over in cosmology is the time of production of non-Gaussianity. Inflationary perturbations exit the horizon and classicalize owing to the accelerated expansion of the universe. Non-Gaussian statistics for the curvature perturbations maybe observed due to other classical effects upon horizon re-entry. These effects are in turn imprinted in the CMB as the curvature perturbations source gravitational wells that redshift radiation by varying degrees (an entirely classical phenomenon). Furthemore, candidate models of inflation may involve multiple fields that interact with each other and indeed cosmologists expect non-Gaussianity to be a probe into the various types of inflationary models.

There are many other mechanisms responsible for creating a non-Gaussian distribution of temperature fluctuations in the CMB besides the inflationary ones. Secondary effects such as, the scattering of photons and classical gravitational effects, occur between the last scattering surface and the observer [117]. Although detection of these non-primordial effects would provide important information for distinguishing structure formation scenarios, they are often regarded as noise of the primary inflationary effects.

We can also turn our attention to tensor modes due to quantum fluctuations of the gravitational field during inflation. Measurement of polarization of the cosmic microwave background due to a long wavelength stochastic background of gravitational waves from inflation in the early Universe would provide additional signatures for the quantization of gravity [118]. Other possibilities have also been suggested, such as using measurements of the scalar modes of the temperature fluctuations to try and access quantum measures of the primordial curvature perturbations, such as violation of Bell inequalities [119] or quantum discord. The issue, as we have pointed out before is that, the conjugate momentum of the field modes decay with the expanding universe. There then does not seem to be enough information to rule out classical curvature perturbations [23], and instead baroque inflationary models need to be assumed for evidence of QG.

3.7 Discussion

We have provided a proposal for a table-top test of QG that uses non-Gaussianity as a QG witness which should be achievable in the near future. This proposal uses a 4×10^9 atoms BEC in a single-well potential and demonstrates a lot of promise as 10^9 atomic BECs have already been created in single wells [95]. The most promising proposal so far for a table-top test of QG is considered to be the BMV proposal, which, in contrast to our quantum gas experiment, uses an opto-mechanical setup and entanglement as a witness of QG. Notably the mass required for our experiment is at least an order of magnitude lower than that used the BMV proposal [68], aiding the prospect of its experimental realization.

Our work suggests that what makes a theory of gravity quantum from a QI perspective is the fact that it can create non-Gaussianity in matter. While entanglement can even be created by classical effects (see Section 3.4), CG can never create non-Gaussianity in the quantum field of matter. An important assumption is that other quantum interactions such as electromagnetic effects are suppressed. Similarly, even though a classically expanding spacetime metric can create entanglement in the quantum field of matter [72–74], it cannot create non-Gaussianity. Furthermore unlike entanglement, a single system suffices to witness this effect.

BECs and cold atoms have been found to be very effective in tests of classical gravity, and experiments using these are now becoming the state-of-the-art for many types of classical gravity measurements [120]. Their effectiveness can be attributed to the extraordinary degree of control that BECs and cold atoms provide in exploring the fundamental behaviour of quantum matter in various settings. In particular, Feshbach resonances enable control of the electromagnetic interactions between atoms, providing a key tool that has led to several scientific breakthroughs [83]. Given their great success in classical gravity measurements and the degree of control offered by these systems, it is perhaps not surprising that we find that BECs could also be very useful for measuring quantum gravitational effects.

We often say that the earth is a sphere, but to be precise, the term sphere refers only to the surface. The correct mathematical term for the solid earth is a ball.

— Leonard Susskind, *The Cosmic Landscape*

4

Quantum Information Theory and the C^0-formulation of the Strong Cosmic Censorship Conjecture

Contents

This chapter is based on a paper written in collaboration with Alexander Yosifov and Vlatko Vedral. The author of this thesis conceptualised the problem statement and investigated the growth of complexity in cold hyperbolic black holes.

4.1 Introduction

While we have explored observational signatures of quantum gravity in the past chapters, an interesting discussion arises when similar considerations are applied to the pathologies that frequently arise in GR. One such overlap between QI and GR is investigated in the following chapter, through the analysis of the cosmic censorship conjecture in the context of the holographic correspondence, as seen in Kerr black holes. This line of inquiry sheds insight on the possible ways a fully quantum theory of gravity would change long held (albeit well motivated) notions in classical GR.

The strong cosmic censorship conjecture [121] was proposed to overcome the inconsistencies that arise during the application of Einstein's field equations to black holes. This was made mathematically explicit while modeling the evolution of space-time inside a rotating black hole. In fact the proponent of the censorship conjecture, Roger Penrose, expected that the lack of predictability could be disregarded as a mathematical novelty as opposed to a statement about the physical world. In the following chapter, we note how ideas from quantum information theory provide physical insights into the recent invalidations of the strong cosmic censorship conjecture. Specifically, we will be invoking insights from AdS/CFT as introduced in Sec.1.4. We have seen that there is a duality between a black hole in asymptotically anti de-Sitter spacetime and a thermal state of a CFT, in which the entropy of the black hole is dual to ordinary thermal entropy. Here we will consider the relation between the black hole interior and the physics of the CFT through the "CV-duality" [45, 46], according to which the complexity at a given boundary/CFT time is proportional to the volume of the maximal slice enclosed within the corresponding Wheeler- DeWitt patch, i.e., within the domain of dependence of a spacelike bulk hypersurface that asymptotes to the given boundary time slice.

4.2 Black Hole Interiors

4.2.1 Volume of a Black Hole

In flat space the volume of a spherical object is well known to be $\sim \frac{4\pi}{3}R^3$. This does not serve as a reasonable estimate of the volume of a spherical black hole owing to the curved geometry of the interior. In fact, black holes have large interiors [122, 123].

The interior volume of a black hole of mass M is $\sim M^5$, while its lifespan is $\sim M^3$. In vacuum, the only non-trivial static, spherically symmetric solution is the Schwarzschild blackhole for which even though the horizon area is time translation invariant for an asymptotic observer, its interior volume, defined in a geometrically covariant way as the maximal spacelike hypersurface bounded by a two-sphere foliating the horizon, is dynamical, and keeps growing. According to classical general relativity, the interior volume continues to grow unbounded. For the simplest case of a Schwarzschild metric, expressed in advanced Eddington-Finkelstein coordinates,

$$ds^2 = -\left(1 - \frac{2M}{r}\right) dv^2 + 2dvdr + r^2 \sin^2\theta d\phi^2 + d\theta^2 \tag{4.1}$$

where $v = t + \int \frac{dr}{1-2M/r}$, and t is Schwarzschild time, the interior volume grows linearly in the advanced time v, where up to a prefactor of $3\sqrt{3}\pi$ it reads

$$V(v) = M^2 v \tag{4.2}$$

The maximum of Eq.(4.2) is obtained by extremizing the integral

$$V = \int^v \int_{S^2} \left[r^2 \left(\frac{2M}{r} - 1\right)^{3/2} \right] \sin\theta d\theta d\phi dv \tag{4.3}$$

which maximizes at $r_{\max} = 3M/2$ and S^2 denotes the two-sphere foliating the horizon.

This non-trivial relation between horizon area and interior volume was further examined in Ref. [124] where it was argued that for a Schwarzschild black hole the volume of the maximal bounded spacelike hypersurface behind the horizon continues to grow until the black hole reaches the Planck scale. Without loss of generality, the results were expanded [125] for the rotating $a \neq 0$ subextremal $|a| < M$ two-parameter family of stationary axisymmetric solutions in asymptotically flat spacetime (i.e. Kerr black hole). Where assuming $M \gg 1$, and the metric curvature is weak at both $r = 2M$ and $r = 3M/2$, then similar reasoning to that in $a = 0$ Schwarzschild geometry was shown to be valid. Namely, for a subextremal Kerr black hole the leading contribution to the interior volume is due to the maximal Cauchy development of initial data defined on a spacelike hypersurface which lies just barely within the black hole.

At first glance a resemblance can be seen with the increase of entropy, but it would be premature to come to this conclusion which doesn't hold under further scrutiny. In fact, black hole interiors grow much beyond thermal equilibriation. This growth of the interior is quantified in the context of AdS/CFT, where the volume of a black hole in d-dimensional asymptotically AdS spacetime was conjectured to be dual to the complexity of a thermal state CFT living on the $(d-1)$-dimensional AdS boundary, hence "complexity=volume" (CV). Interestingly, it was then argued in Ref. [44] that complexity, similar to entropy, admits a Second law.

4.2.2 Cosmic Censorship

In the 1970s, Penrose conjectured that although naked singularities are compatible with GR, any singularities arising in gravitational collapse cannot be visible to observers situated at infinity [121]. That is to say, under physically realistic situations they will be hidden behind an event horizon. This forms the basis of the weak cosmic censorship conjecture. The strong cosmic censorship conjecture stems from the argument that the predictive power of GR as a complete theory of gravity remains unaffected, whether the singularity is visible from infinity or if it can be observed at some finite distance from. Thus, if cosmic censorship were true, then it should forbid the appearance of locally naked singularities, i.e., singularities that lie to the future of some point on an observer's world line and to the past of another point on the same world line. The precise mathematical condition of the strong cosmic censorship conjecture that excludes the locally naked singularities is the demand that space-time be globally hyperbolic. Furthermore, the strong cosmic censorship conjecture requires that the maximal Cauchy development of a generic solution to Einstein's equations with physically realistic matter or asymptotically flat initial data is locally inextendible as a regular Lorentzian manifold.

Note, the existence of a partial Cauchy surface $\mathcal{S}$ with an asymptotically simple past ensures that singularities occurring in space-time arise from an initially regular state and that any Cauchy horizons arising to the future of $\mathcal{S}$ are not artifacts of a bad choice of the initial surface but rather are a result of the genuine breakdown of global hyperbolicity. For example, a partial Cauchy surface in an asymptotically simple and empty space-time (a globally hyperbolic space) with an edge on past null infinity $\mathcal{J}^-$ or future null infinity $\mathcal{J}^+$ would contain a Cauchy horizon.

In a series of extraordinary mathematical results, [47, 126–128] have demonstrated that for a maximal Cauchy development of suitable initial data, considered on a spacelike hypersurface Σ inside a subextremal Kerr (or Reissner-Nordstrom) black hole, the metric is C^0-stable. This implies that while spacetime is extendable to a larger Lorentzian manifold $\tilde{\mathcal{M}} \setminus \mathcal{M}$ across a non-trivial part of the Cauchy horizon, the extension is not smooth enough to qualify as a valid solution of the Einstein's equations. This however, invalidates the C^0 form of Penrose's celebrated SCC while saving the Einstein equations from outputting non unique solutions.

We immediately note the implications of these mathematical results on the predictions of QG at the level of soft singularities especially pertaining to the structure of spacetime. Building on Ref. [47], in this chapter, we revisit the C^0-formulation of the SCC from a quantum complexity-theoretic perspective. We consider an illustrative example of the low-temperature limit of a hyperbolic AdS$_{d+1}$ black hole dual to a CFT living on a $(d-1)$-dimensional hyperboloid to investigate the C^0 formulation of the SCC. We demonstrate that if the metric terminates at the Cauchy horizon, then the CV-duality (i.e. gauge/gravity correspondence) will be violated at late times. In light of this, we propose a novel conjecture relating the C^0-stability of the metric to the complexification of the system, and suggest the extendability of the black hole interior is bounded from below by the classical recurrence time.

The chapter is organized as follows. In Section 4.3 we review the Kerr geometry, and focus on the role of the Cauchy horizon. We then look at the C^0-formulation of Penrose's SCC and its implications for the interior Kerr black hole region. In Section 4.4 we examine the implications of the C^0-instability of the metric for Kerr-AdS spacetime. Section 4.5 is dedicated to the study of the inconsistencies in the bulk/boundary duality yielded by a hypothetical inextendability of the interior metric beyond the Cauchy horizon.

4.3 The Kerr Metric and C^0-inextendability

In GR, black holes are completely characterised by three parameters: mass, rotation (spin) and charge. The Kerr metric is a generalization of the Schwarzschild metric to a rotating body. The subextremal $|a| < M$ Kerr family of solutions describes a metric whose line element, in Eddington-Finkelstein coordinates is given by,

$$\begin{aligned} ds^2 = -\frac{\Delta - a^2 \sin^2\theta}{\rho^2} dv^2 + 2dvdr + \rho^2 d\theta^2 + \frac{A\sin^2\theta}{\rho^2} d\phi^2 \\ - 2a\sin^2\theta dr d\phi - \frac{4aMr}{\rho^2}\sin^2\theta dv d\phi \end{aligned} \quad (4.4)$$

where

$$\begin{aligned} \Delta &\equiv r^2 - 2Mr + a^2 \\ \rho^2 &\equiv r^2 + a^2\cos^2\theta \\ A &\equiv (r^2 + a^2)^2 - a^2\Delta\sin^2\theta \end{aligned} \quad (4.5)$$

Here, $a = J/M$ is the rotation parameter which gives the spin-to-mass ratio of the black hole, where the extremal case corresponds to $a \sim \mathcal{O}(1)$. The metric admits two horizons, respectively at $r_\pm = M \pm \sqrt{M^2 - a^2}$, where $r_-{:=}\{r = \mathcal{CH}^+\}$ is the inner (Cauchy) horizon and $r_+{:=}\{r = \mathcal{H}^+\}$ is the outer (event) horizon. In the following we will focus on the inner horizon, namely the Cauchy horizon.

In Kerr geometry the maximal Cauchy development of generic asymptotically flat initial data, defined on a spacelike hypersurface Σ within the black hole (i.e. the non-empty complement of $\mathcal{M} \setminus J^-(\mathcal{I}^+)$), is non-uniquely extendable as a solution to the vacuum Einstein equations. This means lack of future determinism for all infalling timelike geodesics γ which reach $\tilde{\mathcal{M}} \setminus \mathcal{M}$. Thus, the region beyond the Cauchy horizon $\mathcal{CH}^+$ cannot be uniquely determined, implying a breakdown of global hyperbolicity of the metric, as predicted by classical general relativity. Upon maximal evolution of the initial data on the spacelike hypersurface Σ to a larger Lorentzian manifold $\tilde{\mathcal{M}} \setminus \mathcal{M}$, Σ will no longer be the Cauchy hypersurface for $\tilde{\mathcal{M}}$ which extends across $\mathcal{CH}^+$.

This globally non-hyperbolic future development of the initial data found in Kerr (and also Reissner-Nordstrom) solutions is in sharp contrast to the simple one-parameter Schwarzschild subfamily of solutions, where the maximal Cauchy evolution is future inextendable as a C^0 Lorentzian manifold across $\mathcal{CH}^+$. In Schwarzschild the future is uniquely determined, namely for $r < r_+$ all timelike geodesics γ are incomplete, and asymptote to a spacelike boundary in finite proper time.

In an attempt to preserve the global hyperbolicity of the metric Penrose proposed [129] the so-called strong cosmic censorship conjecture which, generally, reads

Conjecture 1 (the C^0-form of the SCC): The maximal Cauchy evolution of generic asymptotically flat (AdS) vacuum initial data is inextendable to a larger C^0 Lorentzian manifold $\tilde{\mathcal{M}}$ across the Cauchy horizon $\mathcal{CH}^+$.

The role of the C^0-formulation of the SCC is to bring uniqueness to the solutions of the vacuum Einstein equations, and hence make the future of all infalling timelike geodesics deterministic. The C^0-inextendability conjecture restores the predictability of the vacuum equations inside dynamical black holes by introducing a spacelike finite boundary across which the metric cannot be extended even as a (continuous) C^0. Recent advancements, however, see Refs. [47, 130], suggest Conjecture 1 is false, where the main results relevant to us can be summarized by the following theorem

Theorem 1 (Dafermos-Luk): Consider general vacuum initial data corresponding to the expected induced geometry of a dynamical black hole settling down to Kerr (with parameters $0 < |a| < M$) on a suitable spacelike hypersurface Σ_0 in the black hole interior. Then the maximal future development of the spacetime $(\mathcal{M}, g)$ corresponding to Σ_0 is globally covered by a double null foliation and has a non-trivial Cauchy horizon $\mathcal{CH}^+$ across which the metric is continuously extendable.

The theorem suggests that general exterior subextremal spacetimes, emerging from initial data sufficiently close to Kerr data, have C^0-stable non-trivial Cauchy horizons in their interiors. This, together with the global existence statement in the exterior (weak cosmic censorship), are already a strong argument against Conjecture 1. In fact, the weak cosmic censorship (i.e. the completeness of null infinity $\mathcal{I}^+$) makes an even stronger statement as it implies the entire Penrose diagram is nonlinearly stable for solutions to $R_{\mu\nu} = 0$. So given stability in the Kerr exterior $J^-(\mathcal{I}^+)$, we can infer similar properties to hold in the non-empty complement of $\mathcal{M} \setminus J^-(\mathcal{I}^+)$ as well. Moreover, C^0-stability results of $\mathcal{CH}^+$ have also been derived for a broader class of systems, e.g. for Reissner-Nordstrom solutions to the Einstein-Maxwell-real-scalar-field equations [126–128], while in Ref. [131], assuming polynomial decay rate, for suitable initial data of the Einstein-Maxwell-Klein-Gordon equations in a Reissner-Nordstrom background, the spacetime was shown to be continuously extendable. It should be noted, however, that although the metric may admit continuous C^0-extendability across the Cauchy horizon, it may still be inextendible as a C^2 Lorentzian manifold, assuming higher regularity conditions are imposed. Hence, the Christoffel symbols can still fail to be square integrable.

On a linear level, the C^0 SCC, being the strongest inextendability statement, has been shown not to admit a blow up at $\mathcal{CH}^+$ even for the simpler Kerr or Reissner-Nordstrom solutions in asymptotically flat spacetime, given that the polynomially decaying scalar waves solving the Klein-Gordon equation propagate to the black hole interior. Similarly, boundedness at $\mathcal{CH}^+$ has also been demonstrated [132] for Kerr (and Reissner-Nordstrom)-dS spacetime with the decay rate here being exponential. Despite the growing interest in the subject of spacetime extendability in black hole interiors, all C^0 SCC formulations rely on classical geometric arguments and scalar wave decay rate estimations, making the SCC one of the few big problems in gravity yet to receive the quantum treatment. As such, Sections 4.4 and 4.5 constitute the first application of quantum complexity in this context.

4.4 Quantum Complexity and the C^0-stability

In the following we offer a brief introduction to quantum complexity and review the CV-duality in the context of AdS/CFT. We outline a newly-developed methodology of measuring complexity in terms of the flux of a conserved volume current. Having reviewed the C^0-formulation of the SCC (Conjecture 1), we study its implications on the interior of a Kerr-AdS black hole. Although some of the original results were derived for the case of an eternal two-sided Schwarzschild-AdS black hole, Figure 4.1, they have been shown to be valid for a large class of solutions.

4.4.1 Quantum Complexity

Black holes are efficient information scramblers. Quantum circuits models for black hole physics were first developed by Hayden and Preskill [133] to capture their chaotic dynamics. Comparison between black hole scrambling and circuit scrambling motivates us to think of black holes with entropy S as quantum circuits of size K such that $K \sim S$. Quantum computations are the application of unitary operators to a K-qubit system with the complexity of the task, $\mathcal{C}$ defined as the minimum number of gates that it takes to implement the operation.

Quantum complexity increases linearly for time exponential in the entropy $t_{\max} \sim e^S$, known as the classical recurrence time. At this point it saturates and remains at its maximum $\mathcal{C}_{\max} = e^S$ for $t_{\mathrm{qr}} \sim e^{e^S}$, known as the quantum recurrence time, and then fluctuates back to its initial low value [45].

The CV-duality [46] suggests the complexity of the boundary CFT is dual to the volume of the maximal spacelike hypersurface (i.e. codimension-one submanifold) which asymptotes to some time, anchored at the conformal AdS boundary, see Figure 4.1,

$$\mathcal{C} \sim \frac{V}{\hbar G_N l}, \tag{4.6}$$

where l is the characteristic AdS length scale, $\hbar = h/2\pi$ is the reduced Planck constant, and G_N denotes Newton's constant, where we assume $c = \hbar = G_N = 1$.

The CV-duality has been shown to hold for a wide class of theories and in arbitrary number of dimensions. Its validity has been demonstrated for the simplified setting of a (1+1)-dimensional Reissner-Nordstrom background in JT gravity [134], as well as for a $d = 3$ spherically symmetric BTZ-AdS black hole [135, 136]. Recently, a novel way for calculating the volume of maximal spacelike hypersurfaces in the bulk in terms of the flux of the volume current was suggested [137],

$$V_t = \int_{\Sigma_t} v \cdot \epsilon, \tag{4.7}$$

where ϵ is the spacetime volume element, and v denotes the unit timelike vector field orthogonal to the $t = \textit{constant}$ hypersurfaces anchored at the boundary. The

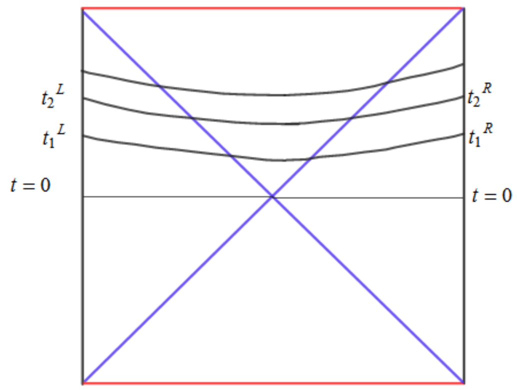

Figure 4.1: A diagram of an eternal two-sided Schwarzschild-AdS black hole. The black lines, denoted by t, describe the boundary Cauchy foliation by slices which are orthogonal to an asymptotic Killing flow yielding time translations, the blue lines indicate the horizons, and the red lines are the singularities. Throughout the chapter we will only focus on the upper ($t > 0$) part of the diagram.

way we think about t in this context is in terms of asymptotic time, i.e. null coordinate which is connected to the Minkowski polar coordinates as $t = r + \tau$ at past infinity, where τ denotes coordinate time, and r is the radial coordinate [122]. Here, $V(\Sigma_t)$ is simply the flux of the volume flow through the hypersurface Σ at boundary time t. The volume current method is valid under the assumption that the whole asymptotically AdS spacetime is foliated (without gaps) by a family of maximal spacelike hypersurfaces (i.e. Cauchy slices Σ_{t_i}) induced by the boundary foliation. As is well known, the CV-duality is intrinsically ill-defined and diverges at asymptotic infinity. This divergence, however, can easily be dealt with by (i) counting only the volume growth within the black hole interior, and (ii) focusing on the volume's time dependence. Following this prescription, one can formulate a pathology-free Second law of complexity and demonstrate that by calculating the volume change between neighboring Cauchy slices behind the horizon in terms of the flow of the volume current (in the black hole interior $r < r_+$ the volume flow is a future-pointing timelike vector, orthogonal to the maximal foliation) as we go to later slices, the interior volume can only grow, bounded from above by the complexity of the holographic CFT.

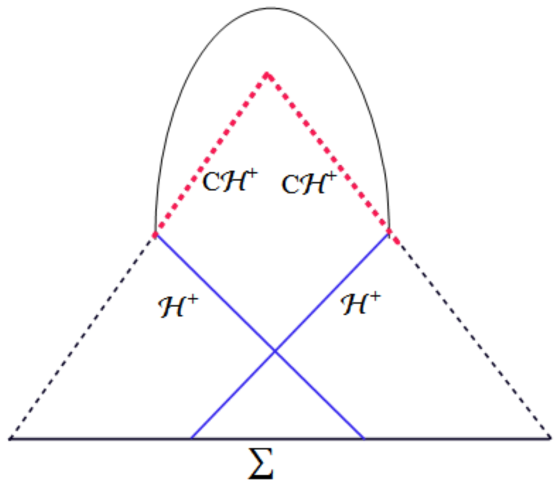

Figure 4.2: Maximum Cauchy evolution of asymptotically flat initial data on a spacelike hypersurface Σ. The region beyond the Cauchy horizon $\mathcal{CH}^+$ corresponds to the larger Lorentzian manifold. The figure was taken from [47].

4.4.2 C^0-instability: What if?

In light of this, the question we address is: What would a hypothetical validity of Conjecture 1 imply from a quantum complexity-theoretic perspective? As is well known, the inextendibility of the metric to a larger Lorentzian manifold $\tilde{\mathcal{M}}$ beyond $\mathcal{CH}^+$ even as a continuous C^0 suggests the Cauchy evolution is spacelike. Namely, the metric terminates at a singular finite boundary, meaning the region beyond $\mathcal{CH}^+$ does not exist. Essentially, this is the statement that timelike geodesics γ cannot reach $\tilde{\mathcal{M}} \setminus \mathcal{M}$.

Loosely speaking, the spacelike finite boundary, corresponding to the maximal Cauchy evolution, could effectively be interpreted as a migrated singularity, where the singularity now lies at some larger r, closer to the outer horizon $\mathcal{H}^+$. In [139], examining AMPS' firewall argument, Susskind proposed that black holes which have evaporated less than half of their initial entropy retain their regular horizon structures but have non-standard singularities instead. In particular, it was suggested that the growing von Neumann entropy of the Hawking radiation is what drives the singularity to migrate, and at late times coincide with the event horizon. This way, by migrating the spacelike finite boundary to coincide or be arbitrarily close to the maximal slice $\Sigma_{\max}$ and $\mathcal{CH}^+$, the Kerr solution obtains the well-defined determinism of the Schwarzschild subfamily.

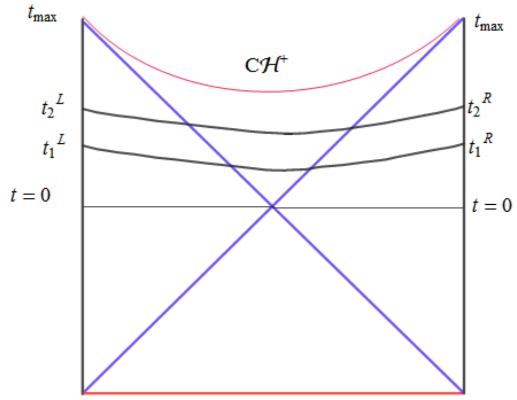

Figure 4.3: A zoomed portion of the upper $t > 0$ part (region II from Figure 1 in [138]) of a maximally-extended two-sided Kerr-AdS black hole, depicting $\mathcal{CH}^+$ as a migrated singularity. Here, $t_{\max}$ denotes the boundary foliation corresponding to $\mathcal{CH}^+$, where "max" refers to the latest slice (i.e. $\mathcal{CH}^+$), assuming Conjecture 1 is true and the spacetime terminates. Note that $\mathcal{CH}^+$ is depicted as a spacelike boundary for illustrative purposes only; in light of its interpretation as a migrated singularity.

To be more precise, suppose we have a subextremal Kerr-AdS black hole, where we require $M > 0$, $a \neq 0$ and $|a| < 1/l$

$$ds^2 = -\frac{\Delta_r}{\rho^2}\left[dt - \frac{a}{\Xi}\sin^2\theta d\phi\right]^2 + \frac{\rho^2}{\Delta_r}dr^2 + \frac{\rho^2}{\Delta_\theta}d\theta^2 + \frac{\sin^2\theta\Delta_\theta}{\rho^2}\left[adt - \frac{(r^2+a^2)}{\Xi}d\phi\right]^2. \tag{4.8}$$

where,

$$\rho^2 = r^2 + a^2\cos^2\theta$$
$$\Delta_\theta = 1 - l^2a^2\cos^2\theta \tag{4.9}$$
$$\Xi = 1 - l^2a^2$$

$l^2 = -\Lambda/3$ is the AdS curvature radius for negative cosmological constant $\Lambda < 0$, and $(r, t, \theta, \phi) \in \mathbb{R}^2 \times \mathbb{S}^2$ denote the coordinates which cover the black hole interior and the near-horizon region just outside the black hole. Here, the polynomial,

$$\Delta_r = (r^2 + a^2)(1 + l^2r^2) - 2Mr, \tag{4.10}$$

vanishes at $\mathcal{H}^+$, where $\mathcal{H}^+$ is a Killing horizon, and $\frac{M}{\Xi^2}$ is the ADM mass. Assuming the weak cosmic censorship, let $(M, a) \in \mathbb{R}^2_{>0}$ be non-degenerate for $|a| < 1/l$. Then, Eq.(4.10) has 2 real roots for $0 < r_- < r_+$, and the metric has both axial ∂_ϕ and timelike ∂_t Killing fields whose relation to the Killing vector field is the standard,

$$\xi = \partial_t + \Omega_{\mathcal{H}^+}\partial_\phi, \tag{4.11}$$

where $\Omega_{\mathcal{H}^+}$ is the angular velocity of $\mathcal{H}^+$. Let us now consider Figure 4.3. Given $\mathcal{CH}^+$ lies at some macroscopic distance from the ringlike curvature singularity r_s, we get,

$$r_s < r_c < M - \sqrt{M^2 - a^2}, \tag{4.12}$$

where r_c denotes the region between $\mathcal{CH}^+$ and the ringlike singularity. Then, assuming the validity of Conjecture 1, a non-negligible macroscopic region of the black hole interior will, essentially, be cut off. As we show in Section 4.5 below, this interior region cut off is very problematic.

4.5 Probing the C^0-instability

In this Section we study low-temperature black holes with hyperbolic horizons in asymptotically AdS spacetime, dual to CFTs living on hyperboloids. In this setting, we examine the C^0-form of the SCC from a quantum complexity-theoretic perspective and argue that if Conjecture 1 is true, then the CV-duality would be violated at late times. We demonstrate that the leading contribution to the interior volume comes from a Cauchy slice which lies in the r_c region between r_s and $\mathcal{CH}^+$, see Eq.(4.12). Given the generic quasi-periodic behavior of quantum complexity, the evolution of the black hole interior will be non-trivially modified. While a macroscopic part of the interior region is cut off, the corresponding complexity of the holographic CFT is expected to continue to evolve until it saturates, hence yielding a deviation from the standard bulk/boundary duality. Therefore, while the complexity of the boundary CFT continues to grow in time, the dual bulk volume will be prematurely saturated. To preserve the CV-duality, we conjecture that the metric must be C^0-extendable at least for as long as quantum complexity increases.

The gravitational dual of a CFT on a $(d-1)$-dimensional hyperboloid H_{d-1} is an AdS_{d+1} black hole with hyperbolic horizon geometry. We investigate the C^0-form of the SCC in the low-temperature limit of these solutions which have been shown to exhibit interesting thermodynamic features. Consequently, we demonstrate that inextendability of the interior metric as a C^0 beyond $\mathcal{CH}^+$ (as suggested by Conjecture 1) violates the CV-duality as it leads to $\mathcal{O}(1)$ variation in the bulk/boundary correspondence at late times. The hyperbolic AdS_{d+1} black hole has $\mathbb{R}^2 \times S^{d-1}$ topology and is given by the metric,

$$ds^2 = -f(r)dt^2 + \frac{dr^2}{f(r)} + \frac{r^2}{l^2}d\Sigma^2_{d-1}, \tag{4.13}$$

where for the hyperbolic CFT metric,

$$f(r) = -1 + \frac{r^2}{l^2} - \frac{M}{r^{d-2}}, \tag{4.14}$$

and

$$d\Sigma^2_{d-1} = l^2 dH^2_{d-1}, \tag{4.15}$$

where dH^2_{d-1} is the unit metric on the H_{d-1} hyperboloid. Here it is convenient to use the convention that lengths are measured in units of the curvature radius (i.e. $l = 1$) for simplicity of notation. The black hole's mass M and temperature T are defined, respectively as,

$$M = r_0^{d-2}(r_0^2 - 1), \tag{4.16}$$

and

$$T = \frac{r_0}{4\pi}\left(d - \frac{d-2}{r_0^2}\right).,\tag{4.17}$$

where for $M = 0$ we get $T = (2\pi)^{-1}$. In this set of coordinates, r_0 is the horizon, and in the near-horizon region $f(r) = 4\pi T(r - r_0)$, while in the asymptotic limit, $f(r) \to r^2/l^2$. We are interested in low-temperature $T = 0$, hyperbolic black holes for which there are solutions that admit regular r_- and r_+ horizons for a family of $-M$ terms. Interestingly, $T = 0$ hyperbolic black holes have global structure whose interior region resembles that of Reissner-Nordstrom, and has two well-defined horizons, similar to Eq.(4.8). We should note that in this respect the negative mass family is special since not all hyperbolic solutions have well-defined black hole configurations, and some have even been shown to break down at r_+. For instance, the $M = 0$ solution only covers part of the manifold (the outside black hole region), and hence is not useful for our considerations. For $T = 0$, in the hyperbolic scenario, there are minimum values for $-M$ and r_+ which are defined, respectively, as,

$$\begin{aligned} M_{\min} &= -\frac{2}{d-2}\left(\frac{d-2}{d}\right)^{d/2} l^{d-2}, \\ r_{\min} &= \left(\frac{d-2}{d}\right)^{3/2} l, \end{aligned} \tag{4.18}$$

where for $d = 4$ they read,

$$\begin{aligned} M_{\min} &= -\frac{l^2}{4}, \\ r_{\min} &= \frac{l}{\sqrt{2}}. \end{aligned} \tag{4.19}$$

Motivated by the CV-duality, the volume of a maximal spacelike hypersurface in $T = 0$ hyperbolic black hole background can be estimated by dividing the hypersurface Σ_{r_i} into individual segments, and approximating the local maximum of the radial function $f(r)$ (to be defined below) on each segment. Where in the hyperbolic AdS_{d+1} background Eq.(4.13), for $r \gg r_{\min}$, the metric asymptotes to an empty AdS_{d+1} solution, while in the near-horizon region, just outside the black hole, the metric is $\mathrm{AdS}_{d+1} \times H_{d-1}$. In this setting, each spacelike hypersurface decomposes as,

$$\Sigma_{t_i} = \Sigma_{\text{in}} \cup \Sigma_{\text{out}}. \tag{4.20}$$

.

Although in [140], $\Sigma_{\text{out}} \sim \Sigma_{\text{R}} \cup \Sigma_{\text{CQM}} \cup \Sigma_{\text{UV}}$, for our analysis we need not consider the details of the exterior components, and will focus only on the interior. As is the standard procedure in the literature, the volume of maximal $r = \textit{constant}$ spacelike hypersurfaces is generally given as,

$$r^{d-1}\sqrt{|f(r)|}, \tag{4.21}$$

where $f(r)$ is a "placeholder," and depends on the region whose contribution to the volume we wish to estimate. For the interior region of Eq.(4.13), $f(r)$ takes the form [141],

$$r^{d-1}\sqrt{\left|1-r^2+\frac{M_{\min}}{r^{d-2}}\right|}, \tag{4.22}$$

and is maximized in the region r_c, Eq.(4.12). It is important to note that for massive non-extremal black holes the region r_c can be arbitrarily big. Therefore, a significant part of the interior volume of low-temperature hyperbolic black holes is contributed by the region r_c, i.e. between $\mathcal{CH}^+$ and the ringlike singularity. The overall complexity of this family of solutions has been demonstrated to evolve as [140],

$$\Delta\mathcal{C}(t)=\frac{2\alpha}{\sqrt{d}}S\log(lT)^{-1}, \tag{4.23}$$

for small t, and at late times as,

$$\Delta\mathcal{C}(t)=\frac{2\alpha}{\sqrt{d}}S\log(lT)^{-1}+\frac{4\pi\alpha}{\sqrt{d}}STt. \tag{4.24}$$

Evidently, the growth rate of complexity is consistent with the classical predictions. Hence, as time goes on the bulk volume will saturate much earlier than the complexity of the dual CFT, yielding a discrepancy in the bulk/boundary description which will only accumulate at late times. Therefore, we conjecture that in order to preserve the complexity-theoretic gauge/gravity black hole framework, the interior metric must be extendable to a larger Lorentzian manifold across $\mathcal{CH}^+$ (i.e. Conjecture 1 must be false) for at least a classical recurrence time. Finally, we ought to draw the readers' attention to some conflicting recent results in the literature for different spacetimes. In [142, 143] the uniform boundedness and the continuity across the Cauchy horizon were demonstrated to remain valid in Reissner-Nordstrom-AdS spacetime for massive scalar waves solving the massive Klein-Gordon equation, assuming a sharp logarithmic decay rate. Despite these promising results invalidating the C^0 SCC, however, the question of boundedness remained open for other general spacetimes. On the other hand, a rigorous proof was presented recently [144], suggesting that if the black hole's mass and angular momentum satisfy some non-Diophantine conditions, then linear scalar perturbations (solving the Klein-Gordon equation) blow up at the Cauchy horizon. Thus, pointing towards a positive resolution of the C^0 SCC for a Kerr-AdS black hole, given the parameters admit Baire genericity. Interestingly, this instability was shown not to result from mere superradiance or blueshift effects but instead from a novel resonance phenomenon (i.e. relation between Diophantine approximation and black hole interiors) found in axisymmetric solutions.

4.6 Discussion

The application of quantum information theory to black holes provides novel insights that overturn widely held notions in GR. For instance, the classical Black hole area theorem states that surface area of a black hole does not decrease with time. We know now, however, that this doesn't hold when considering quantum phenomena such as Hawking radiation that violates the positive energy condition. Similar insights were garnered in attempts to reconcile GR with QM with the black hole information paradox and the firewall problem. In fact, a framework founded on quantum information theory is expected to play a central role in gravity and the emergence of spacetime.

In this spirit, our work examining the C^0 formulation of the SCC from an information theoretic perspective revisits ideas of complexity applied to black hole interiors in the same way quantum entropy redefined horizon area. By means of an example, we showed that in the low-temperature limit of a hyperbolic AdS_{d+1} black hole dual to a CFT living on a $(d-1)$-dimensional hyperboloid H_{d-1}, a significant contribution to the interior volume comes from the region past the inner horizon. Hence, the inextendability of the metric across $\mathcal{CH}^+$ if we imposed Conjecture 1, would lead to late-time violation of the CV-duality as proposed in AdS/CFT. To retain the CV-duality and save the bulk/boundary correspondence, we conjectured imposing a lower bound on metric extendability of order the classical recurrence time.

The AdS/CFT correspondence has also motivated several proposals of "gravitising" quantum mechanics. Notable proposals using the building blocks of quantum information to give rise to an emergent spacetime include [145, 146]. Furthermore, holographic entropy inequalities directly put constraints on the geometries which can emerge through entanglement in AdS/CFT. In future work we can derive insights on QG not only by treating emergent spacetimes by studying regions of allowed entropy space but also complexity space.

यच्च किञ्चिज्जगत्सर्वं दृश्यते श्रूयतेऽपि वा
अन्तर्बहिश्च तत्सर्वं-व्याँप्य नारायणः स्थितः॥

— नारायण सूक्तम

5

Signatures of Causality and Determinism in a Quantum Theory of Events

Contents

This chapter is based on a paper written in collaboration with Eduardo Dias and Vlatko Vedral. The author of this thesis applied quantum information theoretic measures to an event, defined as the moment of coincidence between detectors and the system.

5.1 Introduction

A recurrent theme in quantization efforts of gravity is the commensurate treatment of space and time. In standard quantum mechanics, position is an operator while time is an independent parameter. This asymmetry between space and time is further manifested in the absence of a tensor product description of temporally separated states. The former admits a description that utilizes the tensor product of Hilbert spaces of the subsystems, while an equivalent notion does not exist for the latter. Furthermore, recall that this tensor product structure, along with the quantum superposition principle, yields the property of entanglement between distinct physical systems. Nevertheless, despite the lack of an analogous mathematical construction in the treatment of time, QM also predicts nonclassical temporal correlations [51, 147–150]. These correlations — understood as an entanglement in time — concern timelike events, which refers to measurements performed at different times on the same physical system.

Many ascribe the conflicts between general relativity and QM to the asymmetric formulation discussed above and to our lack of awareness about the very nature of time. In this context, the identification of entanglement in time further encourages the search for a more balanced formulation of QM. Since temporal quantum correlations can also be accessed via Bell-like inequalities [150], one can expect QM to incorporate a tensor product structure for both spacelike events (SLE) and causally connected timelike events (TLE).

Following the above reasoning, proposals for a more symmetric approach to QM involve, for e.g., quantized instances of time called chronos [48], the framework of consistent histories [49, 51], pseudo-density matrices [50], super density operators [52], local event operators that act on Hilbert sub-spaces that are local in spacetime [151], and a quantum formalism of events [152]. It is worth noting that all these works, apart from [152], assume “instantaneous” measurements, so that unlike position, the considered events do not present any time-measurement uncertainty. In fact, for the instant of a measurement to be intrinsically uncertain, it is sufficient if the system under consideration were to travel a certain distance until it reaches the apparatus. A second possibility is that if the interaction time between the detector and the system is not short enough to neglect the evolution that the system would have undergone in the absence of measurements. The former consideration is known as the arrival time problem. It is worth noting that there is still no consensus on the best strategy to determine the arrival time, and that the formalism presented here can be applied to compute it. In addition, none of these formalisms exploit the tensor product structure to study quantum information theoretic aspects of events, especially the causally connected ones

With these motivations in mind, in contrast to previous approaches, barring Ref. [152], we describe spatial and temporal entanglement in the same theoretical framework: via a tensor product structure. We take into account the probabilistic character of the instant at which a measurement (or event) takes place. Although these two features were addressed in Ref. [152], here we use a slightly distinct approach, which encapsulates the super density operators of Ref. [52] as a particular case.

Our strategy lays impetus on the records obtained via the measurements performed by detectors and timers. These registers encompass information about the system under consideration, and of the moment this information was recorded respectively. As our formalism treats all events (measurements) on an equal footing, we will propose methods to characterize and even distinguish SLE and TLE. We reiterate that TLE are restricted to consecutive measurements of the same physical system. In contrast, the spacelike ones refer to independent measurements of two different systems (entangled or otherwise).

We utilize elements of Ref. [152] to recover a tensor product for TLE. Ref. [152] defines states of events by using the Hilbert spaces of the measured system, detectors and timers. Here however, we obtain an equivalent description for SLE and TLE by tracing out the system under measurement and focusing only on the detectors and timers. As a result, in departure from previous approaches, the theoretical framework used here allow us to extend quantum information (QI) tools [153, 154] to events as follows.

Firstly, in this chapter, we will revisit measures of coherence, applied in the context of events, to serve as an indicator of causality when one does not have information about the moment when the events occurred. We will also propose a correlation function of time operators that serves as an indicator of causality. While Ref. [50] outlines a measure of causality, their proposed extension of QM to include a tensor products description of temporally separated events — the so-called pseudo-density matrices (PDM) — results in states with negative eigenvalues.

Here, in contrast, we remain within the scope of traditional QM, with the simple addition of timers and detectors to our description. Secondly, we extend measures of classical correlation [54] and state discrimination criteria [155, 156] to events to quantify, for causally connected events, how much information we know about the outcomes of future events. In the limit of "instantaneous" measurements, we will verify a deterministic property that allows us to predict future events in the specific case of two TLE. Finally, the application of Bell's inequalities in our theoretical framework will also be addressed.

5.2 Describing Events in QM

Consider an event to be a measurement carried out by a detector $\mathcal{D}$ (micro/macroscopic), coupled with a timer $\mathcal{T}$, on a system $\mathcal{S}$. Let $\hat{H}_{\mathcal{S}}$ be the Hamiltonian of $\mathcal{S}$ associated with the degrees of freedom under measurement. In SLE, $\mathcal{S}$ is composed of two systems S_A and S_B (entangled or otherwise) that are measured once, independently. We denote the measurement on $\mathcal{S}_A$ ($\mathcal{S}_B$) by event A (event B). On the other hand, in TLE, we investigate causally connected events such that a single system $\mathcal{S}$ is measured twice. We call the first measurement "event A" and the second "event B." In both SLE and TLE, the observables of $\mathcal{S}$ are $\hat{\alpha}_j = \sum_{\alpha_j} \alpha_j |\alpha_j\rangle_{\mathcal{S}_j}\langle\alpha_j|$, with $j = A, B$.

To record the moment of occurrence of an event, one can consider a Salecker-Wigner-Peres-like timer $\mathcal{T}$ [157]. However, instead of being coupled with the system $\mathcal{S}$, as in Ref. [157], here $\mathcal{T}$ interacts with the detector in such a way $\mathcal{T}$ stops running when $\mathcal{D}$ measures $\mathcal{S}$. Thus, while $\mathcal{D}$ "is" in a ready state $|0\rangle_{\mathcal{D}}$, $\mathcal{T}$ evolves as an ideal clock by the Hamiltonian $\mathcal{H}_{\mathcal{T}}$. We also assume that the time scale of the interaction between the timer and detector is significantly smaller than the characteristic time $\Delta t_{\mathcal{SD}}$ of the measurement of $\mathcal{S}$ by $\mathcal{D}$. An interaction between $\mathcal{T}$ and $\mathcal{D}$ that models this physical picture is $\hat{V}_{\mathcal{TD}} = \mathcal{S} \otimes \hat{\mathrm{H}}_{\mathcal{T}} \otimes |0\rangle_{\mathcal{D}}\langle 0|$ [157], and the total Hamiltonian is $\hat{H} = \hat{H}_{\mathcal{S}} \otimes \mathcal{TD} + \hat{\mathrm{V}}_{\mathcal{SD}} + \hat{\mathrm{V}}_{\mathcal{TD}}$, where $\hat{V}_{\mathcal{SD}}$ is the interaction potential between $\mathcal{S}$ and $\mathcal{D}$. Also, let the timer's observable $\hat{T}$ be such that $\hat{T}|t\rangle_{\mathcal{T}} = t|t\rangle_{\mathcal{T}}$ and $[\hat{T}, \hat{H}_{\mathcal{T}}] = i\hbar$.

By considering a pair of $\mathcal{TD}$ to perform two measurements, regardless of the type of events, the initial condition of the full state is,

$$|\psi(t_0)\rangle = |\varphi(t_0)\rangle_{\mathcal{S}} \otimes |t_0, 0\rangle_A \otimes |t_0, 0\rangle_B \tag{5.1}$$

Here, $|\varphi(t_0)\rangle_{\mathcal{S}}$ is the initial state of $\mathcal{S}$ and $|t_0, 0\rangle_j = |t_0\rangle_{\mathcal{T}_j} \otimes |0\rangle_{\mathcal{D}_j}$ $(j = A, B)$, with $|t_0\rangle_{\mathcal{T}_j}$ being the initial state of the timer $\mathcal{T}_j$ and $|0\rangle_{\mathcal{D}_j}$ the ready state of the detector $\mathcal{D}_j$. Notice that $\mathcal{T}_j\mathcal{D}_j$ register information associated with the event j: for SL events, event j represents the measurement of $\mathcal{S}_j$, whereas for TL events, event j represents the measurement j of $\mathcal{S}$ (with A happening first). To avoid dense notation, we will refrain from using $\otimes$.

To compute $|\psi(t)\rangle = \exp\{-i(t-t_0)\hat{H}/\hbar\}|\psi(t_0)\rangle$, let us break up the Schrodinger evolution into infinitesimal steps $\delta t \ll \Delta t_{\mathcal{SD}}$, so that the eigenvalues of $\mathcal{T}$ (denoted t) in this discrete evolution are $t_0, t_{(1)}, \ldots, t_{(N)}, \ldots$, with $\delta t = t_{(k+1)} - t_{(k)}$. Now, in order to describe two SLE, we model two independent measurements of two systems $\mathcal{S}_A$ and $\mathcal{S}_B$ such that in the first step $t_{(1)}$, the full initial state splits into four branches given by

$$\begin{aligned}
|\psi(t_{(1)})\rangle &= \sqrt{q^A_{(1)} q^B_{(1)}}\ \mathrm{e}^{i(\varphi^A_{(1)}+\varphi^B_{(1)})}|\varphi(t_{(1)})\rangle_{\mathcal{S}}|t_{(1)}, 0\rangle_A|t_{(1)}, 0\rangle_B \\
&+\sqrt{\delta p^A_{(1)}\ q^B_{(1)}}\ \mathrm{e}^{i\varphi^B_{(1)}}\sum_{\alpha_A}\hat{M}^A_{\alpha_A}|\varphi(t_{(1)})\rangle_{\mathcal{S}}\ |t_{(1)}, \alpha_A\rangle_A|t_{(1)}, 0\rangle_B \\
&+\sqrt{q^A_{(1)}\ \delta p^B_{(1)}}\ \mathrm{e}^{i\varphi^A_{(1)}}\sum_{\alpha_B}\hat{M}^B_{\alpha_B}|\varphi(t_{(1)})\rangle_{\mathcal{S}}\ |t_{(1)}, 0\rangle_A|t_{(1)}, \alpha_B\rangle_B \\
&+\sqrt{\delta p^A_{(1)}\delta p^B_{(1)}}\sum_{\alpha_A,\alpha_B}\hat{M}^{AB}_{\alpha_A,\alpha_B}|\varphi(t_{(1)})\rangle_{\mathcal{S}}|t_{(1)}, \alpha_A\rangle_A|t_{(1)}, \alpha_B\rangle_B,
\end{aligned} \tag{5.2}$$

where $\delta p^j_{(1)} \ll 1$ $(q^j_{(1)} = 1 - \delta p^j_{(1)})$ is the probability of $\mathcal{S}_j$ being (not being) measured in the interval $(t_0, t_{(1)}]$. $\varphi^j_{(1)}$ is the phase associated with the undetected branch of $\mathcal{S}_j$. Here $\hat{M}^A_{\alpha_A} = \hat{M}_{\alpha_A} \otimes$ B, $\hat{M}^B_{\alpha_B} =$ A $\otimes \hat{\mathrm{M}}_{\alpha_B}$, $\hat{M}^{AB}_{\alpha_A,\alpha_B} = \hat{M}_{\alpha_A} \otimes \hat{M}_{\alpha_B}$, with $\hat{M}_{\alpha_j} = |\alpha_j\rangle_j\langle\alpha_j|$. Also, $|\varphi(t_{(1)})\rangle_{\mathcal{S}} = \hat{U}_{\mathcal{S}}(t_{(1)}, t_0)|\varphi(t_0)\rangle_{\mathcal{S}}$ where $\hat{U}_{\mathcal{S}}(t_{(1)}, t_0) = \exp\{-i(t_{(1)} - t_0)\hat{H}_{\mathcal{S}}/\hbar\}$. For simplicity we consider that the detectors interact equally with both systems and also with each state $|\alpha_j\rangle_{\mathcal{S}_j}$.

Inspecting Eq.(5.2), we note that in the first branch the detectors do not record any information about $\mathcal{S} = \mathcal{S}_A + \mathcal{S}_B$ with a high probability $q^A_{(1)}q^B_{(1)} = (1 - \delta p^A_{(1)})(1 - \delta p^B_{(1)})$. Thus, the timers will continue to evolve as an ideal quantum clock. In the second branch, with probability $\delta p^A_{(1)}(1 - \delta p^B_{(1)})$, $\mathcal{D}_A$ measures $\mathcal{S}_A$ and

$\mathcal{D}_B$ does not measure $\mathcal{S}_B$, thus $\mathcal{T}_A$ stops running and records the instant of the event A, $t_{(1)}$. In the third branch, the opposite happens. In the last branch both systems are measured in the interval $(t_{(0)}, t_{(1)}]$ and both timers register $t_{(1)}$.

Before proceeding to the next steps of the evolution, we note that the Stern-Gerlach's experiment fits the description of Eq.(5.2). Here, a particle (system $\mathcal{S}$) is subjected to a magnetic field [interaction encompassed in $\hat{U}_{\mathcal{S}}(t_{(1)}, t_0)$] and then detected. For two events, we have two independent Stern-Gerlach's devices, one for each particle. In this context, the branches of $|\psi(t_{(1)})\rangle$ in which the particle is not measured arise from both the uncertainty of the particle's arrival time at the detector and the moment of the detector click, whose duration depends on its interaction with the particle. The click can simply be the transition from the initial state of the detector to an orthogonal one, at which moment, the timer stops running.

We are interested in $|\psi(t)\rangle$ from the moment we can guarantee both $\mathcal{S}_A$ and $\mathcal{S}_B$ have been measured. Thus, we evaluate $|\psi(t_{(N)})\rangle$ when $t_{(N)} \gtrapprox t_0 + t_{\text{a.t.}} + \Delta t_{\mathcal{SD}}$, where $t_{\text{a.t.}}$ is the typical arrival time at the detector. Here, in the continuous limit, WLOG we take $t_{(N)} \to \infty$ [$|\psi_e\rangle \equiv |\psi(t_{(N)} \to \infty)\rangle$] to ensure that the system has completed its interaction with the detector. Note that, we do not invoke environment induced decoherence and consider the complete unitary description of the system-detectors-timers' interactions. Now,

$$|\psi_\varepsilon\rangle = \sum_{\alpha_A, \alpha_B} \int_{t_0}^{\infty} \int_{t_0}^{\infty} dt_A dt_B \; |\Phi_\varepsilon(t_A, \alpha_A; t_B, \alpha_B)\rangle_{\mathcal{S}} \otimes |t_A, \alpha_A\rangle_A \; |t_B, \alpha_B\rangle_B, \tag{5.3}$$

where ε=SL labels SLE. As our interest lies in measurement outcomes recorded by $\mathcal{T}_A\mathcal{D}_A$ and $\mathcal{T}_B\mathcal{D}_B$, we trace out $\mathcal{H}_{\mathcal{S}}$, yielding

$$\hat{\rho}_\varepsilon = \sum_{\alpha_A, \alpha_B} \int_{t_0}^{\infty} \int_{t_0}^{\infty} dt_A dt_B \sum_{\alpha'_A, \alpha'_B} \int_{t_0}^{\infty} \int_{t_0}^{\infty} dt'_A dt'_B \; \mathrm{Tr}_{\mathcal{S}}\Big\{ |\Phi_\varepsilon(t_A, \alpha_A; t_B, \alpha_B)\rangle_{\mathcal{S}} \langle \Phi_\varepsilon(t'_A, \alpha'_A; t'_B, \alpha'_B)| \Big\} \; |t_A, \alpha_A\rangle_A \; |t_B, \alpha_B\rangle_B \; {}_A\langle t'_A, \alpha'_A| \; {}_B\langle t'_B, \alpha'_B|, \tag{5.4}$$

which describes the events A and B with

$$\begin{aligned}
&|\Phi_{\rm SL}(t_A,\alpha_A;t_B,\alpha_B)\rangle_{\mathcal{S}} = \chi_{\rm SL}(t_A,t_B)\\
&\Big[\Theta(t_B,t_A)\hat{U}_{\mathcal{S}}(t_{(N)},t_B)\hat{M}^B_{\alpha_B}\ \hat{U}_{\mathcal{S}}(t_B,t_A)\hat{M}^A_{\alpha_A}\hat{U}_{\mathcal{S}}(t_A,t_0)\\
&+\Theta(t_A,t_B)\hat{U}_{\mathcal{S}}(t_{(N)},t_A)\ \hat{M}^A_{\alpha_A}\hat{U}_{\mathcal{S}}(t_A,t_B)\hat{M}^B_{\alpha_B}\hat{U}_{\mathcal{S}}(t_B,t_0)\\
&+\delta(t_B-t_A)\ \hat{U}_{\mathcal{S}}(t_{(N)},t_A)\ \hat{M}^{AB}_{\alpha_A,\alpha_B}\ \hat{U}_{\mathcal{S}}(t_A,t_0)\Big]|\varphi(t_0)\rangle_{\mathcal{S}}.
\end{aligned} \tag{5.5}$$

Here $t_{(N)} \to \infty$, $\chi_{\rm SL}(t_A,t_B) = \chi_A(t_A)\chi_B(t_B)$, $\chi_j(t_j)$ is the probability density amplitude for $\mathcal{S}_j$ to be measured at the instant t_j, regardless of the outcome α_j, and $\Theta(t_x,t_y)=1$ for $t_x > t_y$, or 0 otherwise. Note, in general situations, $\chi_{\rm SL}(t_A,t_B)$ is non-separable. Inspecting Eqs. (5.4) and (5.5), we observe a superposition of measurements of $\mathcal{S}_A$ and $\mathcal{S}_B$ in an indefinite order. In the second (third) line of Eq.(5.5), $\mathcal{S}_A$ ($\mathcal{S}_B$) is measured first. In the last branch, $\mathcal{S}_A$ and $\mathcal{S}_B$ is measured "simultaneously" in accordance with the coarse-grained nature of the evolution.

In Eq.(5.5), $\chi_j(t_j)$ is the continuous limit of the amplitude

$$\tilde{\chi}_j(t_{(k)},t_{(k-1)}) = \sqrt{\delta p^j_{(k)}}\ \prod_{\ell=1}^{k-1}\sqrt{1-\delta p^j_{(\ell)}}\ \mathrm{e}^{i\varphi^j_{(\ell)}}, \tag{5.6}$$

whose modulus squared is the probability of $\mathcal{S}_j$ being measured in the interval $(t_{(k-1)},t_{(k)}]$. Notice that the outcome of the product operator in (5.6) represents the probability for $\mathcal{S}_j$ not to be measured in the interval $(t_0,t_{(k-1)}]$. To obtain the continuous limit $\chi_j(t_j)$, we can use the relation $|\chi_j(t_{(k)})|^2\ dt = |\tilde{\chi}_j(t_{(k+1)},t_{(k)})|^2$.

For the simplest case where $\delta p^j_{(k)} = \delta p_j \ll 1$, the relation $|\chi_j(t_{(k)})|^2\ dt = |\tilde{\chi}_j(t_{(k+1)},t_{(k)})|^2$ becomes

$$\begin{aligned}
\delta p_j(1-k\delta p_j) &\approx |\chi_j(t_{(k)})|^2\ \delta t\\
\Rightarrow (\delta p_j/\delta t)\mathrm{e}^{-k\delta p_j} &\approx |\chi_j(t_{(k)})|^2
\end{aligned} \tag{5.7}$$

By defining $\delta p_j = \gamma_j\delta t$ and recalling that $t_{(k)} - t_0 = k\delta t$, we have,

$$\chi_j(t_j) = \begin{cases} \sqrt{\gamma_j}\mathrm{e}^{-\gamma_j(t_j-t_0)/2} & \text{for } t_j \geq t_0\\ 0 & \text{otherwise.}\end{cases} \tag{5.8}$$

Equation (5.8) is the time probability amplitude for the measurements of a decay photon. To understand this exponential dependence of χ, first recall that from standard calculations in QM, the probability for an atom initially excited measured at time t_j to be found in the ground state is $\propto 1 - \mathrm{e}^{-\gamma_j(t_j - t_0)/2}$. Then, as it is an irreversible process, the time probability density of decay is simply $\propto -d(\mathrm{e}^{-\gamma_j(t_j-t_0)/2})/dt$, i.e., $\propto |\chi_j(t_j)|^2$ above. In this specific example, the computation of $|\chi_j(t_j)|^2$ is straightforward since the decay is not affected by both the photon measurement and register of the time at which this detection happens.

We note that Eqs. (5.4) and (5.5) can describe, e.g., polarization measurements (and the instant at which these detections occur) of spontaneous decays. Here entangled atoms can emit photons that pass through beam splitters (interaction encompassed in $\hat{H}_{\mathcal{S}}$) before the measurement. Besides, the polarization can also change via $\mathcal{H}_{\mathcal{S}}$ during its measurement. If the entanglement did not affect the decay times, $\chi_{\mathrm{SL}}(t_A, t_B) = \chi_A(t_A)\chi_B(t_B)$. The first reason for this last statement is that the probability for an excited atom to decay in the interval $(t_0, t_{(k)}]$ is proportional to $|\chi_j(t_j)|^2$. Then, as it is an exponential function, the time probability *density* of decay is also $\propto |\chi_j(t_j)|^2$. It is worth pointing out that in this specific example, the computation of $|\chi_j(t_j)|^2$ is straightforward since the decay is a irreversible process and not affected by both the photon measurement and register of the time at which this detection happens.

Finally, one can verify that $\hat{\rho}_\varepsilon$ of Eq.(5.4) can also be applied to TLE ($\varepsilon =$TL), specifically, in the situation where a single system $\mathcal{S}$ is measured twice [152]. Assuming the second measurement (event B) begins soon after the first measurement (event A), we have

$$\begin{aligned} &|\Phi_{\mathrm{TL}}(t_A, \alpha_A; t_B, \alpha_B)\rangle_{\mathcal{S}} = \chi_{\mathrm{TL}}(t_A, t_B)\Theta(t_B > t_A) \\ &\hat{U}_{\mathcal{S}}(t_{(N)}, t_B)\hat{M}_{\alpha_B}\hat{U}_{\mathcal{S}}(t_B, t_A)\hat{M}_{\alpha_A}\hat{U}_{\mathcal{S}}(t_A, t_0)|\varphi(t_0)\rangle_{\mathcal{S}}, \end{aligned} \tag{5.9}$$

where $\chi_{\mathrm{TL}}(t_A, t_B) = \chi_B(t_B|t_A)\,\chi_A(t_A)$, with $\chi_A(t_A)$ as previously discussed. $\chi_B(t_B|t_A)$ is the probability amplitude for the second event to take place at time t_B, given the first measurement happens at t_A. Analogous to SLE, Eqs. (5.4) and (5.9) also describe the experiment involving Stern-Gerlach devices, as well as the spontaneous decay discussed above. However, for TLE, we should have two consecutive SG setups (or beam splitters) measuring the same system $\mathcal{S}$. In the simpler case where the uncertainty in detection time is negligible (χ_j is a Dirac delta function), the timers can be neglected and we recover the formalism of super-density operators [52].

5.3 Signatures of Causality in QM

We analyze the simpler case in which the uncertainty in the detection time (or the duration of the measurement) is negligible. In this case, χ_j is sharp enough to be taken as a Dirac delta function, and $\hat{H}_{\mathcal{S}}$ can be neglected during the measurement; as a result, $\hat{\rho}_\varepsilon$ is represented at a single well-defined instant of time. This time-independent description is also observed when $\mathcal{S}$ is stationary during the measurement ($\chi_j \neq 0$). In these situations the timers can be neglected. It is worth mentioning that in this limit, we recover the formalism of super-density operators [52]. Nevertheless, we will investigate this case in a context different from that of Ref. [52].

In the absence of timers, the detector could be as simple as a two-level atom prepared in the ground state and positioned in one of the arms of the Stern-Gerlach apparatus. For instance, in a specific branch of $|\psi_\varepsilon\rangle$, the atom is excited by coupling to the spin-up particle, and it is left in the ground state in the other branch where the particle is in the spin-down configuration.

We proceed to juxtapose SLE and TLE with only the information gleaned from $\mathcal{D}_A$ and $\mathcal{D}_B$. For two SLE, Eq.(5.4) becomes,

$$\hat{\rho}_{\mathrm{SL}} = \sum_{\alpha_A.\alpha_B} \langle \alpha_A, \alpha_B | \hat{\rho}_{\mathcal{S}} | \alpha_A, \alpha_B \rangle | \alpha_A, \alpha_B \rangle_{AB} \langle \alpha_A, \alpha_B |, \tag{5.10}$$

where $|\alpha_A, \alpha_B\rangle = |\alpha_A\rangle_{\mathcal{S}_A} |\alpha_B\rangle_{\mathcal{S}_B}$. Henceforth, we drop the label $\mathcal{S}_j$ in $|\alpha_j\rangle_{\mathcal{S}_j}$. In the absence of timers, the detector could be a simple two-level atom prepared in the ground state, positioned in an arm of the SG apparatus.

Similarly, utilizing the same picture for two TLE, and allowing the system to evolve between measurements via the unitary operation $\hat{U} = \hat{U}_{\mathcal{S}}$, Eq.(5.4) becomes

$$\hat{\rho}_{\mathrm{TL}} = \sum_{\alpha_A, \alpha'_A} \sum_{\alpha_B} \langle \alpha_B | \hat{U} | \alpha_A \rangle \langle \alpha_A | \hat{\rho}_{\mathcal{S}} | \alpha'_A \rangle \langle \alpha'_A | \hat{U}^\dagger | \alpha_B \rangle \\ | \alpha_A, \alpha_B \rangle_{AB} \langle \alpha'_A, \alpha_B |. \tag{5.11}$$

From Eqs. (5.10) and (5.11), the distinction between SLE and TLE becomes apparent: $\hat{\rho}_{\mathrm{SL}}$ is diagonal in the eigenbasis of the measured observable $\hat{A}_j$, whereas $\hat{\rho}_{\mathrm{TL}}$

contains off-diagonal terms associated with the Hilbert subspace of $\mathcal{D}_A$. Obviously, for $\hat{\rho}_{\mathrm{TL}}$ to maintain its coherence, one should prevent the detectors from decoherence. We are led to the striking conclusion that by simply analyzing the state of the detector (without any information of when and how the events happened), the presence of coherence in $\hat{\rho}_\varepsilon$ indicates a causal relation between the events. Note that it is possible to choose a unitary $\hat{U}$ that destroys these coherence terms in the case of TLE, thereby rendering SLE and TLE indistinguishable. In Ref. [50], the trace norm of the PDM reveals a causal relation between the events. In a similar fashion, here, measures of coherence such as the relative entropy of coherence serve the analogous purpose.

We now proceed to augment the discussion on causality to take into account the uncertainty of the moment of measurement. If the events have non-negligible temporal uncertainty and $\mathcal{S}$ is non-stationary, but the experimentalist lacks access to information recorded by the timers, we should trace the timers out from $\hat{\rho}_\varepsilon$. Here one can confirm that coherence still only exists for $\varepsilon = \mathrm{TL}$. See Eqs. (D.1) and (D.5) in the Appendix D for a visualization.

Finally, for the general event in Eq.(5.4), where the experimentalist learns what the timers register, we consider the following correlation function to differentiate SLE from TLE,

$$C^{\varepsilon}_{AB}(\hat{T}) = \left\langle (\hat{T}_A - \langle \hat{T}_A \rangle_\varepsilon)(\hat{T}_B - \langle \hat{T}_B \rangle_\varepsilon) \right\rangle_\varepsilon . \tag{5.12}$$

$C^{\varepsilon}_{AB}(\hat{T})$ is computed for the state of Eq.(5.4) as follows,

$$\begin{aligned} C^{\mathrm{TL}}_{AB}(\hat{T}) &= \int_{t_0}^{\infty} dt_A t_A |\chi_A(t_A)|^2 \ \mathrm{E}(\hat{T}_B|t_A) \\ &- \int_{t_0}^{\infty} dt_A \ t_A |\chi_A(t_A)|^2 \times \int_{t_0}^{\infty} dt_A |\chi_A(t_A)|^2 \ \mathrm{E}(\hat{T}_B|t_A) \\ &\equiv \langle fg \rangle_{\chi_A} - \langle f \rangle_{\chi_A} \langle g \rangle_{\chi_A} \geq 0 \end{aligned} \tag{5.13}$$

where $\mathrm{E}(\hat{T}_B|t_A) = \int_{t_A}^{\infty} dt_B t_B |\chi_A(t_B|t_A)|^2 > t_A \ \forall t_A$, $f = t_A$, and $g = \mathrm{E}(\hat{T}_B|t_A)$. In the final line of Eq.(5.13), we apply the Chebyshev-Harris inequality [158] for the distribution χ_A.

In SLE with a separable $\chi_{\rm SL}(t_A,t_B)=\chi_A(t_A)\chi_B(t_B)$, the measure is trivially 0 as the probability amplitude of the second event is not conditional upon the moment of occurrence of the first event. In this case the normalization of the probability amplitude coupled with the above independence yields straightforwardly $C^{\rm SL}_{AB}(\hat{T})=0$.

We verify $C^{\varepsilon}_{AB}(\hat{T})>0$ for TLE and is zero for SLE discussed above. To elaborate this suggests, in two causally connected measurements, if the first measurement occurs earlier (later) than its expected time of occurrence, the second one will also (on average) happen earlier (later), resulting in a positive $C^{\rm TL}_{AB}(\hat{T})$.

5.4 QI of Events and Determinism in QM

In spatially entangled systems, one can quantify the information gained about one subsystem given some measurement of the other. Our focus on detectors and timers allows us to similarly quantify, for causally connected events, how much information we know about the future (spatial analogue of the unobserved system) given some information about the past (analogous to observed spatial subsystem). For SLE, the standard interpretation [54, 153, 154, 156] holds.

Again, for simplicity, let us consider the case where χ is very short allowing us to neglect the timers. To analyze equations Eqs. (5.10) and (5.11) in the context of QI [54, 156], we rewrite them in the format

$$\hat{\rho}_{\varepsilon}=\sum_{\alpha_B} p^{\varepsilon}_{\alpha_B}\ \hat{\sigma}^{\varepsilon}_{A,\alpha_B}\otimes|\alpha_B\rangle_B\langle\alpha_B|, \tag{5.14}$$

where, for SLE, we have

$$\hat{\sigma}^{\rm SL}_{A,\alpha_B}=\frac{1}{p^{\rm SL}_{\alpha_B}}\sum_{\alpha_A}\left|\langle\alpha_A,\alpha_B|\varphi(t_0)\rangle_{\mathcal{S}}\right|^2\ |\alpha_A\rangle_A\langle\alpha_A|, \tag{5.15}$$

with $p^{\rm SL}_{\alpha_B}=\sum_{\alpha_A}\left|\langle\alpha_A,\alpha_B|\varphi(t_0)\rangle_{\mathcal{S}}\right|^2$, and for TLE, we have

$$\hat{\sigma}^{\rm TL}_{A,\alpha_B}=|\lambda_{\alpha_B}\rangle_A\langle\lambda_{\alpha_B}|, \tag{5.16}$$

with $|\lambda_{\alpha_B}\rangle_A=1/\sqrt{p^{\rm TL}_{\alpha_B}}\sum_{\alpha_A}\langle\alpha_B|\hat{U}|\alpha_A\rangle\langle\alpha_A|\varphi(t_0)\rangle_{\mathcal{S}}|\alpha_A\rangle_A$ and $p^{\rm TL}_{\alpha_B}=\sum_{\alpha_A}|\langle\alpha_B|\hat{U}|\alpha_A\rangle|^2\ |\langle\alpha_A|\varphi(t_0)\rangle_{\mathcal{S}}|^2$. Notice that $p^{\varepsilon}_{\alpha_B}$ is the probability of $\mathcal{D}_B$ measuring α_B regardless of the value of α_A measured by $\mathcal{D}_A$.

Now, recall Eq.(5.14) and consider that Alice observes $\mathcal{D}_A$ in her laboratory to learn the state of $\mathcal{S}$ while being agnostic to the causal nature of the events. As long as $\mathcal{D}_A$ does not undergo decoherence, Alice can measure $\mathcal{D}_A$ in a basis different from $\{|\alpha_A\rangle_A\}$, which stores information about the states $\{|\alpha_A\rangle\}$ of $\mathcal{S}$. Assuming that Bob always measures $\mathcal{D}_B$ in the basis $\{|\alpha_B\rangle_B\}$, we observe from Eq.(5.14) that Alice can infer the eigenvalue α_B measured by Bob by trying to discriminate between the different states $\hat{\sigma}^{\varepsilon}_{A,\alpha_B}$ of her detector. In particular, for two level systems $\alpha_B = 1, 2$, Alice's highest probability of success is given by $p_{\text{suc}} = 1/2(1 + \text{Tr}|p^{\varepsilon}_2\hat{\sigma}^{\varepsilon}_{A,1} - p^{\varepsilon}_1\hat{\sigma}^{\varepsilon}_{A,2}|)$ according to Helstrom's discrimination criteria. The projection operators with the highest probability of success satisfy constraints outlined in [156]. Note that we are employing QI tools to characterize the detectors' states, instead of the usual application on the systems under measurement. As we will discuss below, this approach allows us to extend the existing information measures and QI protocols to TLE.

Reference [54] provides a way to compute the largest amount of information gained by Alice about Bob's observation. This quantity is a classical correlation function which when employed to our case yields $C_A(\hat{\rho}^{\varepsilon}_B) = \max_{\hat{M}^{\dagger}_{A,i}\hat{M}_{A,i}}\{S(\hat{\rho}^{\varepsilon}_B) - \sum_i\ p_i\ S(\hat{\rho}^{\varepsilon}_{B,i})\}$, where $\hat{\rho}^{\varepsilon}_B = \text{Tr}_A\hat{\rho}_{\varepsilon}$, $\hat{\rho}^{\varepsilon}_{B,i} = \text{Tr}_A(\hat{M}_{A,i}\hat{\rho}_{\varepsilon}\hat{M}^{\dagger}_{A,i})/p_i$ is the state of $\mathcal{D}_A$ after the outcome i is observed by Alice, and $p_i = \text{Tr}_{AB}(\hat{M}_{A,i}\hat{\rho}_{\varepsilon}\hat{M}^{\dagger}_{A,i})$. In [54], C_A was proposed only for SLE, in which its evaluation involved the state of the system under detection [i.e., $C_A(\hat{\rho}_{\mathcal{S}_B})$] and not the states of the detectors as considered here. In SLE, the primary difference between C_A here and that from Ref. [54] is that we compute the correlations between measurement records of subsystems of $\mathcal{S}$ $[C_A(\hat{\rho}^{\varepsilon}_B)]$ and not correlations between subsystems of $\mathcal{S}$. We give an example of Eq.(5.14) and C_A for SLE and TLE as follows.

Consider a spin-half system $\mathcal{S}$, initially in the state $|\varphi(t_0)\rangle_{\mathcal{S}} = |+_x\rangle$, evolving according to $\hat{U} = \exp\{i\pi\sigma_x/4\}$, and subsequently measured in the $\hat{S}_y$ basis by $\mathcal{D}_B$. By knowing this configuration, Alice can predict the outcome measured by $\mathcal{D}_B$ (seen by Bob) by setting $\mathcal{D}_A$ to previously measure $\mathcal{S}$ in the basis $\hat{S}_z$ so that $|\lambda_{+_y}\rangle_A = |+_z\rangle_A$ and $|\lambda_{-_y}\rangle_A = |-_z\rangle_A$. Thus, Eq.(5.14) becomes $\hat{\rho}_{\text{TL}} = 1/2(|+_z\rangle_A\langle +_z| \otimes |+_y\rangle_B\langle +_y| + |-_z\rangle_A\langle -_z| \otimes |-_y\rangle_B\langle -_y|)$, where we verify that, before (after) Bob's observation, if Alice measures $|\pm_z\rangle_A$, she knows Bob will measure (measured) $|\pm_y\rangle_B$. In this manner, Alice looks at a past record in such a way as to precisely learn about a future record. Finally, in Appendix D we show that if the events have non negligible χ but Alice and Bob lack access to the timers, the previous discussion about Alice's predictions still hold.

For SLE, consider $|\varphi(t_0)\rangle_{\mathcal{S}} = \sum_\alpha c_\alpha |\alpha_A\rangle|\alpha_B\rangle$. Thus, Eq.(5.14) becomes $\hat{\rho}_{\mathrm{SL}} = \sum_\alpha |c_\alpha|^2 |\alpha_A\rangle_A\langle\alpha_A| \otimes |\alpha_B\rangle_B\langle\alpha_B|$. Thus clearly the best measurement is in $\{|\alpha_A\rangle\}_A$ of $\mathcal{D}_A$, which results in $C_A(\hat{\rho}_B^{\mathrm{SL}}) = -\sum_\alpha |c_\alpha|^2 \log|c_\alpha|^2$. Analogously for TLE this happens when, e.g., the initial condition is $|\varphi(t_0)\rangle_{\mathcal{S}} = \sum_\alpha c_\alpha|\alpha\rangle$, $\hat{U} =$, and the same observable is measured twice.

We present an interpretation of Alice's prediction for TLE in the following. Recall that for TLE, $\mathcal{D}_A$ and $\mathcal{D}_B$ in Eq.(5.14) record information about the same system $\mathcal{S}$ at an earlier and later time, respectively. Thus, we can say that Alice's guess about the state measured by Bob is a prediction of a future measurement of $\mathcal{S}$, which refers to the knowledge Bob gains while measuring $\mathcal{D}_B$ in the basis $\{|\alpha_B\rangle_B\}$. Recall that $\mathcal{D}_B$ records the value α_B of $\mathcal{S}$. In this manner, by fixing the evolution $\hat{U}$ and the observables of $\mathcal{S}$ measured by $\mathcal{D}_A$ and $\mathcal{D}_B$, Alice can predict the future event of $\mathcal{S}$ (measurement performed by $\mathcal{D}_B$ and checked later by Bob) by measuring $\mathcal{D}_A$ (by observing a past record) in the basis $\{|\lambda_{\alpha_B}\rangle_A\}$, with a probability of success given by p_{suc}. Unlike $\hat{\sigma}^{\mathrm{SL}}_{A,\alpha_B}$, $\hat{\sigma}^{\mathrm{TL}}_{A,\alpha_B}$ is a pure state and hence p_{suc} for a two-level system becomes the original Helstrom's discrimination $p_{\mathrm{suc}} = 1/2(1+\sqrt{1-4p_1p_2|_A\langle\lambda_1|\lambda_2\rangle_A|^2})$ [155]. In general the states of the set $\{|\lambda_{\alpha_B}\rangle_A\}$ are not orthogonal.

If ${}_A\langle\lambda_{\alpha_B}|\lambda_{\alpha'_B}\rangle_A = \delta_{\alpha_B,\alpha'_B}$, $p_{\mathrm{suc}} = 1$ and Alice can predict deterministically what Bob will learn, or learned, about $\mathcal{S}$. Taking a different perspective from the above point of view, let us consider that the observable measured by $\mathcal{D}_{\mathcal{A}}$ is not predetermined. So, given $\hat{U}_{\mathcal{S}}$ and the basis measured by $\mathcal{D}_B$, Alice can always set $\mathcal{D}_A$ to measure an observable of $\mathcal{S}$ prior to Bob's measurement such that ${}_A\langle\lambda_{\alpha_B}|\lambda_{\alpha'_B}\rangle_A = \delta_{\alpha_B,\alpha'_B}$, thus having a deterministic prediction. This striking feature is similar to classical determinism if we assume that the information stored by $\mathcal{D}_A$ defines the initial condition of $\mathcal{S}$. This behaviour comes from the fact that

$\mathcal{D}_A$ and $\mathcal{D}_B$ become maximally correlated for TLE when ${}_A\langle\lambda_{\alpha_B}|\lambda_{\alpha'_B}\rangle_A = \delta_{\alpha_B,\alpha'_B}$ [see Eqs. (5.14) and (5.16)].

5.5 Bell's Inequalities

Bell's theorem demonstrates that under a wide class of conditions pertaining to locality and causality, no other theory can completely reproduce the probabilistic predictions of quantum mechanics. A particular manifestation of Bell's theorem is the fact that entangled states i.e., quantum states of composite systems that cannot be expressed as a (mixtures of) product state, violate Bell's inequalities (BIs).

Since quantum correlations can be accessed by Bell like inequalities, we investigate the extension of BIs to events in our formalism. Traditionally, for a bipartite system $\mathcal{S} = \mathcal{S}_A + \mathcal{S}_B$ living in $\mathcal{H}_{\mathcal{S}_A} \otimes \mathcal{H}_{\mathcal{S}_B}$, the correlation functions of BIs are given by $\mathrm{Tr}(\hat{\rho}_{\mathcal{S}}\hat{A} \otimes \hat{B})$, i.e., they involve the expectation values of observables $\hat{A}$ and $\hat{B}$ of a spatially separated bipartite system ($\mathcal{S}$) chosen to be measured by Alice (A) and Bob (B). Although BIs have been applied to TLE in Ref. [150], due to the space-time asymmetry of QM, the calculation of correlations via $\mathrm{Tr}(\hat{\rho}_{\mathcal{S}}\hat{A} \otimes \hat{B})$ limits BIs to spacelike measurements (or SLE).

In this work, on the other hand, as we focus on the detectors' states and not on the states of $\mathcal{S}$, BIs are calculated identically for SLE and TLE. For a pair of observables $\hat{A}$ and $\hat{B}$, the correlation function is given by $\mathrm{Tr}(\hat{\rho}_{\varepsilon}\hat{A}_{\mathcal{D}_A}\otimes\hat{B}_{\mathcal{D}_B})$, with $\hat{A}_{\mathcal{D}_A}$ ($\hat{B}_{\mathcal{D}_B}$) taken to be the observable of $\mathcal{D}_A$ ($\mathcal{D}_B$) whose eigenstates record information of $\hat{A}$ ($\hat{B}$). Here, $\hat{A}$ ($\hat{B}$) is either the observable of $\mathcal{S}_A$ ($\mathcal{S}_B$) or the observable of the first (second) measurement of $\mathcal{S}$. For example, in CHSH inequality, one has to compute four different density matrices $\hat{\rho}_{\varepsilon}$, one for each pair of observables that Alice and Bob have chosen for $\mathcal{D}_A$ and $\mathcal{D}_B$ to measure. This procedure is faithful to the standard CHSH inequality on a bipartite state and is extendable to subsequent measurements on the same system when we utilize the event state description provided in Eq.(5.4).

5.6 Discussion

Underpinning attempts at a fully quantum theory of gravity is the resolution of the asymmetric treatment of space and time in quantum mechanics, with the former described as an observable while the latter, a parameter. We develop a formalism to describe spacelike and timelike (causally connected) events on an equal footing by utilizing detectors coupled to timers, whose joint state serves as the descriptor of an event. In addition to recovering the notion of a tensor product structure for timelike events our formalism allows for temporal superpositions analogous to the familiar spatial superposition in quantum mechanics. We utilize well known measures from quantum information theory such as coherence and mutual information to indicate and characterize the causal connection between events. Furthermore, we extend the parallel between spacelike and timelike events by illustrating a deterministic relationship between causally connected events (similar to that in spatially entangled physical systems) where observing a previous event (one subsystem), enables us to delineate a later event (the other subsystem).

A future investigation would be the application of QI tools to the timers, i.e., to the case where Alice and Bob have access to when the events take place. It is also interesting to study decohering effects on the detectors in the context of Alice's predictions of Bob's measurements. Another extension of our work is to consider entangled detectors and analyze the properties of $\mathcal{S}$ from the perspective of these quantum observers. It is worth remarking that the temporal superpositions of $\hat{\rho}_\varepsilon$ can naturally give rise to indefinite causal orders, similar to those seen via quantum gates [159–161]. Finally, we believe that the space-time-symmetric description of events presented here, which encompasses indefinite temporal orders, can pave the way forward for a possible quantum theory of gravity, where it is expected to obtain superposition of space-time geometries.

அண்டப் பகுதியின் உண்டைப் பிறக்கம்
அளப்பருந் தன்மை வளப்பெருங் காட்சி
ஒன்றனுக்கொன்று நின்றெழில் பகரின்
நூற்றொரு கோடியின் மேற்பட விரிந்தன
— திருவாசகம் திருவண்டப் பகுதி

6 Summary and Further Work

Since all matter is composed of quantum elementary particles that gravitate, it stands to reason that the mediator of gravitational effects is likely to be quantum as well. A consistent quantum theory of gravity is hoped to overcome pathologies that arise in QFT such as small scale (UV) divergences and singularities in GR. Theories of quantum gravity may possibly revise the most fundamental concepts of space, time and substance. In this thesis, we have explored various problems that merit attention in the treatment of quantum gravity. Our work provides a natural foray into the foundations of quantum gravity and helps ascertain the necessary postulates expected in candidate theories of quantum gravity.

The early universe is regarded as a promising test bed to observe quantum gravitational effects. The paradigm of inflation explains cosmic structure as vacuum fluctuations, stretched to Hubble scales in the expanding universe, amplified by gravitational instability. While inflation indeed places the Bunch-Davies vacuum in the strongest known two-mode squeezed state, probing its quantum nature through conventional methods like the violation of Bell inequalities are tedious due to the lack of conjugate observables. This motivated us to propose other witnesses of quantumness such as non-Gaussianity, which we explored in greater detail for a table-top experiment involving BECs.

We investigated relics of the early universe, primordial massive particles, and showed that they can persist in a superposed state, which in a consistent quantum theory of gravity would manifest as entanglement with the metric itself. Thus gravitationally lensed light would exhibit an interference pattern due to a coherent sum over superpositions of geodesics, in contrast with the classical lensing pattern due to an averaged energy-momentum tensor. In our future work, we will study the qualitative and quantitative differences more precisely. We will resolve the challenges due to the small size of the lensing particles by considering their proximity to Earth and examining alternative lensing systems such as condensates.

We also saw that, similar to the Bohr atom's interaction with light, the interaction of gravitationally bound states of massive particles with gravitational waves (GWs) reflects the quantum nature of gravity and implies the existence of gravitons. We expect that stationary states will absorb or emit GWs in discrete frequencies due to transitions. These absorption lines could be detected by GW detectors. A future direction is to study a complete treatment of this problem and overcome the low absorption cross-section of GWs, by considering the spatial distribution of dark matter, the line widths of the transitions, the location of the source of GWs, and bound systems consisting of more than two particles. Overall, our studies will provide an estimate of the measurement sensitivities required to detect this effect.

The temperature fluctuations of the CMB provide an important probe of the primordial perturbations generated during the inflationary era. By virtue of the coupling between the inflaton and gravity, these are thought to provide information on the quantum state of the primordial gravitational field. If we were able to measure the non-Gaussianity of the quantum state of the CMB radiation and robustly claim that this is due to gravitational interactions, then this would provide evidence of QG through an indirect means of analysing the quantum state of radiation, with no knowledge of the state of the primordial gravitational field required. However owing to the rich phenomenology of non-Gaussianities and the secondary effects involved, further studies are necessary to examine the role of gravitational couplings in the generation of non-Gaussian effects.

In proposing a tabletop experiment involving non-Gaussianity witnesses for a BEC we showed that the quantum self interactions of the gravitational field could be probed. In contrast to entanglement based witnesses, we demonstrated that a single quantum system i.e. a single well BEC alone is sufficient to witness quantum effects of gravity, so long as other non-gravitational quantum interactions can be excluded. The advantage to considering a non-Gaussian signal is that we can immediately neglect all processes generating Gaussian noise, since these will not affect the non-Gaussian measurement.

While non-Gaussianity is a very important resource in QI [77], it is not sufficient for universal speed-up over classical computation. For this, we need negative Wigner function states, and in the case of mixed states, it is possible for a non-Gaussian state to have a positive Wigner function. Given that it is Wigner negative states that are generically associated with non-classicality, it is interesting from a fundamental point-of-view that, it appears to be non-Gaussianity that is a universal indicator of QG, rather than Wigner negativity. Perhaps non-Gaussianity in matter, especially its broader definition as states outside the Gaussian convex hull, is connected with a fundamental property of quantum gravitational degrees of freedom, such as non-commuting variables or quantum contextuality, which will be studied in future work.

As well as proving that gravity obeys a quantum theory if non-Gaussianity is observed, the BEC experiment could also teach us something about QG. For example, the Newtonian interaction used to predict the size of the non-Gaussian signal is derived from the gravity-matter interaction of GR. A measurement of non-Gaussianity would therefore, for instance, provide evidence that the determinant $\mathfrak{g}$ of the 3-metric is quantized and that spatial volume is a quantum variable. This of course would not, however, point us to the appropriate quantization procedure to be followed. Note that in loop QG, volume is a quantum variable with discrete spectrum.

An avenue for future work is apparent if we would like to consider the representation of matter in more fundamental theories like String Theory. In our work, treating gravitating matter as a quantum field allows us to consider non-Gaussianity in its quantum state as a witness of quantum gravity. This description of matter is perfectly extendable to theories like, loop QG, group field theory [162] and asymptotically safe QG [163]. However, this may be considered as an effective field theory description in some candidates for fundamental theories, such as string theory. A future investigation can be to consider non-Gaussianity in the context of these theories. Some semblance with the EFT action being quadratic in the matter terms can be seen in the Polyakov action in curved space [5], suggesting that our notion of non-Gaussianity in matter could also be generalized to strings. Yet again this is something that we do not expect to see in tabletop experiments but is perhaps visible in high energy processes of the early universe.

It was also interesting to examine general relativistic issues from the perspective of quantum information theory. We examined the C^0-formulation of the Strong Cosmic Censorship conjecture from a quantum complexity-theoretic perspective and argued that for generic black hole parameters as initial conditions for the Einstein equations, corresponding to the expected geometry of a hyperbolic black hole, the metric is C^0-extendable to a larger Lorentzian manifold across the Cauchy horizon. To demonstrate the pathologies associated with a hypothetical validity of the C^0 SCC, we proved that it violates the "complexity=volume" conjecture for a low-temperature hyperbolic AdS_{d+1} black hole dual to a CFT living on a $(d-1)$-dimensional hyperboloid H_{d-1}, where in order to preserve the gauge/gravity duality we imposed a lower bound on the interior metric extendability of order the classical recurrence time.

Finally, we defined events from the perspective of a quantum measurement. Any measurement can be modeled as an establishment of correlations between two random variables: one random variable represents values of a quantity pertaining to the system to be measured, while the other random variable represents states of the apparatus used to measure the system. It is by looking at the states of the apparatus and discriminating between them that we infer the states of the system, or even ascertain that an event has indeed happened. This act of introducing detectors and timers into the formalism of events allowed us to unify the description of spacelike and timelike events with notable repercussions to the notion of entanglement in time and in the construction of Bell's inequalities for temporal events. In this quantum formalism of events it is certainly worth extending our results to the case when the detectors or the system decoheres.

Appendices

A
Non-Gaussianity in Quantum Gravity

In the following we demonstrate that the preferential quantization of matter fields while coupling to classical gravity i.e. semi-classical approaches preserve state non-Gaussianity. The Lagrangian densities for a real scalar ϕ, spin-1/2 ψ, and spin-1 field A_μ, which follow from the Einstein Hilbert action, are [74],

$$\mathcal{L}_\phi = \frac{1}{2}\sqrt{g}[g^{\mu\nu}\partial_\mu\phi\partial_\nu\phi - m^2\phi^2] \tag{A.1}$$

$$\equiv \frac{1}{2}e[\eta^{\alpha\beta}e^\mu_\alpha\partial_\mu\phi e^\nu_\beta\partial_\nu\phi - m^2\phi^2], \tag{A.2}$$

$$\mathcal{L}_\psi = \sqrt{g}\left(\frac{1}{2}i[\overline{\psi}\gamma^\mu\nabla_\mu\psi - (\nabla_\mu\overline{\psi})\gamma^\mu\psi] - m\overline{\psi}\psi\right), \tag{A.3}$$

$$\mathcal{L}_A = -\frac{1}{4}\sqrt{g}g^{\mu\nu}g^{\nu\sigma}F_{\mu\rho}F_{\nu\sigma}, \tag{A.4}$$

where the tetrads $e^\mu_\alpha(x)$ are related to the metric tensor by, $g^{\mu\nu}(x) =: e^\mu_\alpha(x)e^\nu_\beta(x)\eta^{\alpha\beta}$, with $\eta^{\alpha\beta}$ taken to be the Minkowski metric.

The electromagnetic stress energy tensor is, $F_{\mu\nu} := \partial_\nu\mathcal{A}_\mu - \partial_\mu\mathcal{A}_\nu$ and $\mathcal{A}_\mu$ is the electromagnetic four-potential. In the fermionic sector, ∇_μ is the covariant derivative; $\gamma^\mu := e^\mu_\alpha\gamma^\alpha$ are the curved space counterparts of the gamma (Dirac) γ matrices, satisfying the anti-commutation relation $\{\gamma^\mu, \gamma^\nu\} = 2g^{\mu\nu}$.

The corresponding Hamiltonian (constraint) densities for the above Lagrangian densities are given by,

$$\mathcal{H}_\phi = \frac{1}{2}\left(\frac{\pi^2}{\sqrt{\mathfrak{g}}} + \sqrt{\mathfrak{g}}\mathfrak{g}^{ab}\partial_a\phi\partial_b\phi + \sqrt{\mathfrak{g}}m^2\phi^2\right), \tag{A.5}$$

$$\mathcal{H}_\psi = \frac{1}{2\sqrt{\mathfrak{g}}}E^a_j\left[i\zeta\tau^j\mathcal{D}_a\xi + \mathcal{D}_a(\zeta\tau^j\xi) + \frac{1}{2}iK^j_a\sigma\xi + c.c.\right], \tag{A.6}$$

$$\mathcal{H}_A = \frac{1}{2\sqrt{\mathfrak{g}}}\mathfrak{g}_{ab}\left[\mathcal{E}^a\mathcal{E}^b + \mathcal{B}^a\mathcal{B}^b\right]. \tag{A.7}$$

Here spacetime has been split into spatial slices and a time axis $M = \mathbb{R}\times\sigma$. Taking n^μ to be the normal vector field of the time slices σ, the tetrad can be written as $e^\mu_\alpha = \mathfrak{e}^\mu_\alpha - n^\mu n_\alpha$, with $\eta^{\alpha\beta}n_\alpha n_\beta = -1$ an internal unit timelike vector (which we may choose to be $n_\alpha = -\delta_{\alpha,0}$), so that $\mathfrak{e}^\mu_\alpha$ is a triad, where $\mathfrak{e}^\mu_\alpha = (0, \mathfrak{e}^\mu_i)$ and we further define $E^a_i = |\det\mathfrak{e}^a_i|\mathfrak{e}^a_i$ with $i, a = 1, 2, 3$. The conjugate momenta to the densitized triad E^a_i is the chiral spin connection $A^i_a := \Gamma^i_a + K^i_a$, where $\Gamma^i_a = \Gamma_{ajk}\epsilon^{jki}$ and $K^i_a = K_{ab}\mathfrak{e}^{bi}$, with Γ_{ajk} the spin-connection and K_{ab} the extrinsic curvature. In (A.5)-(A.7), $\mathfrak{g}$ is then the determinant of the induced spatial metric $\mathfrak{g}^{ab} \equiv \mathfrak{e}^a_i\mathfrak{e}^b_j\delta^{ij}$ on the spatial slices; $\pi := \sqrt{\mathfrak{g}}n^\mu\partial_\mu\phi$ is the momentum conjugate to ϕ; $\mathcal{E}^a := \sqrt{\mathfrak{g}}\mathfrak{g}^{ab}n^\mu F_{\mu b}$ is the electric field; $\mathcal{B}^a := \epsilon^{abc}F_{bc}$ is the magnetic field; τ_i are the generators of the Lie algebra su(2) with the convention $[\tau_i, \tau_j] = \epsilon_{ijk}\tau_k$; $\xi = \sqrt{\mathfrak{g}}\psi$, with ψ a Grassman-valued fermion field; ζ is the momentum conjugate to ξ; and $\mathcal{D}_a\xi := (\partial_a + \tau_j A^j_a)\xi$. For simplicity, we have also assumed that the scalar and fermionic fields are singlets under any internal group symmetry.

In the simplest field theories without additional interactions, it is manifest that the Hamiltonians are quadratic in matter fields consisting only of the kinetic and mass terms. This quadratic scaling generalises to higher spins as well [164].

As shown in the main text the dynamics of the state of these fundamental fields resemble that of the parametric oscillator. Thus without additional source terms and interactions non-Gaussianity is not generated in the semiclassical picture of gravity.

However, if gravity is indeed quantum and admits an operator description we would expect interaction terms involving three or more quantum operators and that create non-Gaussianity in the state. This is made explicit in the following when considering the weak-field and non-relativistic limits of gravity.

A.1 Weak-field limit

In the weak-field limit of gravity typically employed in cosmological perturbation theory the metric can be written as,

$$g_{\mu\nu} = \eta_{\mu\nu} + h_{\mu\nu} \tag{A.8}$$

where $h_{\mu\nu}$ is a perturbation around a space-time background with metric $\eta_{\mu\nu}$. Thus the non-leading interaction term follows as, [91],

$$H_{int} = -\frac{1}{2}\int d^3\boldsymbol{r}\, T^{\mu\nu} h_{\mu\nu}, \tag{A.9}$$

where,

$$\Box h_{\mu\nu} = \frac{16\pi G}{c^4}\left(\frac{1}{2}\eta_{\mu\nu}\eta^{\sigma\rho}T_{\sigma\rho} - T_{\mu\nu}\right), \tag{A.10}$$

with $\Box$ the d'Alembert operator, $T^{\mu\nu}$ the stress-energy tensor for matter, and we have chosen the Lorentz gauge. The stress-energy tensor for a field of arbitrary spin in curved spacetime can be obtained by variation of the action with respect to the metric [74],

$$T_{\mu\nu}(x) = \frac{2}{\sqrt{-g}}\frac{\delta S}{\delta g^{\mu\nu}(x)} \equiv \frac{e_{\alpha\mu}(x)}{e(x)}\frac{\delta S}{\delta e^{\mu}_{\alpha}(x)}. \tag{A.11}$$

For example, when neglecting all other interactions, for a real scalar, spin-1/2 and spin-1 field, the curved space stress-energy tensors are (before taking a weak-field limit) [74],

$$T^{\phi}_{\mu\nu} = (1-2\varepsilon)\partial_\mu\phi\partial_\nu\phi + (2\varepsilon - \frac{1}{2})g_{\mu\nu}g^{\rho\sigma}\partial_\rho\phi\partial_\sigma\phi - 2\varepsilon(\nabla_\mu\partial_\nu\phi)\phi + \frac{1}{2}\varepsilon g_{\mu\nu}\phi\Box\phi \tag{A.12}$$

$$-\varepsilon\Big[R_{\mu\nu} - \frac{1}{2}Rg_{\mu\nu}(1-3\varepsilon)\Big]\phi^2 + \frac{1}{2}\Big[1-3\varepsilon\Big]m^2 g_{\mu\nu}\phi^2, \tag{A.13}$$

$$T^{\psi}_{\mu\nu} = \frac{1}{2}i[\overline{\psi}\gamma_{(\mu}\nabla_{\nu)}\psi - [\nabla_{(\mu}\overline{\psi}]\gamma_{\nu)}\psi], \tag{A.14}$$

$$T^{A}_{\mu\nu} = \frac{1}{4}g_{\mu\nu}F^{\rho\sigma}F_{\rho\sigma} - F^{\rho}_{\mu}F_{\rho\nu}, \tag{A.15}$$

where we have ignored any gauge fixing or ghost terms in $T^{A}_{\mu\nu}$ [74]. Since we have neglected all other interactions, all stress-energy tensors are necessarily just quadratic in matter fields.

In a QG theory we add a hat to both $T_{\mu\nu}$ and $h_{\mu\nu}$. This then results in an interaction Hamiltonian that is cubic in field operators. For example, for a complex scalar field we have terms of the form $\hat{\phi}^\dagger\hat{\phi}\hat{h}_{\mu\nu}$, where we have suppressed any derivatives. On the other hand, for a CG theory, the interaction Hamiltonian contains terms only quadratic in quantum field operators. For example, in the semi-classical theory of gravity with complex scalar matter fields, we have terms of the form $\hat{\phi}^\dagger\hat{\phi}h_{\mu\nu}$, where $h_{\mu\nu}$ is given by the expectation value of the right-hand side of (A.10). Therefore, this weak-field limit of CG cannot produce or change non-Gaussianity in the state of matter, whereas QG can, as expected from the general discussion of GR and QG in the previous section.

A.2 Newtonian limit

We now consider a Newtonian theory of gravity with matter quantized. This can be obtained by starting from Newton's theory and quantizing matter or from taking the non-relativistic limit of the weak-field theory. For the latter, we consider a *closed system* and only the components T_{00} and h_{00}. This results in Poisson's equation,

$$\nabla^2\Phi(\boldsymbol{r}) = 4\pi G\rho(\boldsymbol{r}) \tag{A.16}$$

$$\implies \Phi(\boldsymbol{r}) = -G\int d^3\boldsymbol{r'}\,\frac{\rho(\boldsymbol{r'})}{|\boldsymbol{r}-\boldsymbol{r'}|}, \tag{A.17}$$

and the Newtonian interaction Hamiltonian,

$$H_{int} = \frac{1}{2}\int d^3\boldsymbol{r}\rho(\boldsymbol{r})\Phi(\boldsymbol{r}), \tag{A.18}$$

where $\Phi := -c^2h_{00}/2$ is the Newtonian potential, and $\rho := T_{00}/c^2$ is the matter density. Irrespective of the spin of the field, ρ again contains two copies of the matter field, e.g., for a single non-relativistic scalar matter field Ψ, $\rho = m\Psi^*\Psi$. The interaction Hamiltonians for quantum and classical Newtonian gravity (with quantized scalar matter fields) are then (3.5)-(3.6),

$$\begin{aligned}\hat{H}^{int}_{QG} &= \frac{1}{2}m\int d^3\boldsymbol{r} : \hat{\Psi}^\dagger(\boldsymbol{r})\hat{\Psi}(\boldsymbol{r})\hat{\Phi}(\boldsymbol{r}) : \qquad\qquad (A.19)\\ &= -\frac{1}{2}Gm^2\int d^3\boldsymbol{r'}d^3\boldsymbol{r}\frac{\hat{\Psi}^\dagger(\boldsymbol{r'})\hat{\Psi}^\dagger(\boldsymbol{r})\hat{\Psi}(\boldsymbol{r'})\hat{\Psi}(\boldsymbol{r})}{|\boldsymbol{r}-\boldsymbol{r'}|},\end{aligned}$$

$$\hat{H}^{int}_{CG} = m\int d^3\boldsymbol{r}\hat{\Psi}^\dagger(\boldsymbol{r})\hat{\Psi}(\boldsymbol{r})\Phi[\Psi](t,\boldsymbol{r}), \tag{A.20}$$

where :: refers to normal ordering, and we have made explicit that Φ may depend on the quantum state of matter $\mathit{\Psi}$ in a CG theory, which can result in single-particle gravitational self-interaction, for which we have dropped a factor of 1/2. For example, for the Schrodinger-Newton equations (the non-relativistic limit of semi-classical gravity), Φ is given by the expectation value of the right-hand side of the quantized version of (A.17). Expanding the non-relativistic field in annihilation operators, $\hat{\Psi}(\boldsymbol{r}) = \sum_k \psi_k(\boldsymbol{r})\hat{a}_k$, we again find CG is only quadratic in quantum operators and so cannot change the degree of quantum non-Gaussianity in the state of matter, whereas QG can.

First quantization

The interaction Hamiltonian of classical Newtonian gravity is given by (3.4). The Hamiltonian of QG and CG in the Newtonian limit can then be derived by quantizing the matter density $\rho(\boldsymbol{r})$ and, in the QG case, the gravitational potential $\Phi(\boldsymbol{r})$. In the previous section we took matter to obey a non-relativistic quantum field $\hat{\Psi}$, such that $\hat{\rho} = m\hat{\Psi}^\dagger\hat{\Psi}$, assuming a single type of matter. Since $\hat{\Psi}$ is linear in annihilation operators, and so also in quadratures, the interaction Hamiltonian for CG is at most quadratic, such that an initial Gaussian state of the matter field will always remain Gaussian. However, in the case that we always have definite particle number, which can only be possible in the Newtonian approximation of the respective theories not the full relativistic theories, we could also view QG and CG in a first-quantized form. In this case, assuming a single type of particle, we may quantize $\rho(\boldsymbol{r})$ through,

$$\hat{\rho}(\boldsymbol{r}) = m\sum_{i=1}^{N} \delta^{(3)}(\boldsymbol{r} - \hat{\boldsymbol{r}}_i), \tag{A.21}$$

where N is the total number of particles in the matter system. The respective QG and CG Hamiltonians would then be,

$$\hat{H}^{int}_{QG} = \frac{1}{2}m\sum_{i=1}^{N} \hat{\Phi}(\hat{\boldsymbol{r}}_i), \tag{A.22}$$

$$\hat{H}^{int}_{CG} = m\sum_{i=1}^{N} \Phi[\mathit{\Psi}](\hat{\boldsymbol{r}}_i). \tag{A.23}$$

Since $\Phi(\boldsymbol{r})$ does not need to be a quadratic function of $\boldsymbol{r}$, it is possible here for CG to create non-Gaussianity in the first-quantization picture. For example, in the Schrodinger-Newton equations, where $\Phi(\boldsymbol{r}) = \langle\hat{\Phi}(\boldsymbol{r})\rangle$ with $\hat{\Phi}(\boldsymbol{r})$ obeying Poisson's equation (A.16), the many-body wavefunction of N massive particles would evolve as,

$$i\hbar\partial_t\psi_N(t;\boldsymbol{r}_1,\ldots,\boldsymbol{r}_N) = \Big(-\frac{\hbar^2}{2m}\sum_{i=1}^{N}\nabla_i^2 + V(\boldsymbol{r}_1,\ldots,\boldsymbol{r}_N) - Gm^2\sum_{i,j=1}^{N}\int d^3\boldsymbol{r}'_1\cdots d^3\boldsymbol{r}'_N\frac{|\psi_N(t;\boldsymbol{r}'_1,\ldots,\boldsymbol{r}'_N)|^2}{|\boldsymbol{r}_i-\boldsymbol{r}'_j|}\Big)\psi_N(t;\boldsymbol{r}_1,\ldots,\boldsymbol{r}_N), \tag{A.24}$$

where V is a trapping potential. Although a Gaussian approximation is expected to be very good for table-top experiments, the evolution of ψ_N (and hence its corresponding Wigner function) can, in principle, be non-Gaussian. Therefore, in the BEC experiment proposed in the main text, although the state of the BEC in the second-quantization picture must stay Gaussian under CG, its many-body wave-function need not. Note also that, just as particles tend to automatically get "entangled" in the first-quantization picture when we have identical particles, an identical particle system also tends to become automatically non-Gaussian. That is, if we have two identical particles in positions $\boldsymbol{r}_1$ and $\boldsymbol{r}_2$ and two different states a and b, then the many-body wavefunction is $\psi_N = [\phi_a(\boldsymbol{r}_1)\phi_b(\boldsymbol{r}_2) \pm \phi_a(\boldsymbol{r}_2)\phi_b(\boldsymbol{r}_1)]/\sqrt{2}$, depending on whether the particles are bosons or fermions. The system looks entangled just because of the exchange symmetry of the identical particles (it is so-called "particle" entangled). Similarly, even if each single-particle wavefunction ϕ_a and ϕ_b is Gaussian, ψ_N will, in general, be non-Gaussian due to the exchange symmetry (and the corresponding Wigner function will be non-Gaussian also). However, there has been much discussion on whether this "particle" entanglement is really physical [165].

B

Decoherence of a Massive Particle

B.1 Decoherence in a Photon Bath

We study the decoherence rate of the model from Eq.(2.1) and Eq.(2.2). We can introduce creation and annihilation operations $a^\dagger_{\mathbf{k}}$ and $a_{\mathbf{k}}$ for χ, and $b^\dagger_{\mathbf{k}}$ and $b_{\mathbf{k}}$ for photons respectively, and define $\nu(\mathbf{k})$ to be the Fourier transform of gravitational potential $\phi(\mathbf{x}) = M/|\mathbf{x}|$,

$$\nu(\mathbf{k}) = \frac{1}{2\pi} \int \mathrm{d}^3\mathbf{x}\ \mathrm{e}^{-\mathrm{i}\,\mathbf{k}\cdot\mathbf{x}}\, \phi(\mathbf{x}) = \frac{M}{\pi k^2}. \tag{B.1}$$

Then,

$$H_{\text{int}} = \int \mathrm{d}^3\mathbf{p}\ \mathrm{d}^3\mathbf{k}\ \nu(\mathbf{k})\, \epsilon_{\mathbf{k}}\, a^\dagger_{\mathbf{p}} a_{\mathbf{p}+\mathbf{k}}\, b^\dagger_{\mathbf{k}} b_{\mathbf{k}}. \tag{B.2}$$

We define the Fourier transformed number density of massive particle as,

$$N_{\mathbf{k}} = \int \mathrm{d}^3\mathbf{p}\, a^\dagger_{\mathbf{p}} a_{\mathbf{p}+\mathbf{k}}. \tag{B.3}$$

Then,

$$H_{\text{int}} = \int \mathrm{d}^3\mathbf{k}\ \nu(\mathbf{k})\, \epsilon_{\mathbf{k}}\, N_{\mathbf{k}}\, b^\dagger_{\mathbf{k}} b_{\mathbf{k}}. \tag{B.4}$$

Evolution of density matrix — We now study the evolution of the reduced density matrix ρ of the massive particle to calculate the time of decoherence under this interaction. The master equation has been studied in Ref. [58] and takes the Lindblad form given as follows,

$$\frac{\mathrm{d}\rho}{\mathrm{d}t}\Delta t = \mathrm{i}[\mathrm{tr}_{\mathcal{E}}(U_1\rho_{\mathcal{E}}) - \mathrm{tr}_{\mathcal{E}}(B\rho_{\mathcal{E}}), \rho] + \\ \mathrm{tr}_{\mathcal{E}}\left(U_1\rho_T U_1 - \frac{1}{2}U_1^2\rho_T - \frac{1}{2}\rho_T U_1^2\right), \tag{B.5}$$

where B is an arbitrary Hermitian operator, which would not be relevant in the slow motion approximation where time evolution of $N_{\mathbf{k}}$ is neglected in comparison to the rapidly evolving environment, and U_1 is the time evolution operator defined by,

$$U_1 = -\int_{-\infty}^{\infty} \mathrm{d}t\, H_{\mathrm{int}}(t) \approx -\int \mathrm{d}^3\mathbf{k}\ \nu(\mathbf{k})\,\epsilon_{\mathbf{k}}\,N_{\mathbf{k}}\,b_{\mathbf{k}}^\dagger b_{\mathbf{k}}. \tag{B.6}$$

Here, Δt is the timescale over which we study the evolution of ρ. This timescale is small compared to the evolution of the system but large compared to the evolution of the environment. The right hand side of this equation is also proportional to Δt as calculated in Ref. [58]. We then obtain the following differential equation describing ρ,

$$\frac{\mathrm{d}\rho}{\mathrm{d}t} = -\mathrm{i}\left[H_0 - \int \mathrm{d}^3\mathbf{k}\, d(\mathbf{k}) N_{\mathbf{k}} N_{\mathbf{k}}^\dagger, \rho\right] + \\ \int \mathrm{d}^3\mathbf{k}\, c(\mathbf{k})\left(N_{\mathbf{k}}\rho N_{\mathbf{k}}^\dagger - \frac{1}{2}N_{\mathbf{k}}^\dagger N_{\mathbf{k}}\rho - \frac{1}{2}\rho N_{\mathbf{k}}^\dagger N_{\mathbf{k}}\right). \tag{B.7}$$

Here, H_0 is the free Hamiltonian of the massive particle, $d(\mathbf{k})$ is some function of $\mathbf{k}$ which depends on the operator B in Eq.(B.5), and $c(\mathbf{k})$ is a function describing the photon environment given by,

$$\begin{aligned} c(\mathbf{k}) &= \frac{1}{2\pi}|\nu(k)|^2\,\epsilon_{\mathbf{k}}^2\,\langle b_{\mathbf{k}}^\dagger b_{\mathbf{k}} b_{\mathbf{k}}^\dagger b_{\mathbf{k}}\rangle_{\mathcal{E}} \\ &= \frac{1}{2\pi}|\nu(k)|^2\,\epsilon_{\mathbf{k}}^2\,n_{\mathbf{k}}(n_{\mathbf{k}}+1). \end{aligned} \tag{B.8}$$

Here, we have used the thermal density of photons $n_{\mathbf{k}}$ in place of $\langle b_{\mathbf{k}}^\dagger b_{\mathbf{k}}\rangle$. Notice that the integral containing $d(\mathbf{k})$ in Eq.(B.7) is a c-number due to the slow motion approximation and its commutator with ρ vanishes. We further restrict our focus to the one particle sector for the massive particle. Then the density matrix in

Eq.(B.7) reduces to a function $\rho(\mathbf{k},\mathbf{k}') := \langle \mathbf{k}|\rho|\mathbf{k}'\rangle$ of two momenta, $\mathbf{k}$ and $\mathbf{k}'$. In this representation,

$$\begin{aligned}\langle \mathbf{k}|[H_0,\rho]|\mathbf{k}'\rangle &= \left\langle \mathbf{k}\left|\frac{k^2}{2M}\,\rho-\rho\,\frac{k'^2}{2M}\right|\mathbf{k}'\right\rangle \\ &= \frac{k^2-k'^2}{2M}\,\rho(\mathbf{k},\mathbf{k}'). \end{aligned} \tag{B.9}$$

Further, as $N_{\mathbf{k}}N^\dagger_{\mathbf{k}}$ acting on the one particle state is a c-number, the commutator of $\int \mathrm{d}^3\mathbf{k}\, d(\mathbf{k}) N_{\mathbf{k}}N^\dagger_{\mathbf{k}}$ with ρ vanishes for any function $d(\mathbf{k})$. Likewise,

$$\begin{aligned}&\langle \mathbf{k}|N_{\mathbf{q}}\rho N^\dagger_{\mathbf{q}}|\mathbf{k}'\rangle = \langle \mathbf{k}-\mathbf{q}|\rho|\mathbf{k}'-\mathbf{q}\rangle = \rho(\mathbf{k}-\mathbf{q},\mathbf{k}'-\mathbf{q}),\ \&\\ &\langle \mathbf{k}|N^\dagger_{\mathbf{q}}N_{\mathbf{q}}\rho|\mathbf{k}'\rangle = \langle \mathbf{k}|\rho N^\dagger_{\mathbf{q}}N_{\mathbf{q}}|\mathbf{k}'\rangle = \langle \mathbf{k}|\rho|\mathbf{k}'\rangle = \rho(\mathbf{k},\mathbf{k}').\end{aligned} \tag{B.10}$$

Also, as $\nu(\mathbf{k})$ only depends on the magnitude k, we shall write $\nu(k)$ to denote it. With these simplifications, Eq.(B.7) becomes,

$$\frac{\mathrm{d}\rho}{\mathrm{d}t}(\mathbf{k},\mathbf{k}') = -i\rho(\mathbf{k},\mathbf{k}')\,\frac{k^2-k'^2}{2M}+\frac{1}{2\pi}\int \mathrm{d}^3\mathbf{q}\ |\nu(q)|^2\,\epsilon^2_{\mathbf{q}}\,n_{\mathbf{q}}(n_{\mathbf{q}}+1)\Big[\rho(\mathbf{k}-\mathbf{q},\mathbf{k}'-\mathbf{q})-\rho(\mathbf{k},\mathbf{k}')\Big]. \tag{B.11}$$

Master equation for $\operatorname{tr}\rho^2$ — We now derive a master equation for $\operatorname{tr}\rho^2$. First, in the function form $\rho(\mathbf{k},\mathbf{k}')$, ρ^2 is given by,

$$\rho^2(\mathbf{k},\mathbf{k}') = \int \mathrm{d}^3\mathbf{s}\,\rho(\mathbf{k},\mathbf{s})\rho(\mathbf{s},\mathbf{k}'). \tag{B.12}$$

The evolution of $\operatorname{tr}\rho^2$ is given by,

$$\begin{aligned}\frac{\mathrm{d}(\operatorname{tr}\rho^2)}{\mathrm{d}t} &= \int \mathrm{d}^3\mathbf{k}\ \mathrm{d}^3\mathbf{s}\left(\rho(\mathbf{k},\mathbf{s})\frac{\mathrm{d}\rho(\mathbf{s},\mathbf{k})}{\mathrm{d}t}+\frac{\mathrm{d}\rho(\mathbf{k},\mathbf{s})}{\mathrm{d}t}\,\rho(\mathbf{s},\mathbf{k})\right)\\ &= \frac{1}{2\pi}\int \mathrm{d}^3\mathbf{q}\ |\nu(q)|^2\,\epsilon^2_{\mathbf{q}}\,n_{\mathbf{q}}(n_{\mathbf{q}}+1)\left[-2\operatorname{tr}\rho^2+2\operatorname{Re}\int \mathrm{d}^3\mathbf{k}\ \mathrm{d}^3\mathbf{s}\,\rho(\mathbf{k},\mathbf{s})\rho(\mathbf{s}-\mathbf{q},\mathbf{k}-\mathbf{q})\right].\end{aligned} \tag{B.13}$$

For the purpose of the integrals over $\mathbf{s}$ and $\mathbf{k}$, the direction of $\mathbf{q}$ is arbitrary and can be chosen to be along the z-axis. In other words, the integral only depends on the magnitude of $\mathbf{q}$. We can define,

$$\Lambda(q) := \operatorname{tr}\rho^2 - \operatorname{Re}\int \mathrm{d}^3\mathbf{k}\ \mathrm{d}^3\mathbf{s}\,\rho(\mathbf{k},\mathbf{s})\rho(\mathbf{s}-q\,\hat{z},\mathbf{k}-q\,\hat{z}). \tag{B.14}$$

Then,

$$\frac{\mathrm{d}(\operatorname{tr}\rho^2)}{\mathrm{d}t} = -\frac{1}{\pi}\int \mathrm{d}^3\mathbf{q}\ |\nu(q)|^2\,\epsilon^2_{\mathbf{q}}\,n_{\mathbf{q}}(n_{\mathbf{q}}+1)\,\Lambda(q). \tag{B.15}$$

Bounds on $\Lambda(q)$ — To calculate bounds on $\Lambda(q)$ define,

$$\alpha(q) := \int \mathrm{d}^3\mathbf{k}\, \mathrm{d}^3\mathbf{s}\, \rho(\mathbf{k},\mathbf{s})\rho(\mathbf{s}-q\,\hat{z},\mathbf{k}-q\,\hat{z}) = \mathrm{tr}\,\rho\,\tilde{\rho}_q, \tag{B.16}$$

where $\tilde{\rho}_q(\mathbf{s},\mathbf{k}) := \rho(\mathbf{s}-q\,\hat{z},\mathbf{k}-q\,\hat{z})$ is the "displaced" density matrix. It has been shown [166] that for any real symmetric $n\times n$ matrix B and any arbitrary real $n\times n$ matrix A,

$$\sum_{i=1}^{n} \lambda_i'\,\mu_{n-i+1} \leq \mathrm{tr}(AB) \leq \sum_{i=1}^{n} \lambda_i\,\mu_i. \tag{B.17}$$

Here, λ_i, λ_i' and μ_i denote the i-th eigenvalue of A, the transpose of A and B respectively when arranged in ascending order.

Now, let $A=\rho$, and $B=\tilde{\rho}_q$. A and its transpose have the same set of eigenvalues, say $\{\lambda_i\}$, and let the set of eigenvalues of B be $\{\mu_i\}$. Further, A and B are both valid density matrices and their eigenvalues represent probability to be found in some pure quantum state. Thus, they must all be positive. Thus, the lower bound in Eq.(B.17) is 0. We note that $\mathrm{tr}\,A^2 = \mathrm{tr}\,B^2 = \mathrm{tr}\,\rho^2$, $\mathrm{tr}\,A^2 = \sum_i \lambda_i^2$ and $\mathrm{tr}\,B^2 = \sum_i \mu_i^2$. Then, the upper bound can be obtained using the Cauchy-Schwartz inequality as,

$$\mathrm{tr}(AB) \leq \sum_{i=1}^{n} \lambda_i\,\mu_i \leq \sqrt{\Big(\sum_i \lambda_i^2\Big)\Big(\sum_i \mu_i^2\Big)} = \mathrm{tr}\,\rho^2. \tag{B.18}$$

Thus,

$$\alpha(q) \in [0, \mathrm{tr}\,\rho^2]. \tag{B.19}$$

and,

$$\Lambda(q) = \mathrm{tr}\,\rho^2 - \alpha(q) \in [0, \mathrm{tr}\,\rho^2]. \tag{B.20}$$

Evolution of $\mathrm{tr}\,\rho^2$ — All the terms in Eq.(B.15) only depend on the scalar magnitude of $\mathbf{q}$. Thus, we can integrate out the solid angle to 4π, and substitute ν from Eq.(B.1) and the bounds on $\Lambda(q)$ to get,

$$\frac{\mathrm{d}(\mathrm{tr}\,\rho^2)}{\mathrm{d}t} = -\Gamma\,\mathrm{tr}\,\rho^2, \tag{B.21}$$

where the decay rate $\Gamma \in [0, \Gamma_0]$, with,

$$\Gamma_0 = -\frac{4M^2}{\pi^2}\int_0^\infty \frac{\mathrm{d}q}{q^2}\,\epsilon_{\mathbf{q}}^2 n_{\mathbf{q}}(n_{\mathbf{q}}+1). \tag{B.22}$$

For a thermal bath of photons, $\epsilon_{\mathbf{q}} = q$ is the photon energy and $n_{\mathbf{q}}$ is the number density corresponding to the Planck distribution,

$$n_{\mathbf{q}} = \frac{q^2}{\pi^2(\mathrm{e}^{\beta q} - 1)}, \tag{B.23}$$

in natural units with $\beta = (k_B T)^{-1}$. However, this derivation holds for any species of thermal particles in the background with the right choice of $n_{\mathbf{q}}$ and $\epsilon_{\mathbf{q}}$, and combinations of them with Γ_0 being additive.

B.2 Decoherence due to Fermions

We begin by computing a better bound for $\Lambda(q)$ in place of Eq.(B.20). Observe that when $q = 0$, $\rho_q = \rho$, $\alpha(0) = \mathrm{tr}\,\rho^2$ and thus $\Lambda(0) = 0$. Also, as $\Lambda(q$ is an even function its first derivative must vanish. Then, in the small q limit, it will be approximated by a Taylor expansion with leading term $\propto q^2$. To calculate this approximation, consider the density matrix expressed in terms of its eigenvectors $|\psi_i\rangle$ and corresponding eigenvalues λ_i as,

$$\rho = \sum_i \lambda_i |\psi_i\rangle\langle\psi_i|. \tag{B.24}$$

Then,

$$\rho^2 = \sum_i \lambda_i^2 |\psi_i\rangle\langle\psi_i|. \tag{B.25}$$

Define S_q to be the shift operator in momentum $\exp(\mathrm{i}\,qZ)$, which acts on momentum eigenstates as $S_q|\mathbf{p}\rangle = |\mathbf{p} + q\hat{z}\rangle$. Here Z is the z-component of the position operator. Then,

$$\rho_q = \sum_i \lambda_i^2 S_q |\psi_i\rangle\langle\psi_i| S_q^{-1}. \tag{B.26}$$

Now, $\Lambda(q)$ can be written in terms of λ_i, $|\psi_i\rangle$ and S_q,

$$\Lambda(q) = \sum_{i,j,k} \lambda_i \lambda_j \langle\psi_k|\psi_i\rangle\langle\psi_i|S_q|\psi_j\rangle\langle\psi_j|S_q^{-1}|\psi_k\rangle - \sum_i \lambda_i^2. \tag{B.27}$$

We expand S_q to second order in q and use orthonormality of $|\psi_i\rangle$ to get,

$$\begin{aligned}\Lambda(q) &= \frac{1}{2} q^2 \sum_{i \neq j} \lambda_i \lambda_j |\langle\psi_i|Z|\psi_j\rangle|^2 \\ &\leq \frac{1}{2} q^2 \langle x^2\rangle_\rho \leq q^2 \langle x^2\rangle_\rho \,\mathrm{tr}\,\rho^2.\end{aligned} \tag{B.28}$$

Here, $\langle x^2 \rangle_\rho$ is the expectation value of x^2 under the density matrix ρ. The last inequality is because, we are only interested values of $\operatorname{tr}\rho^2$ close to 1. This, approximation however is only valid in the low q limit, $q \lesssim 1/\sqrt{\langle x^2 \rangle_\rho \operatorname{tr}\rho^2}$. Let $D := \langle x^2 \rangle_\rho \operatorname{tr}\rho^2$. Then, Eq.(2.12) for decoherence due to fermions of mass m becomes,

$$\Gamma_0 = \frac{4M^2 m^2}{\pi^2} \Bigg[\int_0^{\frac{1}{\sqrt{D}}} \mathrm{d}q \, D n_{\mathbf{q}} (n_{\mathbf{q}} + 1) + \\ \int_{\frac{1}{\sqrt{D}}}^{\infty} \frac{\mathrm{d}q}{q^2} n_{\mathbf{q}} (n_{\mathbf{q}} + 1) \Bigg]. \tag{B.29}$$

C
Evolution under Classical Gravity

Here we consider how a single BEC evolves under CG compared to QG. We start with the general Newtonian expressions (3.5) and (3.6). Working in the Schrodinger picture, for QG the evolution of our state vector $|\Psi\rangle$ is given by,

$$i\hbar\frac{d\,|\Psi(t)\rangle}{dt} = \hat{H}_{QG}^{BEC}\,|\Psi(t)\rangle\,, \tag{C.1}$$

where,

$$\hat{H}_{QG}^{BEC} := \int d^3\boldsymbol{r}\Big[-\frac{\hbar^2}{2m}\hat{\Psi}^\dagger(\boldsymbol{r})\nabla^2\hat{\Psi}(\boldsymbol{r}) + V(\boldsymbol{r})\hat{\Psi}^\dagger(\boldsymbol{r})\hat{\Psi}(\boldsymbol{r}) + \frac{1}{2}m : \hat{\Psi}^\dagger(\boldsymbol{r})\hat{\Psi}(\boldsymbol{r})\hat{\Phi}(\boldsymbol{r}) : \Big] \tag{C.2}$$

$$= \int d^3\boldsymbol{r}\Big[-\frac{\hbar^2}{2m}\hat{\Psi}^\dagger(\boldsymbol{r})\nabla^2\hat{\Psi}(\boldsymbol{r}) + V(\boldsymbol{r})\hat{\Psi}^\dagger(\boldsymbol{r})\hat{\Psi}(\boldsymbol{r}) \tag{C.3}$$

$$-\frac{1}{2}Gm^2\int d^3\boldsymbol{r'}\frac{\hat{\Psi}^\dagger(\boldsymbol{r})\hat{\Psi}^\dagger(\boldsymbol{r'})\hat{\Psi}(\boldsymbol{r})\hat{\Psi}(\boldsymbol{r'})}{|\boldsymbol{r}-\boldsymbol{r'}|}\Big], \tag{C.4}$$

with $V(\boldsymbol{r})$ the trapping potential. In contrast, for CG, we have,

$$i\hbar\frac{d\,|\Psi(t)\rangle}{dt} = \hat{H}_{CG}^{BEC}[\Psi](t)\,|\Psi(t)\rangle\,, \tag{C.5}$$

where,

$$\hat{H}_{CG}^{BEC}[\Psi](t) := \int d^3\boldsymbol{r}\Big[-\frac{\hbar^2}{2m}\hat{\Psi}^\dagger(\boldsymbol{r})\nabla^2\hat{\Psi}(\boldsymbol{r}) + V(\boldsymbol{r})\hat{\Psi}^\dagger(\boldsymbol{r})\hat{\Psi}(\boldsymbol{r}) + m\hat{\Psi}^\dagger(\boldsymbol{r})\hat{\Psi}(\boldsymbol{r})\Phi[\Psi(t)](\boldsymbol{r})\Big]. \tag{C.6}$$

In the Schrodinger-Newton example of CG, this is,

$$\hat{H}_{CG}^{BEC}[\Psi](t) = \int d^3\boldsymbol{r}\Big[-\frac{\hbar^2}{2m}\hat{\Psi}^\dagger(\boldsymbol{r})\nabla^2\hat{\Psi}(\boldsymbol{r}) + V(\boldsymbol{r})\hat{\Psi}^\dagger(\boldsymbol{r})\hat{\Psi}(\boldsymbol{r}) \tag{C.7}$$

$$- Gm^2\int d^3\boldsymbol{r'}\frac{\hat{\Psi}^\dagger(\boldsymbol{r})\hat{\Psi}(\boldsymbol{r})\,\langle\Psi(t)|\,\hat{\Psi}^\dagger(\boldsymbol{r'})\hat{\Psi}(\boldsymbol{r'})\,|\Psi(t)\rangle}{|\boldsymbol{r}-\boldsymbol{r'}|}\Big]. \tag{C.8}$$

Note that the evolution of $|\Psi\rangle$ in CG is, in general, 'non-linear' in that $|\Psi\rangle$ is needed to determine Φ. This is often referred to as a wavefunction 'self-interaction' since, in the first quantization picture, the wavefunction of a single-particle will now interact with itself, something that can never occur in a quantum theory of gravity, where (C.1) is said to be 'linear'.

Neglecting any explicit time dependence, the evolution of $|\Psi\rangle$ in QG can, in principle, be solved as,

$$|\Psi(t)\rangle = e^{-i\hat{H}_{QG}^{BEC}t/\hbar}\,|\Psi(0)\rangle\,. \tag{C.9}$$

In contrast, it may not be possible to find an analytic solution in CG due to the potential non-linearities. However, the evolution will still take the form,

$$|\Psi(t)\rangle = \hat{T}\left\{e^{-\frac{i}{\hbar}\int_0^t d\tau \hat{H}_{CG}^{BEC}[\Psi](\tau)}\right\}|\Psi(0)\rangle\,, \tag{C.10}$$

where $\hat{T}$ is the time-ordering operator. Despite the potential non-linearity, since $\hat{H}_{CG}^{BEC}$ is quadratic in matter field operators, it is still a Gaussian process. For example, consider the single-mode BEC experiment introduced in the main text where we assume $\hat{\Psi}(\boldsymbol{r}) = \psi(\boldsymbol{r})\hat{a}$. Neglecting the trapping potential and free dynamics, we then have,

$$|\Psi(t)\rangle = \hat{T}\left\{e^{-\frac{i}{\hbar}\int_0^t d\tau \lambda_{CG}[\Psi](t)\hat{a}^\dagger\hat{a}}\right\}|\Psi(0)\rangle\,, \tag{C.11}$$

with,

$$\lambda_{CG}[\Psi](t) = m\int d^3\boldsymbol{r}|\psi(\boldsymbol{r})|^2\Phi[\Psi](t,\boldsymbol{r}). \tag{C.12}$$

Equation (C.11) can be written as,

$$|\Psi(t)\rangle = e^{-\frac{i}{\hbar}\Lambda_{CG}[\Psi](t)\hat{a}^\dagger\hat{a}}\,|\Psi(0)\rangle\,, \tag{C.13}$$

where,

$$\Lambda_{CG}[\Psi](t) := \int_0^t d\tau \lambda_{CG}[\Psi](\tau). \tag{C.14}$$

The evolution of $|\Psi\rangle$ in this case is then, in general, a non-linear Gaussian process. However, it need not always be non-linear. For instance, in the Schrodinger-Newton case we have,

$$\lambda_{CG}[\Psi](t) = -Gm^2 \langle\Psi(t)| \hat{N} |\Psi(t)\rangle \int d^3\boldsymbol{r} d^3\boldsymbol{r'} \frac{|\psi(\boldsymbol{r'})|^2|\psi(\boldsymbol{r})|^2}{|\boldsymbol{r}-\boldsymbol{r'}|}, \tag{C.15}$$

where $\hat{N} := \hat{a}^\dagger\hat{a}$. Since $\hat{N}$ is a constant of motion (it commutes with $\hat{H}_{CG}^{BEC}$), we have,

$$\lambda_{CG} = -Gm^2 N \int d^3\boldsymbol{r} d^3\boldsymbol{r'} \frac{|\psi(\boldsymbol{r'})|^2|\psi(\boldsymbol{r})|^2}{|\boldsymbol{r}-\boldsymbol{r'}|}, \tag{C.16}$$

where $N := \langle\hat{N}\rangle$. Therefore, $|\Psi(t)\rangle$ evolves as,

$$|\Psi(t)\rangle = e^{-\frac{i}{\hbar}\gamma_{CG}\hat{a}^\dagger\hat{a}t} |\Psi(0)\rangle, \tag{C.17}$$

where,

$$\gamma_{CG} := \int d^3\boldsymbol{r} \Big[-\frac{\hbar^2}{2m}\psi^*(\boldsymbol{r})\nabla^2\psi(\boldsymbol{r}) + V(\boldsymbol{r})|\psi(\boldsymbol{r})|^2 \Big] - \lambda_{CG}, \tag{C.18}$$

such that $|\Psi(t)\rangle$ evolves under a Gaussian phase-shift channel. For example, if the BEC were initially in a coherent state $|\alpha\rangle$, it would then stay a coherent state but with just a time-dependent phase,

$$|\Psi(t)\rangle = |\alpha e^{-i\gamma_{CG}t/\hbar}\rangle, \tag{C.19}$$

with $N = |\alpha|^2$.

D

Fuzzy Time Events without Observing the Timers

We considered events of a long duration where it was necessary to include a timer to record the instance of measurement. Here we consider the situation where the experimentalist does not have access to the information stored in the timers for which we obtain

$$\begin{aligned}\hat{\rho}_{\mathrm{TL}} = \sum_{\alpha_A,\alpha_B} \sum_{\alpha'_A} \int_{t_0}^{\infty} \int_{t_A}^{\infty} \ dt_A dt_B \ |\chi_B(t_B|t_A)|^2 |\chi_A(t_A)|^2 \\ \langle \alpha_B | \hat{U}_{\mathcal{S}}(t_B,t_A)|\alpha_A\rangle \ \langle \alpha_A|\hat{U}_{\mathcal{S}}(t_A,t_0)|\psi(t_0)\rangle_{\mathcal{S}} \\ {}_{\mathcal{S}}\langle \psi(t_0)|\hat{U}^{\dagger}_{\mathcal{S}}(t_A,t_0)|\alpha'_A\rangle\langle\alpha'_A|\hat{U}^{\dagger}_{\mathcal{S}}(t_B,t_A)|\alpha_B\rangle \\ |\alpha_A\alpha_B\rangle_{AB}\langle\alpha'_A\alpha_B|. \end{aligned} \tag{D.1}$$

By rewriting this equation in the notation of Eq. (5.14), with $p^{\varepsilon}_{\alpha_B} \ \hat{\sigma}^{\varepsilon}_{A,\alpha_B} = \int dt_B \int dt_A \ p'^{\varepsilon}_{\alpha_B}(t_A,t_B) \ \hat{\rho}'^{\varepsilon}_{\alpha_B}(t_A,t_B)$, we obtain

$$\begin{aligned} p'^{\mathrm{TL}}_{\alpha_B}(t_A,t_B) = \sum_{\alpha_A} |\langle \alpha_B|\hat{U}_{\mathcal{S}}(t_B,t_A)|\alpha_A\rangle|^2 \\ |\langle\alpha_A|\hat{U}_{\mathcal{S}}(t_A,t_0)|\psi(t_0)\rangle_S|^2 \end{aligned} \tag{D.2}$$

and

$$\hat{\rho}'^{\mathrm{TL}}_{\alpha_B}(t_A,t_B) = |\lambda_{\alpha_B}(t_A,t_B)\rangle\langle\lambda_{\alpha_B}(t_A,t_B)|, \tag{D.3}$$

with

$$|\lambda_{\alpha_B}(t_A,t_B)\rangle = \frac{1}{\sqrt{p'^{\mathrm{TL}}_{\alpha_B}(t_A,t_B)}}\sum_{\alpha_A}\langle\alpha_B|\hat{U}_{\mathcal{S}}(t_B,t_A)|\alpha_A\rangle$$
$$\langle\alpha_A|\hat{U}_{\mathcal{S}}(t_A,t_0)|\psi(t_0)\rangle_S|\alpha_A\rangle. \tag{D.4}$$

Similarly, for SLE, we have

$$\hat{\rho}_{\mathrm{SL}} = \sum_{\alpha_A,\alpha_B}\int_{t_0}^{\infty}\int_{t_0}^{\infty} dt_A dt_B\ |\chi_B(t_B)|^2|\chi_A(t_A)|^2$$
$$\left|\langle\alpha_A\alpha_B|\hat{U}_{\mathcal{S}_A}(t_A,t_0)\otimes\hat{U}_{\mathcal{S}_B}(t_B,t_0)|\psi(t_0)\rangle_{\mathcal{S}}\right|^2$$
$$|\alpha_A\alpha_B\rangle_{AB}\langle\alpha_A\alpha_B| \tag{D.5}$$

where we assume the separable evolution of the system $\hat{U}_{\mathcal{S}}(t,t_0) = \hat{U}_{\mathcal{S}_A}(t,t_0)\otimes\hat{U}_{\mathcal{S}_B}(t,t_0)$ that stops after their measurements, i.e., $\hat{U}_{\mathcal{S}_j}(t,t_j) = 0$ with t_j being the detection time of $\mathcal{S}_j$.

Now the notation of Eq. (5.14) yields

$$p'^{\mathrm{SL}}_{\alpha_B}(t_A,t_B) =$$
$$\sum_{\alpha_A}\left|\langle\alpha_A\alpha_B|\hat{U}_{\mathcal{S}_A}(t_A,t_0)\otimes\hat{U}_{\mathcal{S}_B}(t_B,t_0)|\psi(t_0)\rangle_{\mathcal{S}}\right|^2 \tag{D.6}$$

and

$$\hat{\rho}'^{\mathrm{SL}}_{\alpha_B}(t_A,t_B) = \frac{1}{p'^{\mathrm{SL}}_{\alpha_B}(t_A,t_B)}$$
$$\sum_{\alpha_A}\left|\langle\alpha_A\alpha_B|\hat{U}_{\mathcal{S}_A}(t_A,t_0)\otimes\hat{U}_{\mathcal{S}_B}(t_B,t_0)|\psi(t_0)\rangle_{\mathcal{S}}\right|^2|\alpha_A\rangle\langle\alpha_A|. \tag{D.7}$$

Note that in the SL case we need to consider three terms corresponding to the order of the measurements. Furthermore, from the above results it is evident that the coherence is retained in the state describing TLE while it is absent in SLE.

Extraordinary claims require extraordinary evidence

— Carl Sagan, *Cosmos*

References

[1] C. J. Isham. "Structural issues in quantum gravity". In: *14th International Conference on General Relativity and Gravitation (GR14)*. Aug. 1995, pp. 167–209. arXiv: gr-qc/9510063.

[2] C. Rovelli. "Strings, loops and others: A Critical survey of the present approaches to quantum gravity". In: *15th International Conference on General Relativity and Gravitation (GR15)*. Dec. 1997, pp. 281–331. arXiv: gr-qc/9803024.

[3] *Approaches to Quantum Gravity: Toward a New Understanding of Space, Time and Matter*. Cambridge University Press, 2009.

[4] C. Rovelli. "Notes for a brief history of quantum gravity". In: *9th Marcel Grossmann Meeting on Recent Developments in Theoretical and Experimental General Relativity, Gravitation and Relativistic Field Theories (MG 9)*. June 2000, pp. 742–768. arXiv: gr-qc/0006061.

[5] Joseph Polchinski. *String Theory*. Vol. 1. Cambridge Monographs on Mathematical Physics. Cambridge University Press, 1998.

[6] Carlo Rovelli. *Quantum Gravity*. Cambridge Monographs on Mathematical Physics. Cambridge University Press, 2004.

[7] Sougato Bose et al. "Spin Entanglement Witness for Quantum Gravity". In: *Phys. Rev. Lett.* 119 (24 Dec. 2017), p. 240401. URL: https://link.aps.org/doi/10.1103/PhysRevLett.119.240401.

[8] C. Marletto and V. Vedral. "Gravitationally Induced Entanglement between Two Massive Particles is Sufficient Evidence of Quantum Effects in Gravity". In: *Phys. Rev. Lett.* 119 (24 Dec. 2017), p. 240402. URL: https://link.aps.org/doi/10.1103/PhysRevLett.119.240402.

[9] C. Wan et al. "Free Nano-Object Ramsey Interferometry for Large Quantum Superpositions". In: *Phys. Rev. Lett.* 117 (14 Sept. 2016), p. 143003. URL: https://link.aps.org/doi/10.1103/PhysRevLett.117.143003.

[10] Dvir Kafri and J. M. Taylor. *A noise inequality for classical forces*. 2013. URL: https://arxiv.org/abs/1311.4558.

[11] C. Marletto and V. Vedral. "Gravitationally Induced Entanglement between Two Massive Particles is Sufficient Evidence of Quantum Effects in Gravity". In: *Phys. Rev. Lett.* 119 (24 Dec. 2017), p. 240402. URL: https://link.aps.org/doi/10.1103/PhysRevLett.119.240402.

[12] Tanjung Krisnanda et al. "Revealing Nonclassicality of Inaccessible Objects". In: *Phys. Rev. Lett.* 119 (12 Sept. 2017), p. 120402. URL: https://link.aps.org/doi/10.1103/PhysRevLett.119.120402.

[13] Richard Howl, Roger Penrose, and Ivette Fuentes. "Exploring the unification of quantum theory and general relativity with a Bose–Einstein condensate". In: *New Journal of Physics* 21.4 (Apr. 2019), p. 043047. URL: https://doi.org/10.1088%2F1367-2630%2Fab104a.

[14] Richard Howl et al. "Gravity in the quantum lab". In: *Advances in Physics: X* 3.1 (Dec. 2017), p. 1383184. URL: https://doi.org/10.1080%2F23746149.2017.1383184.

[15] Carlos Sabín et al. "Phonon creation by gravitational waves". In: *New Journal of Physics* 16.8 (Aug. 2014), p. 085003. URL: https://doi.org/10.1088/1367-2630/16/8/085003.

[16] Dennis Rätzel et al. "Dynamical response of Bose–Einstein condensates to oscillating gravitational fields". In: *New Journal of Physics* 20.7 (July 2018), p. 073044. URL: https://doi.org/10.1088/1367-2630/aad272.

[17] Alan H. Guth. "Inflationary universe: A possible solution to the horizon and flatness problems". In: *Phys. Rev. D* 23 (2 Jan. 1981), pp. 347–356. URL: https://link.aps.org/doi/10.1103/PhysRevD.23.347.

[18] Robert H. Brandenberger. "Inflationary cosmology: Progress and problems". In: *IPM School on Cosmology 1999: Large Scale Structure Formation Tehran, Iran, January 23-February 4, 1999.* 1999. arXiv: hep-ph/9910410 [hep-ph].

[19] Andrei D. Linde. "A New Inflationary Universe Scenario: A Possible Solution of the Horizon, Flatness, Homogeneity, Isotropy and Primordial Monopole Problems". In: *Phys. Lett.* 108B (1982). [Adv. Ser. Astrophys. Cosmol.3,149(1987)], pp. 389–393.

[20] Andreas Albrecht et al. "Inflation and squeezed quantum states". In: *Phys. Rev.* D50 (1994), pp. 4807–4820. arXiv: astro-ph/9303001 [astro-ph].

[21] Jonathan L. Ball, Ivette Fuentes-Schuller, and Frederic P. Schuller. "Entanglement in an expanding spacetime". In: *Physics Letters A* 359.6 (Dec. 2006), pp. 550–554. URL: https://doi.org/10.1016%2Fj.physleta.2006.07.028.

[22] Ivette Fuentes et al. "Entanglement of Dirac fields in an expanding spacetime". In: *Phys. Rev. D* 82 (4 Aug. 2010), p. 045030. URL: https://link.aps.org/doi/10.1103/PhysRevD.82.045030.

[23] J. Maldacena. "A model with cosmological Bell inequalities". In: *Fortschritte der Physik* 64.1 (Dec. 2015), pp. 10–23. URL: http://dx.doi.org/10.1002/prop.201500097.

[24] Stephen J. Summers and Reinhard Werner. "The vacuum violates Bell's inequalities". In: *Physics Letters A* 110.5 (1985), pp. 257–259. URL: https://www.sciencedirect.com/science/article/pii/0375960185900933.

[25] Atsushi Higuchi et al. "Entanglement of the vacuum between left, right, future, and past: The origin of entanglement-induced quantum radiation". In: *Phys. Rev. D* 96 (8 Oct. 2017), p. 083531. URL: https://link.aps.org/doi/10.1103/PhysRevD.96.083531.

[26] Edward Witten. "APS Medal for Exceptional Achievement in Research: Invited article on entanglement properties of quantum field theory". In: *Rev. Mod. Phys.* 90 (4 Oct. 2018), p. 045003. URL: https://link.aps.org/doi/10.1103/RevModPhys.90.045003.

[27] W. G. Unruh. "Notes on black-hole evaporation". In: *Phys. Rev. D* 14 (4 Aug. 1976), pp. 870–892. URL: https://link.aps.org/doi/10.1103/PhysRevD.14.870.

[28] K. -E. Hellwig and K. Kraus. “Formal Description of Measurements in Local Quantum Field Theory”. In: *Phys. Rev. D* 1 (2 Jan. 1970), pp. 566–571. URL: https://link.aps.org/doi/10.1103/PhysRevD.1.566.

[29] H. Reeh and S. Schlieder. “Bemerkungen zur unitäräquivalenz von lorentzinvarianten feldern”. In: *Nuovo Cim.* 22.5 (1961), pp. 1051–1068.

[30] Rafael D. Sorkin. “Impossible measurements on quantum fields”. In: *Directions in General Relativity: An International Symposium in Honor of the 60th Birthdays of Dieter Brill and Charles Misner*. Feb. 1993. arXiv: gr-qc/9302018.

[31] Eduardo Martín-Martínez. “Causality issues of particle detector models in QFT and quantum optics”. In: *Phys. Rev. D* 92 (10 Nov. 2015), p. 104019. URL: https://link.aps.org/doi/10.1103/PhysRevD.92.104019.

[32] Grant Salton, Robert B Mann, and Nicolas C Menicucci. “Acceleration-assisted entanglement harvesting and rangefinding”. In: *New Journal of Physics* 17.3 (Mar. 2015), p. 035001. URL: https://dx.doi.org/10.1088/1367-2630/17/3/035001.

[33] Jorma Louko and Alejandro Satz. “How often does the Unruh–DeWitt detector click? Regularization by a spatial profile”. In: *Classical and Quantum Gravity* 23.22 (Oct. 2006), p. 6321. URL: https://dx.doi.org/10.1088/0264-9381/23/22/015.

[34] Paul Langlois. “Causal particle detectors and topology”. In: *Annals of Physics* 321.9 (2006), pp. 2027–2070. URL: https://www.sciencedirect.com/science/article/pii/S0003491606000480.

[35] Eduardo Martín-Martínez, Miguel Montero, and Marco del Rey. “Wavepacket detection with the Unruh-DeWitt model”. In: *Phys. Rev. D* 87 (6 Mar. 2013), p. 064038. URL: https://link.aps.org/doi/10.1103/PhysRevD.87.064038.

[36] Antony R. Lee and Ivette Fuentes. “Spatially extended Unruh-DeWitt detectors for relativistic quantum information”. In: *Phys. Rev. D* 89 (8 Apr. 2014), p. 085041. URL: https://link.aps.org/doi/10.1103/PhysRevD.89.085041.

[37] R B Mann and T C Ralph. “Relativistic quantum information”. In: *Classical and Quantum Gravity* 29.22 (Oct. 2012), p. 220301. URL: https://doi.org/10.1088/0264-9381/29/22/220301.

[38] Juan Maldacena. In: *International Journal of Theoretical Physics* 38.4 (1999), pp. 1113–1133. URL: https://doi.org/10.1023%2Fa%3A1026654312961.

[39] Sean A. Hartnoll. “Lectures on holographic methods for condensed matter physics”. In: *Class. Quant. Grav.* 26 (2009). Ed. by A. M. Uranga, p. 224002. arXiv: 0903.3246 [hep-th].

[40] Hong Liu, Krishna Rajagopal, and Urs Achim Wiedemann. “Calculating the Jet Quenching Parameter”. In: *Phys. Rev. Lett.* 97 (18 Nov. 2006), p. 182301. URL: https://link.aps.org/doi/10.1103/PhysRevLett.97.182301.

[41] Jorge Casalderrey-Solana et al. *Gauge/String Duality, Hot QCD and Heavy Ion Collisions*. Cambridge University Press, 2014. arXiv: 1101.0618 [hep-th].

[42] Makoto Natsuume. *AdS/CFT Duality User Guide*. 2014. URL: https://arxiv.org/abs/1409.3575.

[43] Barak Bringoltz and Michael Teper. “The pressure of the SU(N) lattice gauge theory at large N”. In: *Physics Letters B* 628.1 (2005), pp. 113–124. URL: https://www.sciencedirect.com/science/article/pii/S0370269305012323.

[44] Adam R. Brown and Leonard Susskind. "Second law of quantum complexity". In: *Physical Review D* 97.8 (Apr. 2018). URL: https://doi.org/10.1103%2Fphysrevd.97.086015.

[45] Leonard Susskind. *Computational Complexity and Black Hole Horizons*. 2014. URL: https://arxiv.org/abs/1402.5674.

[46] Leonard Susskind. *Addendum to Computational Complexity and Black Hole Horizons*. 2014. URL: https://arxiv.org/abs/1403.5695.

[47] Mihalis Dafermos and Igor Rodnianski. "Lectures on black holes and linear waves". In: (2008). URL: https://arxiv.org/abs/0811.0354.

[48] David Finkelstein. "Space-Time Code". In: *Phys. Rev.* 184 (5 Aug. 1969), pp. 1261–1271. URL: https://link.aps.org/doi/10.1103/PhysRev.184.1261.

[49] C. J. Isham. "Quantum logic and the histories approach to quantum theory". In: *Journal of Mathematical Physics* 35.5 (May 1994), pp. 2157–2185. URL: https://doi.org/10.1063%2F1.530544.

[50] Joseph Fitzsimons, Jonathan Jones, and Vlatko Vedral. *Quantum correlations which imply causation*. 2013. URL: https://arxiv.org/abs/1302.2731.

[51] Marcin Nowakowski. "Quantum entanglement in time". In: *AIP Conference Proceedings*. Author(s), 2017. URL: https://doi.org/10.1063%2F1.4982771.

[52] Jordan Cotler et al. "Superdensity operators for spacetime quantum mechanics". In: *Journal of High Energy Physics* 2018.9 (Sept. 2018). URL: https://doi.org/10.1007%2Fjhep09%282018%29093.

[53] Don N. Page and William K. Wootters. "Evolution without evolution: Dynamics described by stationary observables". In: *Phys. Rev. D* 27 (12 June 1983), pp. 2885–2892. URL: https://link.aps.org/doi/10.1103/PhysRevD.27.2885.

[54] L Henderson and V Vedral. "Classical, quantum and total correlations". In: *Journal of Physics A: Mathematical and General* 34.35 (Aug. 2001), pp. 6899–6905. URL: https://doi.org/10.1088%2F0305-4470%2F34%2F35%2F315.

[55] Itamar Allali and Mark P. Hertzberg. "Gravitational decoherence of dark matter". In: *Journal of Cosmology and Astroparticle Physics* 2020.07 (July 2020), pp. 056–056. URL: http://dx.doi.org/10.1088/1475-7516/2020/07/056.

[56] Itamar J. Allali and Mark P. Hertzberg. "General Relativistic Decoherence with Applications to Dark Matter Detection". In: *Phys. Rev. Lett.* 127 (3 July 2021), p. 031301. URL: https://link.aps.org/doi/10.1103/PhysRevLett.127.031301.

[57] Itamar J. Allali and Mark P. Hertzberg. "Decoherence from general relativity". In: *Physical Review D* 103.10 (May 2021). URL: http://dx.doi.org/10.1103/PhysRevD.103.104053.

[58] J J Halliwell. "Two derivations of the master equation of quantum Brownian motion". In: *Journal of Physics A: Mathematical and Theoretical* 40.12 (Mar. 2007), pp. 3067–3080. URL: https://doi.org/10.1088/1751-8113/40/12/s11.

[59] B. Paczynski. "Gravitational microlensing by the galactic halo". In: *Astrophysical Journal* 304 (May 1986), p. 1. URL: https://doi.org/10.1086/164140.

[60] Kim Griest. "Galactic microlensing as a method of detecting massive compact halo objects". In: *Astrophysical Journal* 366 (Jan. 1991), p. 412. URL: https://doi.org/10.1086/169575.

[61] Gianfranco Bertone and Dan Hooper. "History of dark matter". In: *Reviews of Modern Physics* 90.4 (Oct. 2018). URL: https://doi.org/10.1103/revmodphys.90.045002.

[62] Don N. Page and C. D. Geilker. "Indirect Evidence for Quantum Gravity". In: *Phys. Rev. Lett.* 47 (14 Oct. 1981), pp. 979–982. URL: https://link.aps.org/doi/10.1103/PhysRevLett.47.979.

[63] Cécile Morette Dewitt and Dean Rickles. *The role of gravitation in physics report from the 1957 Chapel Hill Conference.* eng. Max Planck Research Library for the History and Development of Knowledge; Sources 5. epubli GmbH, 2011.

[64] Andrea Palessandro and Martin S. Sloth. "Gravitational absorption lines". In: *Phys. Rev. D* 101 (4 Feb. 2020), p. 043504. URL: https://link.aps.org/doi/10.1103/PhysRevD.101.043504.

[65] Niklas G. Nielsen, Andrea Palessandro, and Martin S. Sloth. "Gravitational atoms". In: *Phys. Rev. D* 99 (12 June 2019), p. 123011. URL: https://link.aps.org/doi/10.1103/PhysRevD.99.123011.

[66] C. Marletto and V. Vedral. "When can gravity path-entangle two spatially superposed masses?" In: *Phys. Rev. D* 98 (4 Aug. 2018), p. 046001. URL: https://link.aps.org/doi/10.1103/PhysRevD.98.046001.

[67] M. Carlesso et al. "Testing the gravitational field generated by a quantum superposition". In: 21.9 (Sept. 2019), p. 093052. URL: https://doi.org/10.1088/1367-2630/ab41c1.

[68] S. Bose et al. "Spin Entanglement Witness for Quantum Gravity". In: *Phys. Rev. Lett.* 119 (24 Dec. 2017), p. 240401. URL: https://link.aps.org/doi/10.1103/PhysRevLett.119.240401.

[69] R. J. Marshman, A. Mazumdar, and S. Bose. "Locality and entanglement in table-top testing of the quantum nature of linearized gravity". In: *Phys. Rev. A* 101 (5 May 2020), p. 052110. URL: https://link.aps.org/doi/10.1103/PhysRevA.101.052110.

[70] R. Howl et al. "Non-Gaussianity as a Signature of a Quantum Theory of Gravity". In: *PRX Quantum* 2.1 (Feb. 2021). URL: http://dx.doi.org/10.1103/PRXQuantum.2.010325.

[71] Niklas G. Nielsen, Andrea Palessandro, and Martin S. Sloth. "Gravitational atoms". In: *Physical review. D* 99.12 (June 2019). URL: https://explore.openaire.eu/search/publication?articleId=dedup_wf_001::2791f48e68abbf89a4c754076794a1be.

[72] L. Parker. "Particle Creation in Expanding Universes". In: *Phys. Rev. Lett.* 21 (8 Aug. 1968), pp. 562–564. URL: https://link.aps.org/doi/10.1103/PhysRevLett.21.562.

[73] Leonard Parker. "Quantized Fields and Particle Creation in Expanding Universes. I". In: *Phys. Rev.* 183 (5 July 1969), pp. 1057–1068. URL: https://link.aps.org/doi/10.1103/PhysRev.183.1057.

[74] N. D. Birrell and P. C. W. Davies. *Quantum Fields in Curved Space.* Cambridge Monographs on Mathematical Physics. Cambridge University Press, 1982.

[75] Michael J W Hall and Marcel Reginatto. "On two recent proposals for witnessing nonclassical gravity". In: *Journal of Physics A: Mathematical and Theoretical* 51.8 (Jan. 2018), p. 085303. URL: https://doi.org/10.1088/1751-8121/aaa734.

[76] Marios Christodoulou et al. *Locally mediated entanglement through gravity from first principles.* 2022. URL: https://arxiv.org/abs/2202.03368.

[77] Seth Lloyd and Samuel L. Braunstein. "Quantum Computation over Continuous Variables". In: *Phys. Rev. Lett.* 82 (8 Feb. 1999), pp. 1784–1787. URL: https://link.aps.org/doi/10.1103/PhysRevLett.82.1784.

[78] R D Sorkin. "Expressing entropy globally in terms of (4D) field-correlations". In: *Journal of Physics: Conference Series* 484 (Mar. 2014), p. 012004. URL: https://doi.org/10.1088/1742-6596/484/1/012004.

[79] Jürgen Berges, Stefan Floerchinger, and Raju Venugopalan. "Dynamics of entanglement in expanding quantum fields". In: *Journal of High Energy Physics* 2018.4 (Apr. 2018). URL: https://doi.org/10.10072Fjhep0428201829145.

[80] Christian Weedbrook et al. "Gaussian quantum information". In: *Rev. Mod. Phys.* 84 (2 May 2012), pp. 621–669. URL: https://link.aps.org/doi/10.1103/RevModPhys.84.621.

[81] Karsten Lange et al. "Entanglement between two spatially separated atomic modes". In: *Science* 360.6387 (2018), pp. 416–418. eprint: https://www.science.org/doi/pdf/10.1126/science.aao2035. URL: https://www.science.org/doi/abs/10.1126/science.aao2035.

[82] Philipp Kunkel et al. "Spatially distributed multipartite entanglement enables EPR steering of atomic clouds". In: *Science* 360.6387 (2018), pp. 413–416. URL: https://www.science.org/doi/abs/10.1126/science.aao2254.

[83] Lev Pitaevskii and Sandro Stringari. *Bose-Einstein Condensation and Superfluidity.* Oxford University Press, Jan. 2016. URL: https://doi.org/10.1093/acprof:oso/9780198758884.001.0001.

[84] E. Wigner. "On the Quantum Correction For Thermodynamic Equilibrium". In: *Phys. Rev.* 40 (5 June 1932), pp. 749–759. URL: https://link.aps.org/doi/10.1103/PhysRev.40.749.

[85] Michael E. Peskin and Daniel V. Schroeder. *An Introduction to quantum field theory.* Reading, USA: Addison-Wesley, 1995.

[86] J F Corney and P D Drummond. "Gaussian operator bases for correlated fermions". In: *Journal of Physics A: Mathematical and General* 39.2 (Dec. 2005), pp. 269–297. URL: https://doi.org/10.1088/0305-4470/39/2/001.

[87] Thomas Thiemann. *Modern Canonical Quantum General Relativity.* Cambridge Monographs on Mathematical Physics. Cambridge University Press, 2007.

[88] Bryce S. DeWitt. "Quantum Theory of Gravity. II. The Manifestly Covariant Theory". In: *Phys. Rev.* 162 (5 Oct. 1967), pp. 1195–1239. URL: https://link.aps.org/doi/10.1103/PhysRev.162.1195.

[89] John F. Donoghue. "Leading quantum correction to the Newtonian potential". In: *Phys. Rev. Lett.* 72 (19 May 1994), pp. 2996–2999. URL: https://link.aps.org/doi/10.1103/PhysRevLett.72.2996.

[90] John F. Donoghue. "General relativity as an effective field theory: The leading quantum corrections". In: *Phys. Rev. D* 50 (6 Sept. 1994), pp. 3874–3888. URL: https://link.aps.org/doi/10.1103/PhysRevD.50.3874.

[91] Michele Maggiore. *Gravitational Waves: Volume 1: Theory and Experiments.* Oxford University Press, Oct. 2007. URL: https://doi.org/10.1093/acprof:oso/9780198570745.001.0001.

[92] Simon A Haine. “Searching for signatures of quantum gravity in quantum gases”. In: *New Journal of Physics* 23.3 (Mar. 2021), p. 033020. URL: https://doi.org/10.10882F1367-26302Fabd97d.

[93] B. Dubost et al. “Efficient Quantification of Non-Gaussian Spin Distributions”. In: *Phys. Rev. Lett.* 108 (18 May 2012), p. 183602. URL: https://link.aps.org/doi/10.1103/PhysRevLett.108.183602.

[94] Richard Howl, Roger Penrose, and Ivette Fuentes. “Exploring the unification of quantum theory and general relativity with a Bose–Einstein condensate”. In: *New Journal of Physics* 21.4 (Apr. 2019), p. 043047. URL: https://doi.org/10.1088/1367-2630/ab104a.

[95] Dale G. Fried et al. “Bose-Einstein Condensation of Atomic Hydrogen”. In: *Phys. Rev. Lett.* 81 (18 Nov. 1998), pp. 3811–3814. URL: https://link.aps.org/doi/10.1103/PhysRevLett.81.3811.

[96] K. M. R. van der Stam et al. “Large atom number Bose-Einstein condensate of sodium”. In: *Review of Scientific Instruments* 78.1 (2007), p. 013102. eprint: https://doi.org/10.1063/1.2424439. URL: https://doi.org/10.1063/1.2424439.

[97] Marios Christodoulou and Carlo Rovelli. “On the possibility of laboratory evidence for quantum superposition of geometries”. In: *Physics Letters B* 792 (2019), pp. 64–68. URL: https://www.sciencedirect.com/science/article/pii/S0370269319301698.

[98] C. K. Law, H. Pu, and N. P. Bigelow. “Quantum Spins Mixing in Spinor Bose-Einstein Condensates”. In: *Phys. Rev. Lett.* 81 (24 Dec. 1998), pp. 5257–5261. URL: https://link.aps.org/doi/10.1103/PhysRevLett.81.5257.

[99] W. Muessel et al. “Scalable Spin Squeezing for Quantum-Enhanced Magnetometry with Bose-Einstein Condensates”. In: 113.10, 103004 (Sept. 2014), p. 103004. arXiv: 1405.6022 [quant-ph].

[100] Philipp Kunkel et al. “Spatially distributed multipartite entanglement enables EPR steering of atomic clouds”. In: *Science* 360.6387 (2018), pp. 413–416. eprint: https://www.science.org/doi/pdf/10.1126/science.aao2254. URL: https://www.science.org/doi/abs/10.1126/science.aao2254.

[101] S. Wüster et al. “Quantum-field dynamics of expanding and contracting Bose-Einstein condensates”. In: *Phys. Rev. A* 77 (2 Feb. 2008), p. 023619. URL: https://link.aps.org/doi/10.1103/PhysRevA.77.023619.

[102] Mattias T. Johnsson and Simon A. Haine. “Generating Quadrature Squeezing in an Atom Laser through Self-Interaction”. In: *Phys. Rev. Lett.* 99 (1 July 2007), p. 010401. URL: https://link.aps.org/doi/10.1103/PhysRevLett.99.010401.

[103] S. S. Hodgman et al. “Direct Measurement of Long-Range Third-Order Coherence in Bose-Einstein Condensates”. In: *Science* 331.6020 (2011), pp. 1046–1049. eprint: https://www.science.org/doi/pdf/10.1126/science.1198481. URL: https://www.science.org/doi/abs/10.1126/science.1198481.

[104] Ch. Kurtsiefer, T. Pfau, and J. Mlynek. “Measurement of the Wigner function of an ensemble of helium atoms”. In: 386.6621 (Mar. 1997), pp. 150–153.

[105] Jeff S. Lundeen et al. “Direct measurement of the quantum wavefunction”. In: *Nature* 474.7350 (June 2011), pp. 188–191. URL: https://doi.org/10.1038%2Fnature10120.

[106] Charles Bamber and Jeff S. Lundeen. “Observing Dirac’s Classical Phase Space Analog to the Quantum State”. In: *Phys. Rev. Lett.* 112 (7 Feb. 2014), p. 070405. URL: https://link.aps.org/doi/10.1103/PhysRevLett.112.070405.

[107] S. E. Pollack et al. “Extreme Tunability of Interactions in a ^{7}Li Bose-Einstein Condensate”. In: *Phys. Rev. Lett.* 102 (9 Mar. 2009), p. 090402. URL: https://link.aps.org/doi/10.1103/PhysRevLett.102.090402.

[108] M. Fattori et al. “Magnetic Dipolar Interaction in a Bose-Einstein Condensate Atomic Interferometer”. In: *Phys. Rev. Lett.* 101 (19 Nov. 2008), p. 190405. URL: https://link.aps.org/doi/10.1103/PhysRevLett.101.190405.

[109] Harold Weinstock, ed. *SQUID Sensors: Fundamentals, Fabrication and Applications*. Springer Netherlands, 1996. URL: https://doi.org/10.1007/978-94-011-5674-5.

[110] I. K. Kominis et al. “A subfemtotesla multichannel atomic magnetometer”. In: *Nature* 422.6932 (Apr. 2003), pp. 596–599. URL: https://doi.org/10.1038/nature01484.

[111] Cheng Chin et al. “Precision Feshbach spectroscopy of ultracold Cs_2”. In: *Phys. Rev. A* 70 (3 Sept. 2004), p. 032701. URL: https://link.aps.org/doi/10.1103/PhysRevA.70.032701.

[112] Randy K. Dumas and Tom Hogan. “Recent Advances in SQUID Magnetometry”. In: *Magnetic Measurement Techniques for Materials Characterization*. Springer International Publishing, 2021, pp. 39–62. URL: https://doi.org/10.1007/978-3-030-70443-8_3.

[113] Cheng Chin et al. “Feshbach resonances in ultracold gases”. In: *Rev. Mod. Phys.* 82 (2 Apr. 2010), pp. 1225–1286. URL: https://link.aps.org/doi/10.1103/RevModPhys.82.1225.

[114] P. G. Mickelson et al. “Spectroscopic Determination of the s-Wave Scattering Lengths of ^{86}Sr and ^{88}Sr”. In: *Phys. Rev. Lett.* 95 (22 Nov. 2005), p. 223002. URL: https://link.aps.org/doi/10.1103/PhysRevLett.95.223002.

[115] Pascal G. Mickelson et al. “Observation of an Optical Feshbach Resonance in 88Sr”. In: *Conference on Lasers and Electro-Optics/International Quantum Electronics Conference*. OSA, 2009. URL: https://doi.org/10.1364/iqec.2009.ipda3.

[116] Timothy Clifton et al. “Modified gravity and cosmology”. In: *Physics Reports* 513.1-3 (Mar. 2012), pp. 1–189. URL: https://doi.org/10.1016%2Fj.physrep.2012.01.001.

[117] E. Komatsu, D. N. Spergel, and B. D. Wandelt. “Measuring Primordial Non-Gaussianity in the Cosmic Microwave Background”. In: *The Astrophysical Journal* 634.1 (Nov. 2005), pp. 14–19. URL: https://doi.org/10.1086/491724.

[118] Lawrence M. Krauss and Frank Wilczek. “Using cosmology to establish the quantization of gravity”. In: *Phys. Rev. D* 89 (4 Feb. 2014), p. 047501. URL: https://link.aps.org/doi/10.1103/PhysRevD.89.047501.

[119] Jérôme Martin and Vincent Vennin. “Obstructions to Bell CMB experiments”. In: *Phys. Rev. D* 96 (6 Sept. 2017), p. 063501. URL: https://link.aps.org/doi/10.1103/PhysRevD.96.063501.

[120] Kai Bongs et al. “Taking atom interferometric quantum sensors from the laboratory to real-world applications”. In: *Nature Rev. Phys.* 1.12 (2019), pp. 731–739.

[121] R. Penrose. “Gravitational collapse: The role of general relativity”. In: *Riv. Nuovo Cim.* 1 (1969), pp. 252–276.

[122] Marios Christodoulou and Carlo Rovelli. “How big is a black hole?” In: *Phys. Rev. D* 91 (6 Mar. 2015), p. 064046. URL: https://link.aps.org/doi/10.1103/PhysRevD.91.064046.

[123] Yen Chin Ong. “Never Judge a Black Hole by Its Area”. In: *JCAP* 04 (2015), p. 003. arXiv: 1503.01092 [gr-qc].

[124] Marios Christodoulou et al. “Gravity entanglement, quantum reference systems, degrees of freedom”. In: (July 2022). arXiv: 2207.03138 [quant-ph].

[125] Ingemar Bengtsson and Emma Jakobsson. “Black holes: Their large interiors”. In: *Modern Physics Letters A* 30.21 (June 2015), p. 1550103. URL: https://doi.org/10.1142%2Fs0217732315501035.

[126] Mihalis Dafermos. “Stability and instability of the Cauchy horizon for the spherically symmetric Einstein-Maxwell-scalar field equations”. English. In: *Ann. Math. (2)* 158.3 (2003), pp. 875–928. URL: annals.math.princeton.edu/issues/2003/Dafermos.pdf.

[127] Mihalis Dafermos and Igor Rodnianski. “The Red-shift effect and radiation decay on black hole spacetimes”. In: *Commun. Pure Appl. Math.* 62 (2009), pp. 859–919. arXiv: gr-qc/0512119.

[128] Paul M. Chesler. *Singularities in rotating black holes coupled to a massless scalar field.* 2019. URL: https://arxiv.org/abs/1905.04613.

[129] Naresh Dadhich, Sushant G. Ghosh, and Sanjay Jhingan. “Gravitational collapse in pure Lovelock gravity in higher dimensions”. In: *Phys. Rev. D* 88 (2013), p. 084024. arXiv: 1308.4312 [gr-qc].

[130] Jonathan Luk, Sung-Jin Oh, and Yakov Shlapentokh-Rothman. *A scattering theory approach to Cauchy horizon instability and applications to mass inflation.* 2022. URL: https://arxiv.org/abs/2201.12294.

[131] Mihalis Dafermos and Yakov Shlapentokh-Rothman. “Rough initial data and the strength of the blue-shift instability on cosmological black holes with {*upLambda*”. In: *Classical and Quantum Gravity* 35.19 (Sept. 2018), p. 195010. URL: https://doi.org/10.1088%2F1361-6382%2Faadbcf.

[132] Peter Hintz and Andrá s Vasy. “Analysis of linear waves near the Cauchy horizon of cosmological black holes”. In: *Journal of Mathematical Physics* 58.8 (Aug. 2017), p. 081509. URL: https://doi.org/10.1063%2F1.4996575.

[133] Patrick Hayden and John Preskill. “Black holes as mirrors: quantum information in random subsystems”. In: *Journal of High Energy Physics* 2007.09 (Sept. 2007), pp. 120–120. URL: https://doi.org/10.1088%2F1126-6708%2F2007%2F09%2F120.

[134] Adam R. Brown et al. “Complexity of Jackiw-Teitelboim gravity”. In: *Physical Review D* 99.4 (Feb. 2019). URL: https://doi.org/10.1103%2Fphysrevd.99.046016.

[135] Albert M Sirunyan et al. “Measurement of nuclear modification factors of $\Upsilon(1S)$, $\Upsilon(2S)$, and $\Upsilon(3S)$ mesons in PbPb collisions at $\sqrt{s_{\mathrm{NN}}} = 5.02$ TeV”. In: *Phys. Lett. B* 790 (2019), pp. 270–293. arXiv: 1805.09215 [hep-ex].

[136] Oscar J.C. Dias, Harvey S. Reall, and Jorge E. Santos. “The BTZ black hole violates strong cosmic censorship”. In: *Journal of High Energy Physics* 2019.12 (Dec. 2019). URL: https://doi.org/10.1007%2Fjhep12%282019%29097.

[137] Josiah Couch et al. "Holographic complexity and volume". In: *Journal of High Energy Physics* 2018.11 (Nov. 2018). URL: https://doi.org/10.1007%2Fjhep11%282018%29044.

[138] M Giammatteo and Ian G Moss. "Gravitational quasinormal modes for Kerr anti-de Sitter black holes". In: *Classical and Quantum Gravity* 22.9 (Apr. 2005), pp. 1803–1824. URL: https://doi.org/10.1088%2F0264-9381%2F22%2F9%2F021.

[139] Leonard Susskind. *Singularities, Firewalls, and Complementarity.* 2012. URL: https://arxiv.org/abs/1208.3445.

[140] José L. F. Barbón and Javier Martín-García. "Holographic complexity of cold hyperbolic black holes". In: *Journal of High Energy Physics* 2015.11 (Nov. 2015). URL: https://doi.org/10.1007%2Fjhep11%282015%29181.

[141] Yu-Sen An, Rong-Gen Cai, and Yuxuan Peng. "Time dependence of holographic complexity in Gauss-Bonnet gravity". In: *Phys. Rev. D* 98 (10 Nov. 2018), p. 106013. URL: https://link.aps.org/doi/10.1103/PhysRevD.98.106013.

[142] Christoph Kehle. *Uniform boundedness and continuity at the Cauchy horizon for linear waves on Reissner-Nordström-AdS black holes.* 2018. URL: https://arxiv.org/abs/1812.06142.

[143] Christoph Kehle. *Blowup of the local energy of linear waves at the Reissner-Nordström-AdS Cauchy horizon.* 2021. URL: https://arxiv.org/abs/2108.04280.

[144] Christoph Kehle. *Diophantine approximation as Cosmic Censor for Kerr-AdS black holes.* 2020. URL: https://arxiv.org/abs/2007.12614.

[145] Ning Bao et al. "Consistency conditions for an AdS multiscale entanglement renormalization ansatz correspondence". In: *Physical Review D* 91.12 (June 2015). URL: https://doi.org/10.1103%2Fphysrevd.91.125036.

[146] ChunJun Cao and Sean M. Carroll. "Bulk entanglement gravity without a boundary: Towards finding Einstein's equation in Hilbert space". In: *Physical Review D* 97.8 (Apr. 2018). URL: https://doi.org/10.1103%2Fphysrevd.97.086003.

[147] A. J. Leggett and Anupam Garg. "Quantum mechanics versus macroscopic realism: Is the flux there when nobody looks?" In: *Phys. Rev. Lett.* 54 (9 Mar. 1985), pp. 857–860. URL: https://link.aps.org/doi/10.1103/PhysRevLett.54.857.

[148] Edward S. Fry et al. "Atomic coherence effects within the sodium D_1 line: Lasing without inversion via population trapping". In: *Phys. Rev. Lett.* 70 (21 May 1993), pp. 3235–3238. URL: https://link.aps.org/doi/10.1103/PhysRevLett.70.3235.

[149] Daniel Collins et al. "Bell-Type Inequalities to Detect True N-Body Nonseparability". In: *Physical Review Letters* 88.17 (Apr. 2002). URL: https://doi.org/10.1103%2Fphysrevlett.88.170405.

[150] Caslav Brukner et al. *Quantum Entanglement in Time.* 2004. URL: https://arxiv.org/abs/quant-ph/0402127.

[151] T. C. Ralph, G. J. Milburn, and T. Downes. "Quantum connectivity of space-time and gravitationally induced decorrelation of entanglement". In: *Physical Review A* 79.2 (Feb. 2009). URL: https://doi.org/10.1103%2Fphysreva.79.022121.

[152] Eduardo O. Dias. "Quantum formalism for events and how time can emerge from its foundations". In: *Phys. Rev. A* 103 (1 Jan. 2021), p. 012219. URL: https://link.aps.org/doi/10.1103/PhysRevA.103.012219.

[153] Michael A. Nielsen and Isaac L. Chuang. *Quantum Computation and Quantum Information: 10th Anniversary Edition.* Cambridge University Press, 2010.

[154] Vlatko Vedral. *Introduction to Quantum Information Science.* Oxford University Press, Sept. 2006. URL: https://doi.org/10.1093/acprof:oso/9780199215706.001.0001.

[155] Carl W. Helstrom. "Quantum detection and estimation theory". In: *Journal of Statistical Physics* 1.2 (June 1969), pp. 231–252.

[156] A.S Holevo. "Statistical decision theory for quantum systems". In: *Journal of Multivariate Analysis* 3.4 (1973), pp. 337–394. URL: https://www.sciencedirect.com/science/article/pii/0047259X73900286.

[157] Asher Peres. "Measurement of time by quantum clocks". In: *American Journal of Physics* 48.7 (July 1980), pp. 552–557.

[158] T. E. Harris. "A lower bound for the critical probability in a certain percolation process". In: *Mathematical Proceedings of the Cambridge Philosophical Society* 56.1 (1960), pp. 13–20.

[159] Giulio Chiribella et al. "Quantum computations without definite causal structure". In: *Physical Review A* 88.2 (Aug. 2013). URL: https://doi.org/10.1103%2Fphysreva.88.022318.

[160] Daniel Ebler, Sina Salek, and Giulio Chiribella. "Enhanced Communication with the Assistance of Indefinite Causal Order". In: *Phys. Rev. Lett.* 120 (12 Mar. 2018), p. 120502. URL: https://link.aps.org/doi/10.1103/PhysRevLett.120.120502.

[161] David Felce and Vlatko Vedral. "Quantum Refrigeration with Indefinite Causal Order". In: *Phys. Rev. Lett.* 125 (7 Aug. 2020), p. 070603. URL: https://link.aps.org/doi/10.1103/PhysRevLett.125.070603.

[162] Daniele Oriti. "A quantum field theory of simplicial geometry and the emergence of spacetime". In: *Journal of Physics: Conference Series* 67 (May 2007), p. 012052. URL: https://doi.org/10.1088/1742-6596/67/1/012052.

[163] Steven Weinberg. "ULTRAVIOLET DIVERGENCES IN QUANTUM THEORIES OF GRAVITATION". In: *General Relativity: An Einstein Centenary Survey.* 1980, pp. 790–831.

[164] M. M. Hatalkar. "Theory of Elementary Particles in General Relativity". In: *Phys. Rev.* 94 (6 June 1954), pp. 1472–1475. URL: https://link.aps.org/doi/10.1103/PhysRev.94.1472.

[165] "Quantum Correlations in Systems of Indistinguishable Particles". In: *Annals of Physics* 299.1 (2002), pp. 88–127. URL: https://www.sciencedirect.com/science/article/pii/S0003491602962688.

[166] J.B. Lasserre. "A trace inequality for matrix product". In: *IEEE Transactions on Automatic Control* 40.8 (1995), pp. 1500–1501.